Insight Development on Tribological Characteristics of Molybdenum Disulphide-Titanium Dioxide as Soft Composite Coating Material for Machining Applications

A Thesis submitted in the partial fulfilment of the requirements for the award of the degree of

DOCTOR OF PHILOSOPHY

By

Borgaonkar Avinash Vitthal

(ROLL NO: 716123)

Under the supervision of

Dr. Syed Ismail

DEPARTMENT OF MECHANICAL ENGINEERING

NATIONAL INSTITUTE OF TECHNOLOGY

WARANGAL (T.S) INDIA 506 004

2021

In memory of my father

With love and eternal appreciation

Late Vitthal Ganapati Borgaonkar

NATIONAL INSTITUTE OF TECHNOLOGY

WARANGAL (T.S) INDIA 506 004

DECLARATION

This is to certify that the work presented in the thesis entitled **"Insight Development on Tribological Characteristics of Molybdenum Disulphide-Titanium Dioxide as Soft Composite Coating Material for Machining Applications"**, is a bonafied work done by me under the supervision of Dr. Syed Ismail and was not submitted elsewhere for the award of any degree.

I declare that this written submission represents my idea in my own words and where other's ideas or words have not been included. I have adequately cited and referenced the original sources. I also declare that I have adhered to all principles of academic honesty and integrity and have not misinterpreted or fabricated or falsified any idea/data/fact/source in my submission. I understand that any violation of the above will be a cause for disciplinary action by the Institute and can also evoke penal action from the sources which have thus not been properly cited or from whom proper permission has not taken when needed.

Date: **(Avinash V. Borgaonkar)**

Place: Warangal Research Scholar,

Roll No.716123

NATIONAL INSTITUTE OF TECHNOLOGY
WARANGAL (T.S) INDIA 506 004

CERTIFICATE

This is to certify that the thesis entitled **"Insight Development on Tribological Characteristics of Molybdenum Disulphide-Titanium Dioxide as Soft Composite Coating Material for Machining Applications"** that is being submitted by **Mr. Borgaonkar Avinash Vitthal** in partial fulfilment for the award of Doctor of Philosophy (Ph.D) in the Department of Mechanical Engineering, National Institute of Technology, Warangal, is a record of bonafied work carried out by him under my guidance and supervision. The results of embodied in this thesis have not been submitted to any other Universities or Institutes for the award of any degree or diploma.

Dr. Syed Ismail
Assistant Professor
Department of Mechanical Engineering
NIT-Warangal

ACKNOWLEDGEMENT

I take the opportunity to express my heartfelt adulation and gratitude to my supervisor, **Dr. Syed Ismail**, Assistant Professor, Mechanical Engineering Department, National Institute of Technology, Warangal for their unreserved guidance, constructive suggestions, thought provoking discussions and unabashed inspiration in nurturing this research work. It has been a benediction for me to spend many opportune moments under the guidance of the perfectionist at the acme of professionalism. The present work is a testimony to their alacrity, inspiration and ardent personal interest, taken by them during the course of this thesis work in its present form.

I wish to sincerely thank university authorities, **Prof. Ramana Rao**, Director, National Institute of Technology, Warangal and other top officials who gave me an opportunity to carry out research work. I also sincerely thank **Prof. A. Kumar**, Head, Mechanical Engineering Department, National Institute of Technology, Warangal for his continuous support towards carrying out research work.

Thanks are also due to **Prof. R. Narasimha Rao, Prof. N. Selvaraj, Prof. P. Bangaru Babu, Prof. S. S. Rao** and **Prof. C.S.P. Rao,** former Head(s), Mechanical Engineering Department, National Institute of Technology, Warangal, for their timely suggestions, support and for providing necessary department facilities and services during successful completion of research work. I wish to express my sincere and whole hearted thanks and gratitude to **Prof. K. V. Sai Srinadh, Prof. V. Suresh Babu** and **Dr. K. Gopi Krishna** (DSC members) for their kind help, encouragement and valuable suggestions for successful completion of research work. I wish to thank **Dr. G. Raghavendra** and **Dr. B. Satish Ben** for their extended help during this work.

I would like to express my sincere thanks to **Prof. Shirish Sonawane**, Chemical Engineering Department, National Institute of Technology, Warangal for their cooperation and the help extended during this work.

The authors would like to thank **Prof. Mihir Sarangi** and **Mr. Soumya Ranjan Guru,** Mechanical Engineering Department, Indian Institute of Technology Kharagpur, for their support in the research work. Authors would also acknowledge **Central workshop** and **Center for Advanced Instrumentation,** National Institute of Technology Warangal for their support in the research work.

I wish to express my sincere and whole hearted thanks and gratitude to **Dr. M. B. Mandale**, Head, Mechanical Engineering Department, Rajarambapu Institute of Technology, Sakharale. I would like to express my sincere thanks to all my friends and colleagues specially, to **Dr. Ganesh Warkhade, Dr. Amrut Mulay, Dr. Venkateswara Babu, Dr. Uday Bagale, Dr. Prashant Suryawanshi, Dr. Abhay Lingayat, Dr. Vinay Rangari, Dr. Harshal Patil, Dr. Gajanan Suryawanshi, Mr. Roshan Bodile, Mr. Ganesh Gawale, Mr. Upendra Mourya, Mr. Kishor Ingale, Mr. Sandip Khobragade, Mr. Sri Chaitanya, Mr. Nagendra Prasad, Mr. Ramana Reddy, Mr. Satish, Mr. Shyam Kumar, Mr. Markandeyulu**,. I would like to thank **Mr. Yellaiah**, Tribology Lab technician for his support during the completion of the research work.

Words are inadequate to express my thanks to my wife **Shital**, my son **Advait,** I cannot finish the thesis without their support and understanding.

At the end, I must appreciate to all my family members, my mother Smt. **Madhuri**, brother Mr. **Mahendra**, and sister in law **Sarita**, nephew **Abhinav**, father in law **Balasaheb**, mother in law **Kumudini**, and family members **Vaibhav, Varsha, Supriya, Shraddha, Shubhra, Manaswi** for exhibiting patience during this long and arduous journey.

I want to express my sincere thanks to all those who directly or indirectly helped me at various stages of this work. Above all, I express my indebtedness to the **"Almighty"** for all his blessing and kindness.

(Avinash V. Borgaonkar)

Abstract

MoS_2 is popularly used solid lubricant in various applications due to its superior tribological behavior. However, it possesses low hardness poor scratch and wear resistance which requires further improvement. In the present work an efforts have been made to enhance hardness and scratch resistance of pure MoS_2 coating film by doping TiO_2 nanoparticles as a reinforcement material. The Manganese phosphating is selected as a pre-treatment method to improve the bond strength between coating and substrate. The developed composite coating is bonded with the substrate material employing sodium silicate as a binder. The mechanical properties such as hardness and adhesion strength of the different coating samples are evaluated. Among pure MoS_2 and composite MoS_2-TiO_2 coating, coating with 15 wt. % TiO_2 exhibits superior hardness and bond strength. Further the tribological performance of composite MoS_2-TiO_2 coating (with different crystallite size and wt. % addition of TiO_2) considering different operation conditions such as contact pressure, sliding speed and temperature is investigated. In addition the effect of coating thickness is also considered. The test results reveal that, in comparison with the application of pure MoS_2 coating, the composite MoS_2-TiO_2 coating exhibits excellent tribological performance in all considered operating conditions due to the synergistic effect of both MoS_2 and TiO_2. The crystallite size of TiO_2 is not influential on COF and wear rate as compared to wt. % addition of TiO_2. However, at high contact pressure and higher sliding speed, the sample C (27.69 nm crystallite size) with 15% wt. of TiO_2 depicts the lowest COF and wear rate. In addition, a positive effect on COF and negative effect on wear rate is observed with the increase in temperature of the coated pin surface. The similar trend is also observed with the increase in coating film thickness.

The parametric optimization of the factors affecting the tribological behavior of this composite MoS_2-TiO_2 coating have been investigated using Taguchi approach with standard L27 orthogonal array. The developed model is validated through Analysis of variance (ANOVA) technique. The optimization study was performed by considering the various input parameters such as addition of wt. % of TiO_2 into the MoS_2 base matrix, contact pressure, sliding speed and temperature which affects the tribological properties of the coating material. The artificial neural network (ANN) tool is also implemented for predicting the output tribological responses. The study reveals that temperature has the highest influence followed by contact pressure and addition of wt. % of TiO_2. The predicted results have been verified by performing confirmation tests. The responses predicted using both Taguchi and ANN were compared. The study shows that ANN helps to predict the responses more accurately as compared

to Taguchi approach. Machining is one of the most basic and indispensable processes in the manufacturing industry. The machining responses such as cutting forces, surface finish and cutting temperature at the tool-chip interface, specific energy and tool life decisively plays important role to evaluate the machining performance. In the present work, composite MoS_2-TiO_2 coating is used in milling of AISI 52100 steel with HSS end mill cutter. The machining performance is compared with plain conventional, MoS_2 coated and composite MoS_2-TiO_2 coated tool under different lubricated condition. The use of solid lubricant in the form of coating or lubricant (third body) exhibited improved machining performance.

Keywords: Composite MoS_2-TiO_2 coating; cutting forces; cutting temperature; friction coefficient hardness; MoS_2; machining; milling operation; scratch strength; solid lubricants; surface finish; TiO_2; tribological properties; wear rate.

Table of Contents

List of Tables

List of Figures

List of Abbreviations

Abbreviations	Description
MoS_2	Molybdenum disulfide
TiO_2	Titanium dioxide
BSL	Bonded Solid Lubricants
ANN	Artificial Neural network
ANOVA	Analysis of Variance
ASTM	American Society for Testing of Materials
DOE	Design of Experiments
DOF	Degree of Freedom
F- ratio	Ratio of Variance between the groups to the variance within the group
FFBP	Feed forward back propagation
HV	Vickers hardness
HSS	High Speed Steel
LEARNGD	Adaptation Learning Function
LM	Levenberg Marquardt
LOGSIG	Log Sigmoid Transfer Function
TANSIG	Tan Sigmoid Transfer Function
PURELIN	Pure Linear Transfer Function
MAPE	Mean Absolute Percentage Error
MSE	Mean Square Error
OA	Orthogonal Array
PVC	Polyvinylchloride
R	Correlation Coefficient
R^2	Coefficient of Determination
R_a	Average Surface Roughness
RPM	Revolution Per Minute
S/N ratio	Signal to Noise Ratio
SEM	Scanning Electron Microscope
COF	Friction coefficient

WR	Wear rate
TMDs	Transition-Metal Dichalcogenides
PVD	Physical Vapour Deposition
CVD	Chemical Vapour Deposition
DLC	Diamond Like Carbon
RT	Room Temperature
ACP	Aluminum Chromium Phosphate
WC	Tungsten Carbide
EMSL	Electrostatic Micro-Solid Lubricant
NOX	Nitrogen Oxides
VOC	Volatile Organic Compounds
AFM	Atomic Force Microscopy
XRD	X-ray diffraction
EDX	Energy Dispersive X-ray analysis
AE	Acoustic Emission
L_C	Critical Load
FFMLP	Feed Forward Multi-Layer Perceptron
BP	Back Propagation
SLT	Self-Lubricated Tool

Chapter 1

Introduction

The chapter briefly introduces solid lubricants and their classification, reinforcement materials, binding materials, coating deposition processes. This chapter also outlines the motivation behind the present research. At last, the organization of the dissertation is discussed.

1.1 Background

Solid lubricants have been used for the lubrication of interacting surfaces from the past few decades. The usage of solid lubricant is inevitable in uncommon circumstances where oil and greases are unsuitable. The examples are space-related technologies (where liquid lubricants are avoided due to their release of gases under vacuum and extreme temperature conditions), textile and food sector (where products are possibly contaminated with the usage of oils and greases) and chemically reactive environments (where liquid lubricants would decompose or freeze in hostile environments) (Savan et al., 2000). Physical vapour deposition (PVD), chemical vapour deposition (CVD), bonding, burnishing, thin-film coating and particle embodiment have been used as different techniques to deposit solid lubricant as coating material onto the contacting surfaces. The direct deposition of soft coating material onto the substrate surface resulted into poor adhesion. Rovani et al. (2018) reported that various pre-treatment processes like phosphating, salt-bath nitriding and shot blasting help to improve the adhesion strength between substrate and coating. Many researchers (Azhaarudeen et al., 2018, Li et al., 2004, Tamilselvi et al., 2015) reported that phosphating was popularly employed as a pre-treatment process, as it helps to improve the adhesion between the coating and substrate by enhancement in the porous nature.

In general, the coatings are divided into two categories i.e. soft coatings (hardness less than 10 GPa) and hard coatings (hardness greater than 10 GPa) (Donnet and Erdemir (a), 2004). On the basis of soft and hard category, the coating materials are represented in table 1.1.

Table 1.1 Classification of coating materials

Hard coatings	**Soft coatings**
Nitrides	Soft metals
TiN, CrN, ZrN, BN, $BaSO_4$	Ag, Au, Pb, In, Cr, Sn, Cu, Ni
Carbides	Lamellar solids
TiC, CrC, WC	MoS_2, Graphite,WS_2, HBN, H_3BO_3, GaSe, GaS
Oxides	Halides sulphates, sulphur
Al_2O_3, Cr_2O_3, ZnO,TiO_2, CdO, Cs_2O, ReO_7, PbO	CaF_2, PbS, BaF_2, $CaSO_4$, $BaSO_4$
Borides	Polymers
TiB_2	PTFE, Polyimide, PE, DLC
DLC and Diamond a-C, a-C:H, ta-C, ta-C:H, a-C:X(:H), CNx, (nc) diamond	
DLC = diamondlike carbon a = amorphous ta = tetrahedral amorphous X = a metal nc = nanocrystalline PTFE = polytetrafluorethylene PE = polyethylene	

In tribological applications, both soft and hard coatings are used to enhance frictional and wear characteristics of interacting surfaces.

1.1.1 Hard coatings

Hard coating possesses high hardness i.e. ability to resist permanent deformation during mechanical loading. Specifically, it is beneficial in case of erosive or abrasive wear. If coating material is harder than the abrasive particles, there is less chance of abrasive wear likely to occur. Commonly, the hard coatings are classified into three groups according to their chemical bonding character such as metallic materials, covalent materials, and ionic (ceramic) materials (Voevodin et al., 2014).

Metallic materials

Metallic materials possess the ability to develop semi-coherent or coherent interfaces with substrate metallic materials, results into low energy interfaces with optimum adherence. This includes carbides, borides, and nitrides of transitional metals like Titanium-based carbides, borides, and nitrides; which are widely used in industrial applications because of their good adhesion to steel substrates, high hardness as well as chemical stability and su-

perior wear and corrosion resistance over a wide temperature range (Bunshah and Weissmantel, 2000).

Covalent materials

Covalent hard materials contain nitrides, borides and carbides of Al, Si and B and diamond. Boron carbide (B_4C) is distinct from other covalent materials since it has the ability to maintain its hardness even at higher temperatures. Therefore this material has been used in high-temperature and wear resistant applications (e.g., wheel dressing tools, blast nozzles, light and weight armour plates) (Abou et al., 2010). Under high humid environment, B_4C converts into boric acid (H_3BO_3) due to chemical reaction and it forms a structure similar to graphite which results in lower COF and wear rate between the interacting surfaces (Cuong et al., 2006). Over the past few years, diamond and DLC-based coatings have drawn the researcher's attentions of as they possess high hardness and abrasion resistance. These are extensively used in machining applications (i.e. cutting tools) (Clausing et al., 2012).

Ionic (ceramic) materials

Coatings formulated using Ionic (ceramic) materials such as oxides of Zr, Al, Ti and Be have been employed in the case of metal cutting tools to enhance the wear resistance. It also helps to improve the hardness and high temperature strength. Besides, it does not affect the toughness and adherence of the coating (Chen et al., 2008).

1.1.2 Soft coatings

The primary purpose of the application of the soft coating is to reduce friction between the interacting surfaces. It includes soft metal coating, polymer coating and lamellar coating. Recently, several solid lubricant materials like MoS_2, graphite, WS_2, CaF_2, DLC, HBN, H_3BO_3 and PTFE, etc., have been identified in the field of advanced tribology which controls the friction between the rubbing surfaces (Donnet and Erdemir (b), 2004).

Soft metal coating

The soft metal coating involves materials like Pb, Ag, Au and In. These materials possess a crystal structure with multiple slip planes. This helps to provide the lower shear ability, which makes them suitable for tribological applications. Besides, the point and dislocation defects that occurred during shear deformation were rapidly nullified due to the generation of frictional heat between the contacting surfaces. The film thickness influences the tribo-

logical behavior of the soft metal coating, bond strength between the coating and substrate (Donnet and Erdemir (a), 2004).

Polymer coatings

Among the soft coatings, polymer coatings are popular since they possess excellent self-lubricating properties, better wear and corrosion resistance and low noise emission. Besides, they are economical to synthesize (Holmberg, 2009). The most commonly used polymer coatings are polytetrafluoroethylene (PTFE), polyimides and elastomers. The tribological behavior of the polymeric coatings depends on the polymeric tribo-film developed due to rubbing of the parts against each other.

Lamellar coating

The most popularly used lamellar coatings are MoS_2 and graphite. The layered inorganic compound offers low friction because of its anisotropic layered structure i.e. weak Van der Waals forces and covalent bonding between the adjacent lamellae. When the interacting surfaces are in a sliding motion, the basal planes are adjusted parallel to the interacting surfaces. This leads to the generation of (002)-oriented transfer layers under a steady-state. When slide one over the other these parallel basal planes produce easy shear due to inter and intra-crystalline slip (Voumard et al., 2001).

The soft coating possesses lower shear strength, due to which it is worn out from the substrate surface and adheres onto the wear track. Eventually, this assists to mitigate the friction between the contacting surfaces. From the referred literature related to soft coatings, the MoS_2 has been popularly used. Because of its easy shearing ability and lamellar structure, it exhibits excellent tribological properties (Haider and Hashmi, 2011). The properties of MoS_2 have been listed in the following subsection.

1.1.3 MoS_2 coating material

The structure of Molybdenum disulphide (MoS_2) is comprised of Molybdenum (M) atoms in hexagonal planes sandwiched between of sulphur (S) atoms. The M atoms are equispaced from six atoms of S present at the corners of a triangular prism as depicted in Fig. 1.1. The M and S atoms are strongly bonded with each other. The spacing between S atoms is comparatively higher and the weak van der Waals forces between them resulted into easy shear between the basal planes. Under sliding condition, the lubricant film gets compacted and rearrangement of the structure at the surface took place; which makes the

basal lattice planes parallel to the sliding direction. In general, MoS_2 is dark grey to black in colour, extra shiny and smooth in nature when burnished (Reeves et al., 2013).

Under the early sliding or running in period, persistent layers of MoS_2 are accumulated within the contact surface of the substrate and counterbody due to which the COF reduces till it reaches to the steady state. This steady state prolongs based on the effects of environmental conditions, temperature, coating film thickness, surface finish and pre-treatment on the substrate (Clauss, 2012). Many researchers examined the effectiveness of the usage of MoS_2 as a solid lubricant in tribological and machining applications and concluded that the performance could be enhanced to a greater extent fulfilling the societal demands (cleaner, healthier and safer operating). The reported studies (Donnet and Erdemir (b), 2004, Tedstone et al., 2015) highlighted the benefits of MoS_2 coating in improving the tribological and machining characteristics under various environmental conditions. The enhanced performance is attributed to the soft lamellar crystal structure of MoS_2 and its weak Van der Waals forces enabling easy shear at the interface between MoS_2 basal planes.

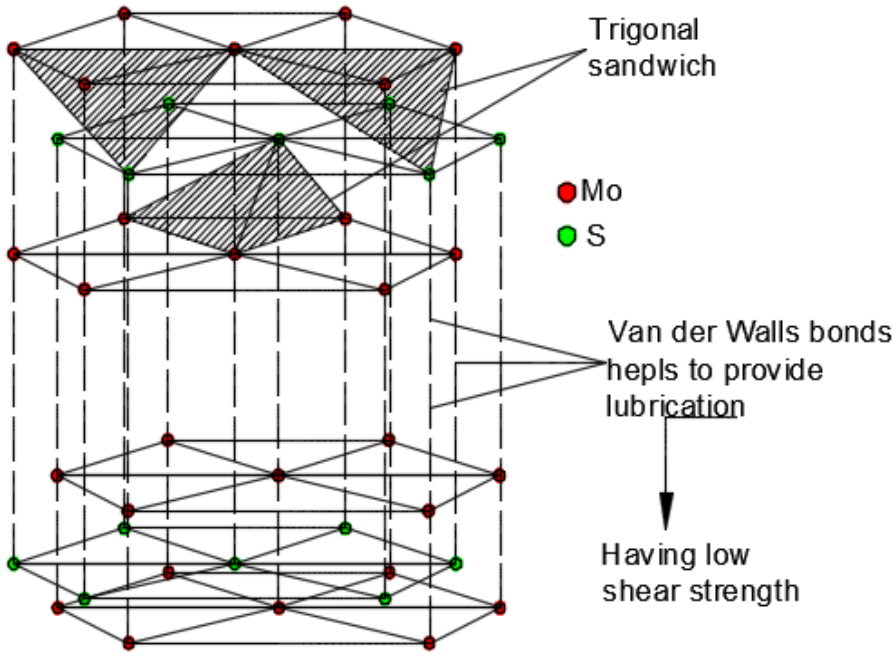

Fig. 1.1 The crystallographic structure of MoS_2

The pure MoS_2 coating exhibits poor wear resistance (Shankara et al., 2008, Shang et al., 2018). Further research work has been carried out to improve the wear resistance of pure MoS_2 coating material. It has been observed that the doping of reinforcement material into the MoS_2 base matrix significantly improves the wear resistance. The different rein-

forcement materials employed to enhance the wear resistance of pure MoS_2 coating have been listed in the following subsection.

1.1.4 Reinforcement materials

In order to improve the wear resistance of pure MoS_2 coating, various reinforcement materials such as lead (Pb) and titanium (Ti) have been used (Shang et al., 2018). The addition of Pb and Ti elements with their alternate layers help to reduce the hole and defect associated with coatings and resulted into improvement in the compactness and density of the coatings. A significant enhancement in the elastic modulus and hardness of the composite MoS_2/Pb-Ti coatings was found as compared with pure MoS_2 coating. Eventually, this resulted into improved tribological and anti-corrosion performance of the composite MoS_2/Pb-Ti coating. Dominguez et al. (2017) reported that layered TMD (MoS_2-WSe_2) and their combinations with WC phase resulted into enhanced load bearing capacity and wear resistance. Essa et al. (2017) demonstrated that the M50 steel fabricated with the addition of ZnO and MoS_2 exhibits enhanced tribological performance at high temperatures. Shankara et al. (2008) fabricated composite MoS_2-ZrO_2 coating and studied the tribological and mechanical properties. The doping of ZrO_2 resulted into an increase in the hardness of the coating and exhibited improved endurance life.

The performance of MoS_2 based composite coatings have been extensively studied, which include (YSZ–Ag–Mo–MoS_2 Muratore et al., 2006, Mo_2N/MoS_2/Ag Aouadi et al., (a, b) 2009, and Ag/MoS_2/graphite Chen et al., 2012). A thermal barrier coating is one of the approaches to protect the oxidation of MoS_2 (Muratore et al., 2009). Zhang et al. (2009) achieved an excellent tribological performance at 300°C employing CNT/MoS_2 composite coating. In addition, the CNT/MoS_2 composite coating exhibits enhanced mechanical properties because of the high load bearing capacity of CNTs. Voevodin et al. (2002) and Baker et al. (2007) demonstrated that DLC could also be doped to increase the service temperature range of the MoS_2 based composite coating. The DLC phase increases the hardness of the coating film and generates a resource of carbon for efficient lubrication in a humid environment.

In general, the binder is used to restrain the coating materials (in powder form dispersed within the binder) on the substrate surface. In the past few years, there has been an increase in demand of various binders for specific applications. The binder establishes the adhesion of the solid lubricant onto the substrate surface and helps to control the wear of solid lubricant coating due to its high hardness and mechanical strength. Based on the type

of coatings, the binders have been used for the specific applications. The different types of binders used are listed as follows.

1.1.5 Binding materials

Bonded solid lubricants provide improved endurance life, better abrasion resistance and adhesion. The commonly used solid lubricants like MoS_2 and graphite have some limitations when air is an operating medium at a higher temperature. In such cases, MoS_2 oxidizes to MoO_3 at 400 °C, which becomes abrasive in nature (McDonald and Hamilton, 2009). Similarly graphite also has a limitation i.e. loss of absorbed water layer with the increase in temperature. These problems can be resolved with the use of bonded solid lubricant films, in which binder acts as a barrier to protect against the failure of the solids lubricants. The binders are available in organic and inorganic form. The organic binders include Epoxy phenolic resin, Epoxy and Polyamide-imide; whereas inorganic binders include Sodium Silicate and Silicone (Burke et al., 2001).

Resin-bonded solid lubricants were used for the last few decades and these are classified into heat cured and air-cured materials. The air-cured solid lubricants bonded using thermoplastic resins such as cellulosic and acrylics. These resins produce quite a hard film that does not possess resistance against solvents. The heat-cured solid lubricants bonded using binders such as thermosetting and include alkyds, phenolics, epoxies and silicones. These resins possess outstanding solvent resistance and better adhesion strength but are softer than phenolics. Alkyds are economical, easy to handle and cured at lower temperatures. Whereas phenolics possess high surface adhesion and high hardness than alkyds; but they requires high temperature for curing (Ma et al., 2019).

The inorganic binders include Sodium Silicate and Silicone. Silicones can operate at higher operating temperatures but are soft in nature and possess good adhesion strength (Sunil et al., 2016). From the past few decades, soluble silicates have been used as binders in many applications since these are not having problem-related to handling, safety and environmental issues associated with nitrogen oxides (NOX) and volatile organic compounds (VOC). In addition, these are economical since they are not subjected to fluctuating market prices as like petroleum or sugar-based binders (McDonald and Hamilton 2009). From the available silicates based binders, sodium silicate is most widely used since it demonstrates a high level of binder performance. It has good binding strength, durability and water resistance.

Surface engineering includes the application of coatings and surface treatments. Among these, coatings is the most efficient and flexible solutions for tribological applications. The application of the coating leads to a decrease in the COF; increases the surface hardness by modification of the surface chemistry. Eventually, coating helps to enhance wear resistance and endurance life of interacting surfaces (Bhushan, 2000). In the past few decades, numerous coating deposition techniques have been successfully developed and employed to mitigate the friction and/or to protect the interacting surfaces from the failure of mechanical systems. These are listed in the following subsection.

The solid lubricants in the form of coating, deposited on the substrate surface using different coating deposition techniques. The different coating deposition techniques have been explained below.

1.1.6 Coating deposition methods

The solid lubricants in their dry form are deposited using different deposition techniques, namely physical vapour deposition (PVD), chemical vapour deposition (CVD), bonded solid lubricants (BSL) and burnished films (Gradt and Schneider 2016, Renevier et al., 2003). The PVD process is carried out by application of a high voltage across a low pressure gas; this results in the development of plasma which comprises of gas ions and electrons in a high energy state. These energised plasma ions strike to the target containing the desirable coating material and result in ejection of molecules from the target that contains adequate energy to travel and bond with the substrate. The PVD coated films usually possess thickness less than 2μm and possess excellent adhesion with the substrate (Totten 2017).

The CVD technique is used to deposit bonded solid lubricant films on various kinds of substrates materials such as metallic, ceramic, and polymeric. The solid lubricant films produced using this technique are in gradient, duplex, multiplex, and nanostructured or nanocomposite forms which results into improved performance and durability under severe conditions (Renevier et al., 2003).

Bonded solid lubricants (BSL) are similar to paints with higher content of solid. The BSL is comprised of either a single or a mixture of one or more lubricants in the powder form. They include volatile solvents or water-based or a mixture of both and can be subsequently cured in air at room temperature or at temperatures up to 180°C in the furnace. BSL can be applied by dipping, brushing or spraying onto the substrate surface (Erdemir 2000).

Burnished films are the simplest among all the methods; this process consists of rubbing the dry solid lubricant in the powder form between the interacting surfaces. The coating film produced with this technique is up to 1μm thick. However, the coating thickness is not uniform and coating film possesses lower endurance life (Fatah 2017).

1.2 Motivation and scope of the current research

In case of rolling/sliding contact conditions due to direct metal-metal contact, a higher amount of wear at the contacting surfaces takes place which results into failure of the entire system. In order to mitigate the friction and wear currently, different solid lubricants are employed in the form of coatings. The significance of solid lubricant coatings in enhancing the tribological performance pursuit to researchers and scientists to develop a new and effective solid lubricant based composite coatings. The developed coating should possess higher endurance life. There is a lack of research for understanding the benefits of the applications of composite coating in tribological and machining sectors.

To this date, a scarce amount of work was reported on the development of solid lubricant based composite coatings, its characterization and tribological evaluation. There is no data available in the open literature related to the development of composite MoS_2-TiO_2 solid lubricant based coatings, its characterization and tribological analysis and their performance in machining application (i.e. milling operation) in terms of cutting forces, cutting temperatures and surface finish of machined work material. Due to these mentioned limited work in the development of new composite MoS_2-TiO_2 solid lubricant-based coating there is a motivation to investigate its tribological performance, mechanical properties like hardness and adhesion strength and benefits in machining process.

1.3 Organization of the thesis

The thesis has been organized under seven chapters, with the contents summarized as follows:

Chapter 1 deals with the background of solid lubricant coating materials and their classification, reinforcement materials, binding materials, coating deposition processes. This chapter also outlines the motivation behind the present research. At last, the organization of the dissertation is discussed.

An extensive literature survey in the area of solid lubricant based coatings has been outlined in **Chapter 2**. This chapter reviews the solid lubricant materials and the coating dep-

osition methods being used to produce solid lubricant coatings and their use in tribological and machining applications. Eventually, the research gaps were identified and a framework is established to fulfil the identified gaps.

Chapter 3 presents the basics of the development of composite MoS_2-TiO_2 solid lubricant-based coatings, pre-treatment of the substrate to enhance adhesion strength between substrate and coating, deposition of the developed composite coating. This chapter deals with the characterisation of the developed coating in terms of adhesion strength and hardness of the coating.

The tribological behavior of composite MoS_2-TiO_2 coatings considering the effect of crystallite size and wt. % of TiO_2 into the MoS_2 base matrix has been explained in **Chapter 4**. The tribological investigation is performed considering various operating conditions like contact pressure, sliding speed and temperature. In addition, the effect of coating thickness is studied.

Chapter 5 demonstrates parametric optimization of the factors (wt. % addition of TiO_2 into the MoS_2 base matrix, contact pressure, sliding speed and temperature) affecting the tribological behavior of composite MoS_2-TiO_2 coating employing Taguchi approach with standard L27 orthogonal array. The developed model is validated by applying the Analysis of variance (ANOVA) technique. The tribological behavior of the developed composite coating is also investigated employing an Artificial Neural Network (ANN). In addition, the comparative study of the responses obtained using both Taguchi and Artificial Neural Network (ANN) is outlined in this chapter.

The machining performance of composite MoS_2-TiO_2 coated tool in machining operation (i.e. milling process) is discussed in **chapter 6.** A comprehensive experimental investigation is carried out with different environmental conditions in terms of cutting forces, surface finish, cutting temperatures, specific energy and tool life.

Eventually, **chapter 7** presents the overall conclusions drawn from the investigations carried out and it also suggests further recommendations for future work.

We should not give up and we should not allow the problem to defeat us.
Confidence and hard work is the medicine to kill the disease called failure. It will make you successful person. Dr. A P J ABDUL KALAM

Chapter 2

Literature Review

In the previous chapter, the research goal and working approach are addressed. The current chapter deals with an extensive literature survey which includes applications of the bonded solid lubricants (BSL), pre-treatment process required to ensure sufficient adhesion, reinforcement materials to enhance the wear resistance, binding materials to hold the solid lubricants on the substrate surface and coating deposition processes. This chapter also provides a summary of the literature review, gaps identified in the existing research and objectives of the present work.

2.1 Applications of the solid lubricants

Generally, solid lubricants are used in machining and tribological applications for controlling friction and wear between the interacting surfaces. The solid lubricants have been also used in automotive and aerospace industries, manufacturing industries, food and textile industries and nuclear industries. The literature review of solid lubricants used in machining and tribological applications is shown below.

2.1.1 Machining applications

The solid lubricants have been used in various machining applications like turning, grinding, milling and metalworking etc. The reviews of these machining applications are summarized below.

Turning

Dilbag and Rao (2008) performed hard turning operation on bearing steel using ceramic inserts at various operating conditions for different tool geometry (Refer Fig.2.1(a)). The machining was carried out at dry and lubricated condition employing graphite and MoS_2 solid lubricants. Their study revealed that solid lubricants help to improve the surface finish significantly. The surface roughness has been decreased by 8 % and 15 % with the use of graphite and MoS_2 respectively in comparison with dry machining.

The MoS_2 powder lubricant (third body) has been employed in turning operation due to its friction control and heat dissipation ability which is generated at the machining zone (Mukhopadhyay et al., 2007 and Wenlong et al., 2010).

Jianxin et al. (2008) deposited composite MoS_2-Zr coatings on the surface of carbide tools by combination of sputtering and ion plating process. The composite coating exhibits high hardness and superior adhesion with the substrate compared to pure MoS_2 coating. The test results show that with the application of composite MoS_2-Zr coating, decrease in COF compared to conventional carbide tool. The wear of composite MoS_2-Zr coating observed to be affected with cutting speed. Paturi and Narala (2015) studied the tribological properties of electrostatic micro-solid lubricant (EMSL) bonded MoS_2 coating on carbide tools in dry sliding condition. EMSL coatings possess good adhesion strength and superior wear resistance. The coating reduces the friction in turns helps to control the heat generation at the contact faces. From overall test results friction was reduced about to 50 % compared to that of uncoated tool. This is because of the inherent low shear strength of MoS_2 which allows transfer of worn out MoS_2 particles at the contact zone. The 42% reduction in specific wear rate of EMSL coating is observed as compared to conventional tool.

The influence of graphite as a coating material in turning operation was successfully studied by Shaji and Radhakrishnan (2003) and Matthew et al. (2009). These reported studies concluded that in comparison with the cutting fluid, graphite found to be efficient in reducing surface roughness of machined work material. The reduction in friction was observed due to its hexagonal layer lattice structure and its easy shearing ability (Teer 2001).

Boric acid (H_3BO_3) is a soft in nature and eco-friendly material. It possesses lubricity due to its lamellar crystal structure (Lovell et al., 2006). Boric acid is a favorable solid lubricant in industrial applications due to its reasonably high load carrying capacity and better frictional and wear characteristics (Krishna et al., 2009). The application of boric acid in turning process demonstrated effective lubrication resulted into reduced tool wear and cutting forces. In addition it also provides improved surface finish. (Vamsi et al., 2010, Krishna and Rao 2008) investigated the effect of graphite and boric acid on turning performance by supplying these lubricants in dry powder form at the tool-workpiece interface under same cutting conditions. The significant decrement in flank wear was noticed due to reduced friction at the contact zone. As compared to graphite, boric acid demonstrated sig-

nificant machining performance by reducing tool flank wear, cutting forces and improved surface finish (Rao and Xie 2006, Rao et al., 2011).

Agarwal and Venkateswara (2007) and Agarwal and Agarwal (2021) performed turning operation using coated carbide tool for the AISI 304 steel workpiece employing boric acid as a solid lubricant. The experimental results shows that there is 35 to 60 % reduction in the average flank wear, 40 to 49 % reduction in net cutting specific energy, 40 to 60 % reduction in tool-chip contact length, 32 to 65 % reduction in chip thickness ratio and 10 to 39 % reduction in the surface roughness with boric acid as a solid lubricant compared to that of dry and wet (with cutting fluid) machining. Wenlong et al. (a), (b) 2011 fabricated carbide tools with four micro-holes using EDM process on flank and rake face of the tool. The tools fabricated with and without MoS_2 powder filled into produced micro-holes and termed as Self-Lubricated Tool (SLT). They observed that tools embedded with MoS_2 powder showed enhanced tool life compared to tools without MoS_2 powder. The experimental results validated with numerical analysis. The results obtained from both the methods are in close agreement.

Grinding

Venu Gopal and Venkateswara (2004) used graphite powder between the interacting surfaces (Refer Fig. 2.1(b)). The effect of third body element (graphite powder) on the grinding forces, surface finish and specific energy was evaluated. The significant improvement was observed in terms of surface finish, specific energy and surface damage as compared to dry grinding.

Shaji and Radhakrishnan (2002, 2003) have experimented surface grinding operation in presence of graphite. They observed reduction in the tangential force as well as specific cutting energy due to lower frictional forces and improved surface finish.

Drilling

Renevier et al. (2000) performed drilling operation using high speed steel (HSS) drill bits. The drill bits were coated using TiN, TiCN, TiAlN, TiN+MoST(MoS_2+Ti) (Singh et al., 2015) and TiCN+MoST coating (Refer Fig. 2.1(c)). The experimental investigation showed that MoST coating improved the machining efficiency two folds for TiN bits and 4.1 to 4.8 times for TiCN bits under dry machining. However, the applicability of TiAlN coating was limited to dry machining. Moreover MoST mixed with PAO oil exhibits improved the machining efficiency by 2.4 times.

Milling

Suresh and Venkateswara (2005) performed milling operation on steel specimen in dry and lubricated condition using graphite (third body element) (Refer Fig. 2.1(d)). The machining performance was quantified in terms of cutting force, specific energy and surface finish. It was found that graphite assists to reduce the frictional heat produced at the contact zone. Their study demonstrated that significant improvement in the performance was observed with graphite assisted machining as compared to machining with cutting fluids.

Kiliçay and Ulutan (2016) evaluated the performances of various commercial boron compounds such as boron oxide, boron pentahydrate, boric acid, and Etidot-67 as solid lubricants in milling operation. The milling operation was performed using HSS end mills for machining AISI 1020 steel and the performance was judged in terms of cutting forces and surface quality. They observed a significant enhancement in the machining performance with the use of commercial boron compounds. It has been observed that in case of boric acid, the cutting forces were decreased by 15 to 50 % and the surface finish was improved by 20 to 32 %, compared to dry machining.

Renevier et al. (2000) also performed milling operation on stainless steel specimen. The Carbide end mills were coated with TiCN and TiCN/MoST. The experimental results showed that TiCN/MoST coated end mills exhibits enhanced tool life and decrement in cutting forces and improved surface finish compared to TiCN coatings alone.

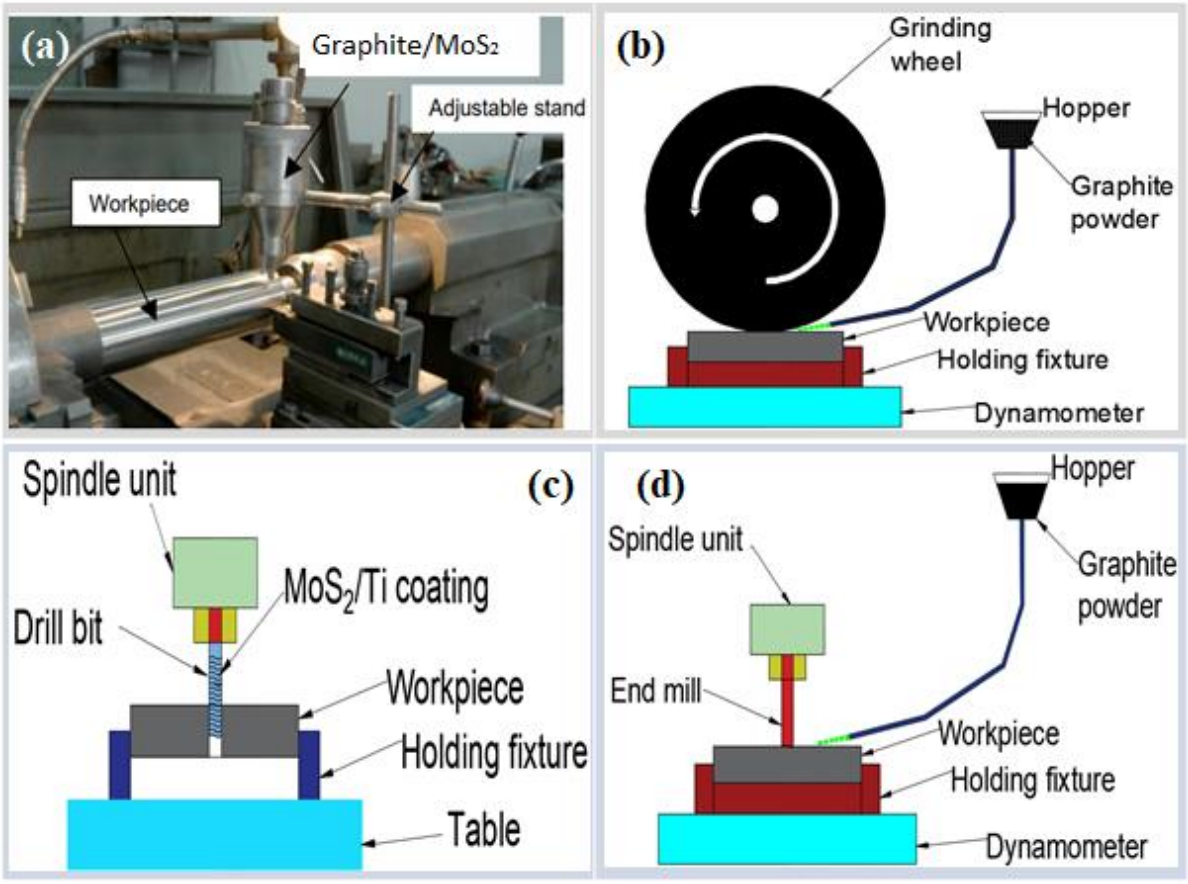

Fig. 2.1 Solid lubricants in different machining operations (a) turning Dilbag and Rao (2008), (b) grinding Venu Gopal and Venkateswara (2004), (c) drilling Renevier et al. (2000), (d) milling Suresh and Venkateswara (2005)

Metalworking

Renevier et al. (2000) performed different sheet metal working operations employing MoST coatings. The operations are briefly described as below.

Forming

The MoST composite coating was deposited on the ejector pin surface used in plastic moulds in forming applications. The number of shots carried out using coated and uncoated pins was compared to examine the effectiveness of the coating. The bare ejector pins performs 2000 shots prior to failure which got increased to 100000 for MoST coated pins. This is almost 50 times improvement and helps to cut down the cost significantly.

Piercing

The performance of MoS_2 and MoST coating was investigated in piercing operation. The experimental study showed that, conventional tool was able to pierce 5000 parts, MoS_2

coated tool able to pierce 6000 parts, and with MoST coated tool able to pierce 27000 parts.

Blanking

The blanking operation was carried out with bare and MoST coated punches. With the bare punches 3000 parts were produced, whereas, with application MoST coating the number of parts produced enhanced from 3000 to 12000 parts.

Drawing

The drawing operation was performed using bare tools, tools with CrN coating and tools with CrN/MoST coating. Their investigation shows that, conventional tool was able to draw 15000 parts, CrN coated tool able to draw 50000 parts and CrN/MoST coated tool able to draw 100000 parts (Carrera et al., 2003).

2.1.2 Tribological applications

The solid lubricants have been used in various tribological applications like roller bearings, slide bearings, slide guide way and flexible elements etc. The reviews of these tribological applications are summarized below.

Lubrication in Roller-Bearing

Based on the demand, the roller bearings are lubricated using greases, oils or solid lubricants. Many special types of grease, with or without addition of solid lubricants, enable customization for specific application. In specific conditions like high temperature, low speed and high contact pressure and environmental factors (like chemical and humid) solid lubricants or greases comprised with solid lubricants have been mostly used (Fleischauer et al., 2002, Miyoshi 2019). The solid lubricant film ensures reliable separation between roller and ring at lower speeds and higher loads which cannot be sustained by pure grease. The solid lubricants are also used in a vacuum, for example, in aerospace and nuclear sector, for micro-setting movements or in extreme temperature conditions (Rossi et al., 2003).

Slide Bearing, Slide Surface Lubrication and Slide Guide way

Similar to roller-bearing lubrication solid lubricants have been used for slide-bearing lubrication. The slide guide ways and other sliding surfaces are principally operating in boundary or mixed lubrication regime. The application of PTFE belts and epoxy resin mixed with solid lubricants like MoS_2, polyurethane or graphite is the best solution for such oper-

ational requirements. Lubricating varnishes comprising solid lubricants or pastes are also suitable which offers lubrication during running in phase and warm up and cool down phases in normal operating conditions (Erdemir 2001).

Lubrication in flexible elements

The hydrodynamic lubrication is not possible in case of chain and link due to higher surface pressure and lower sliding velocity between these elements. In such mixed lubrication condition, use of solid lubricants can reduce wear and assist to attain designed service life for the machine components. While selecting an appropriate lubricant, special focus should be provided not only to the various chain-drive mechanisms, but also to the material pairs and the operating conditions. The solid lubricants possess sufficient adhesion strength due to which it is not spun off at higher chain speeds or higher centrifugal forces at the turning point (pinion and wheel). The typical application of composite MoS_2-Ti coating in industrial elements is depicted in Fig. 2.2 (Renevier et al., 2001)

Fig. 2.2 Industrial applications of MoS_2-Ti (MoST) coating (a) bearings, (b) gears, (c) hobs, (d) punches and dies Renevier et al. (2001)

From the few years different soft-layered lamellar solid lubricants have been used in tribological applications, among these MoS_2 is popularly used since it offers lower fric-

tion coefficient, reasonably good wear resistance and ability to sustain at moderate loads (Hu et al., 2005 and Voumard et al., 2001). The tribological characterization of MoS_2 was performed on bearing applications by Heshmat et al. (2005). A systematic investigation of the tribological behavior of MoS_2 coatings were carried out employing on shaft surfaces of foil air bearings. The application of MoS_2 coatings resulted into reduced friction coefficient and enhanced wear resistance in oil free air craft engine (DellaCorte et al., 2004).

Meng et al. (2019) studied the tribological properties of textured pin and flat counterbody surfaces using different solid lubricants such as CaF_2, h-BN, WS_2, and graphite. The experimental tests showed that severe plastic deformation took place on both patterned and flat samples. Among these mentioned solid lubricants, CaF_2 has not shown any significant tribological response. The hBN also was squeezed outside the contacting surface, resulting into higher friction, whereas WS_2 and graphite have demonstrated comparatively lower friction coefficient. Li et al. (2018) were studied tribological behavior of CaF_2 and hBN doped Fe-based impregnated diamond bit matrix. Their study demonstrated that with increase in content of CaF_2 and hBN deteriorates the mechanical properties of the samples. The rise in hardness of the samples was observed with increase in content of CaF_2. The CaF_2 specimen demonstrated enhanced tribological performance as compared to hBN specimen. Chen et al. (2010) examined the tribological performance of Si_3N_4-hBN composites, against stainless steel counter-disc using pin-on-disc wear test rig in dry sliding condition. They reported that the addition of hBN to Si_3N_4 significantly reduces the COF and wear rate compared to pure Si_3N_4 specimens.

Deshmukh et al. (2006) analyzed the tribological performance of commercial transmission fluid mixed with boric acid. They observed this mixture demonstrated superior tribological performance. Vadiraj et al. (2012) examined the tribological behavior of MoS_2, graphite, boric acid and TiO_2 at different sliding speeds in dry sliding condition. They observed that MoS_2 and graphite exhibits 30 to 50% reduction in wear rate as compared to remaining lubricants at all sliding speeds. The reduction in COF was observed with increase in sliding speed for all the conditions. Among these MoS_2 depicted lower COF whereas boric acid and TiO_2 film shows higher COF due to poor adhesion and lubricity.

Luo et al. (2015) evaluated the torsional fretting wear of the bonded MoS_2 coating onto a steel substrate. With the application of coating, reduction in the frictional torque was observed as compared to uncoated specimens. The mechanism of the torsional fretting wear was mainly discovered as a combination of oxidation, abrasive wear, and delamina-

tion. Many attempts have been made by Fu et al. (2000), Xu et al. (2007), (Ye et al. (a) (2009), and Luo et al. (a, b) (2011) with the purpose of analyzing the performance of bonded coatings under fretting conditions. All these studies showed that the application of bonded coatings significantly enhanced the wear resistance. Because of the superior tribological properties, bonded MoS_2 coatings are employed in various applications like automotive, industrial, space mechanisms and nuclear power plants (Xu et al., 2003). Shen et al. (2017) analyzed the frictional and wear behaviour of bonded MoS_2 coatings in dual-rotary fretting (DRF). The DRF is a complicated fretting mechanism which combines torsional and rotational fretting. They noticed that MoS_2 coating exhibits superior tribological properties as compared to the uncoated substrate. Besides, it was observed that the coating endurance life was greatly depends on the fretting modes. The coating demonstrated higher wear resistance when the DRF was principally dominated by the torsional fretting than the rotational fretting. Wan et al. (2016) were prepared Polyimide/Epoxy resin MoS_2 bonded coatings using polyfluo-wax (PFW) as filler. The tribological properties of prepared coating were studied using a reciprocating ball-on-disc tribometer. Their study reveals that the incorporation of filler proved to be effective, improving the tribological performance of the coating. Moreover, reduction in COF was observed with increasing the content of PFW filler from 2 to 10%, and optimum filler content observed to be 6 %. Yin et al. (2011) examined the tribological behavior of epoxy bonded self-lubricating coatings doped with MoS_2 and graphite under dry sliding motion. The test results showed that the coating exhibits enhanced tribological properties at various operating conditions. Besides with the increase in sliding speed, decrease in load carrying capacity of the bonded coatings was observed. Ye et al. (b) (2009) examined the frictional and wear characteristics of bonded MoS_2 films reinforced with nano-LaF_3 filler under dry sliding conditions. The anti-corrosion ability of bonded films was also studied. With increase in the content of nano-LaF_3 filler (0 to 5 wt. %) the wear resistance of the coating increases. The doping of LaF_3 filler also helped to enhance the corrosion resistance of the coating. This was attributed due to the improved interfacial bonding between the MoS_2 and nano-LaF_3 mixed with the polymeric matrix. However, higher content of nano-LaF_3 filler leads to increase in the surface and interfacial defects and eventually results into deteriorating the anti-corrosion performance.

Ravindran et al. (2013) investigated the tribological performance of powder metallurgy processed aluminium metal matrix composites with different wt. % of graphite (AMMCG) using Taguchi approach. Their study shows that with increase in applied load

and sliding speed, COF and wear rate of AMMCG composite increases. The 5 wt. % addition of graphite exhibits lowest COF and wear rate for constant load and sliding speed. Saravanakumar et al. (2021) investigated the tribological behaviour of MoS_2 and graphite reinforced aluminium matrix (AA2219) composites. The optimization of factors affecting tribological properties was performed using Taguchi's method. The tribological properties significantly influenced by applied load followed by wt. % of solid lubricants. Their study shows that COF and wear rate increases along with the increase in normal load and sliding distance. The addition of MoS_2 exhibits lower COF; whereas addition of graphite exhibits lower wear rate for the selected operating parameters. Kavimani and Prakash (2017) fabricated Magnesium Metal Matrix Composite (MMC) reinforced with reduced graphene oxide (r-GO). The experimental investigation demonstrates improvement in the microhardness and decrement in specific wear rate with doping of r-GO. Taguchi coupled Artificial Neural Network (ANN) approach was employed to optimize the input parameters like load, wt. % of reinforcement material, sliding speed and sliding distance to achieve minimum specific wear rate. The ANOVA results reveal that specific wear rate significantly influenced by applied load and followed by wt. % of r-GO. The developed ANN model exhibits better prediction with R^2-value of 98.4% with lowest MSE in comparison with regression model obtained using Taguchi. Stojanovic et al. (2018) evaluated the frictional and wear behavior of aluminium hybrid composites (A356) reinforced with graphite. Taguchi coupled ANN technique was implemented to optimize the input parameters to achieve minimum COF and wear rate. The ANOVA results showed that COF and wear rate significantly influenced by sliding speed followed by wt. % addition of graphite and applied load. The developed ANN model exhibits better prediction of tribological properties with R^2-value of 98.9 % with lowest MSE compared to regression model obtained using Taguchi. Tyagi et al. (2020) modified the steel substrate surface using electric discharge coating (EDC). The green compact sintered electrodes were used (prepared by mixing WS_2 and Cu powder in different proportions). They have studied the effect of input parameters (peak current, duty factor and powder mixing ratio) on output performance parameters (microhardness, mass transfer rate, coating film thickness and tool wear rate). The ANN was developed for predicting the output responses. The ANN predicted results exhibits close agreement with experimental results.

As the direct deposition of the solid lubricants onto the substrate surface results in to poor adhesion. Hence in order to enhance the adhesion between substrate and coating

different pre-treatment processes have been employed (Ebnesajjad 2010). The pre-treatment processes are listed in the following subsection.

2.2 Pre-treatment processes

Rovani et al. (2018) and Liang (2013) reported that various pre-treatment techniques like shot blasting, ion plating, phosphating, sand blasting and salt-bath nitriding assists to enhance adhesion between substrate and coating. Korsunsky and Kim (2010) employed different pre-treatments like shot peening and grit blasting for steel substrates. The fretting tests were performed on pre-treated samples coated using DLC and MoS_2 coatings. They observed that in case of both DLC and MoS_2 coatings, grit blasting pre-treatment exhibits excellent bond strength resulted into enhanced endurance life and reduction in COF.

In another study, (Zhu and Zhou 2001 and Xu et al., 2003) employed sand blasting as a pre-treatment on steel substrates. The pre-treated samples were coated with novolac epoxy resin bonded MoS_2 coating. The fretting tests were carried out on coated samples. The test results shown that the pre-treatment help to enhance the adhesion between substrate and coating as compared to un-treated samples. Xu et al. (2003) deposited MoS_2 coatings by sputtering process on pre-treated steel substrate. Ion-plating and shot-peening processes were employed as pre-treatments. The fretting tests were performed on coated samples. They observed that shot-peening process exhibits excellent adhesion strength between substrate and coating as compared to ion-plating and results into enhanced endurance life of the coating.

To ensure the advantages of the phosphating process Shankara et al. (2008) developed composite MoS_2 based coating by adding zirconia and graphite and deposited onto the phosphated steel substrate. The experiments were performed on reciprocating tribometer. The composite coating exhibits enhanced frictional and wear properties compared to pure MoS_2. Beside the presence of moisture, affects the service life of the coating. At high temperature the moisture evaporates and improved the service life of the coating. Hu et al. (2020) studied the corrosion resistance of zinc phosphate coating applied on mild steel, using nano-MoS_2 as an accelerator. The test results demonstrated that dispersed nano-MoS_2 particles serves as nucleation sites for phosphate crystals to catch the metallic ions and helps to develop a dense and uniform phosphate coating. This developed coating shows remarkable improvement in the corrosion resistance of the steel. Liu et al. (2014) developed adaptive phosphate coatings with addition of MoS_2 and Ag using ACP as a binder and were deposited at a higher temperature on steel substrate. The tribological per-

formance of the fabricated coating was investigated in the temperature range from room temperature (RT) to 700 °C. The test results show that the composite Ag/MoS_2 coating (with mass ratio of 2 : 1) demonstrate a stable and lower COF and relative lower wear rates over the entire temperature range. This was attributed due to the tribo-chemical reaction takes place between Ag and MoS_2 during rubbing process which leads to formation of Ag/MoS_2 compounds lubricating film. Several studies (Azhaarudeen et al., 2018, Li et al., 2004 and Tamilselvi et al., 2015) reported that phosphating is most popularly used pre-treatment process as it assists to improve the bond strength between the substrate and coating. The schematic of the phosphated substrate surface is shown in Fig. 2.3.

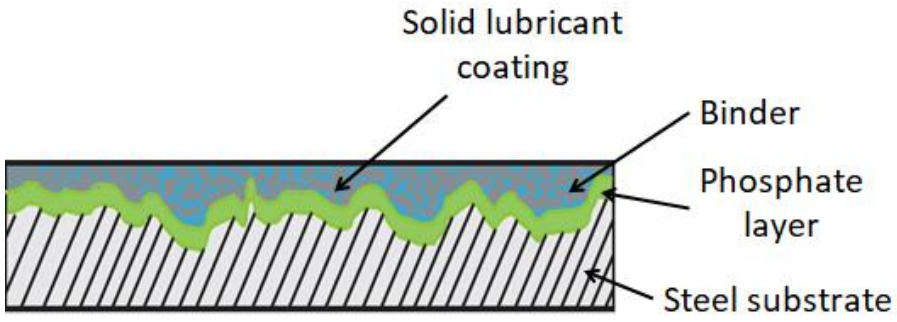

Fig. 2.3 Phosphating as a pre-treatment Li et al. (2004)

The pure MoS_2 coating exhibits higher wear rate due to poor bond strength between substrate and coating. As the MoS_2 coating delaminates from the substrate the friction coefficient increases (Shang et al., 2018 and Shankara et al., 2008). Further to improve the wear resistance of poor MoS_2 coating, different reinforcement materials were added into the MoS_2 base matrix. The different reinforcement materials were used to enhance the tribological performance of the solid lubricant coatings have been listed in the below subsection.

2.3 Reinforcement materials

Zhu et al. (2003) investigated frictional and wear behavior of sputtered pure MoS_2 and composite MoS_2/Ti coatings in fretting and pin-on disk tests under different operating conditions. They observed that MoS_2 exhibits a superior performance in fretting with corundum balls in comparison with steel balls. The easy shearing ability of the MoS_2 coating leads to transfer the film under fretting conditions. The MoS_2/Ti composite coating proved to be excellent in pin-on-disk tests as compared to pure MoS_2, since the pure MoS_2 coating

exhibits poor mechanical properties. Bulbul and Efeoglu (2010) deposited MoS_2-Ti composite coating on AISI 52100 steel using sputtering process. The mechanical and tribological properties of the developed coatings have been evaluated. The addition of Ti into MoS_2 leads to increase the hardness due to compressive stress induced in the matrix structure. The composite MoS_2-Ti coating with 8.54 wt. % of Ti exhibited excellent tribological performance. Renevier et al. (2001) examined the frictional and wear behavior of MoS_2-Ti composite coatings. These developed composite coating exhibits high hardness, high load capacity and high adhesion. Due to this, the wear resistance has been significantly improved and at the same time MoS_2 exhibits low friction. They studied the application of developed coating in cutting and forming tools.

Asmoro et al. (2018) analyzed the tribological response of brake lining composite lubricated with MoS_2 and graphite. The experimental tests were performed using pin-on-disc tribometer at different loads and speeds. The composites made with different wt. % addition of MoS_2 and graphite. The test results shows that compare to graphite, MoS_2 exhibits lowest frictional properties. In addition, with increase of MoS_2 wt. %, decrements in specific wear rate and heat generation was observed. Cho et al. (2006) investigated the tribological behaviour of brake material doped with various solid lubricants like graphite, Sb_2S_3 and MoS_2 with different volume fractions. The tribological responses of the developed materials were tested using a brake dynamometer. The test results reveal that the materials composed of graphite and Sb_2S_3 improves the friction stability and fade resistance. However, the materials composed with MoS_2 and Sb_2S_3 decreases the resistance to wear and fading.

Ma et al. (2013) evaluated the frictional and wear characteristics of Ni/MoS_2-C composite coating deposited on steel substrates using electro-brush plating process. The experimental tests carried out under different environmental conditions like in high vacuum, humid air, atomic oxygen, erosion and ultraviolet irradiation. The nano graphite particles showed enhancement in the moisture resistance with reducing the residual stress which in turn improves the mechanical properties of the developed coating. The coating exhibited excellent lubricity for longer duration in all environmental conditions. The test results reveal that the Ni/MoS_2-C coating has outstanding space-tribological properties and better compatibility in harsh environments. Efeoglu et al. (2008) investigated the frictional and wear response of MoS_2 co-sputtered with Nb. The experiments were performed in various environments such as air, dry nitrogen, distilled water and PAO oil using pin-on disc tribometer. The higher friction and wear rate was observed in dry nitrogen whereas lower

in case of oil. The MoS_2-Nb film produces a dense structure. The NbS_2 phase observed in humid air demonstrated superior lubricating properties compared to dry nitrogen conditions.

Dominguez et al. (2017) examined the tribological properties of multiphase MoS_2 and WSe_2 films and their combinations with WC deposited using sputtering process. The tests were carried out in ambient air and dry nitrogen environment. The WSe_2 films exhibited same frictional and wear characteristics under both the environments. The addition of the WC phase is only significant for MoS_2 coating in ambient air. The enhanced performance of the multiphase MoS_2 and WSe_2 films doped with WC makes an alternative for pure MoS_2 coating in space and vacuum applications. Chan et al. (2016) studied the tribological performance of multi-layered MoS_2 and WC coated substrate in sliding against Aluminium alloy material using a pin-on-disc tribometer. They observed that application of MoS_2 on hard WC coating helped to lower the punch forces required for aluminium sheet metal forming and also exhibit better surface finish. The coating prevents the accumulation of aluminium debris on the tool surfaces. However, due to the shorter life of MoS_2 coating, for each pass of the tool requires MoS_2 coating to be applied by a spraying method. It is also observed that the worn out MoS_2 particles partially protects the tool surface.

Xu et al. (2020) developed composite MoS_2-Si coating and studied its tribological behavior. The test results showed that with increase of Si content the typical porous with columnar morphology changes to a non-porous morphology. The 14.7 at. % Si content found to be optimum exhibiting better tribological properties. However, the higher Si content inhibits the formation of the transfer film resulted into poor tribological properties.

In general, binder is used to restrain the coating materials (in powder form dispersed within the binder) on the substrate surface. From past few years there has been growing interest in the demand of various binders for specific applications. The binder establishes adhesion to the solid lubricant onto the substrate surface and helps to control the wear of solid lubricant due to its high hardness and strength. Based on the type of the coatings the binders have been used for specific application. The categories of the bonded coatings and corresponding binders used are listed as follows.

2.4 Binding materials

The binders are available in the organic, inorganic ceramic materials. The organic binders include Epoxy phenolic resin, Epoxy and Polyamide-imide; whereas inorganic binders include Sodium Silicate and Silicone (Burke 2005).

Organic bonded coatings

Resin bonded solid lubricants were used from last few decades and these are classified into heat cured and air cured materials.

Heat cured resin bonded coatings

In general phenolics and epoxies are used as the binding agents. Phenolics offer superior adhesion with the surface, and comparatively harder than epoxies, whereas epoxies possess excellent solvent resistance. The synthesized epoxy-phenolics binder demonstrates combined properties of both. Other materials, such as polyimides and silicones are also used as binders for specific application. Silicones can withstand at higher temperatures compared to phenolics, but are soft in nature and provide good adhesion. Polyimides are suitable for high loading conditions (Ma et al., 2019).

Air cured resin bonded coatings

The air cured organic binder offers a moderate performance lies in between unbonded/burnished coatings and heat cured bonded coatings. The most commonly used binders are thermoplastic resins, such as celluloses, alkyds, acrylics, vinyls, epoxies and acetates (Burke, 2005).

Inorganic (non-ceramic) bonded coatings

The inorganic binders like silicates (e.g., Na_2SiO_3) and phosphates (e.g., $AlPO_4$) were principally employed for space applications (Jia et al., 2017). Besides organometallics, aluminates and other compounds have been also used. These inorganics binders have several merits over organic binders. These inorganic binders are useful in such applications where liquid oxygen compatibility is required and can sustain at moderately elevated temperatures. Besides, these are harder than organic binders and can tolerate higher loads (Lince 2020). However, inorganic binders are comparatively brittle and wear out more easily, due to which it exhibit lower cycle life than organic binders (Lince et al., 2014).

Ceramic bonded coatings

Ceramics binders are mostly employed in high temperature applications (up to 1100°C), where resins and inorganic binders unable to sustain. TMDs like MoS_2 cannot sustain at such high temperature, so other lubricants like CaF_2, CaF_2/BaF_2 and MgF_2 eutectic mixtures are used. Beside PbO can also be used. In certain applications, aluminium phosphate is often added for strength (Bruce 2012). The most of the ceramic bonded coatings require

higher temperature (above 500°C for curing), hence the refractory metals and their alloys, or other high-temperature materials can be employed (Reeves et al., 2013).

From the last several decades, soluble silicates are being used as binders in many applications since these are easy for handling. Whereas environmental and safety issues are associated with nitrogen oxides (NOX) and volatile organic compounds (VOC). Beside these are economical since they are not subjected to fluctuating market prices as like petroleum or sugar-based binders (McDonald and Hamilton 2009). From the available silicates based binders, sodium silicate is most widely used since it demonstrates a high level of binder performance. It is having good binding strength, durability and water resistance.

2.5 Coating deposition processes

Generally, the solid lubricants have been applied on the substrate surface using different methods such as bonding, burnishing, particle embodiment, thin-film coating (George 2017). Among these bonding is used for the parts and components those are non-accessible for lubrication after machine assembly (Vazirisereshk et al., 2019). Burnishing is the easier and cheaper method by which a very thin film can be applied with rubbing dry lubricant powder in between the interacting surfaces. Burnishing can be used for the parts/components having close-fitting tolerance. Generally, the particle embodiment method is used for fabricating a self-lubricating coated layer over the metallic surfaces. The thin film coatings have been developed using commercial techniques like CVD and PVD. These are costlier and are efficient to produce precise thin films as per the requirement (Gradt and Schneider 2016, Renevier et al., 2003). In the recent years, several researchers employed bonded solid lubricants (BSL) since these are easy to apply, economical and possess excellent frictional and wear characteristics. The typical bonded solid lubricant is depicted in Fig. 2.4.

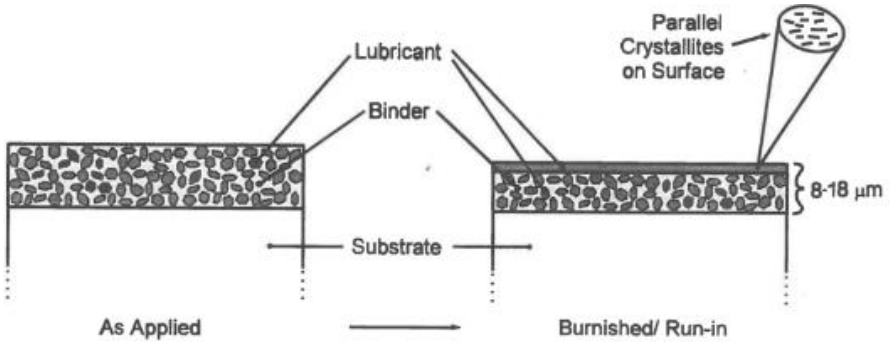

Fig. 2.4 Schematic representation of bonded MoS_2 coating (Left as-applied coating, right-after run in period) Liang (2013)

The following observations have been listed from the comprehensive literature review.

2.6 Observations from the literature

- Pure MoS_2 used as a solid lubricant to improve the tribological properties.
- Improvement in the tribological properties has been observed with addition of different reinforcement materials such as metals (MoS_2-Pb-Ti, MoS_2-Ti), selenide (MoS_2-WSe_2) and oxides (MoS2-ZnO) (MoS_2-ZrO_2).
- Pre-treatment process gives bond strength and optimum coating thickness. Various pre-treatment techniques like sand-blasting, phosphating, salt-bath nitriding, shot peening, micro-arc oxidation; and abrasive blasting process have been used.
- Phosphating was popularly used as it creates micro-pores nature which helps to trap the solid lubricant into the interstices between the phosphate crystals which results in enhanced bond strength.
- Lead and Graphite based lubricants lead to environment pollution, health and safety issues when mixed with atmosphere. Hence, there is need to investigate eco-friendly, stable and easily disposable solid lubricants.

2.7 Gaps in the existing research

The literature review carried out in the area of solid lubricant coating, coating deposition methods, coating materials, MoS_2 based coatings in machining and tribological applications. The literature review outlined the key gaps as follows.

- Very few studies reported on fabrication, characterization of composite coating material
- Based on the referred literature, lack of study related to the investigation of the tribological performance of composite MoS_2-TiO_2 coating material
- Lack of studies related to the investigation of the individual and combined factors affecting the tribological response of composite coating material using Taguchi and Artificial Neural network (ANN)
- Limited work has been reported on the use of composite coating material in the machining process
- Lack of studies available related to investigation of the tribological properties of the composite coating in combination with surface texturing

- Lack of studies available related to investigation of the corrosion resistance of the composite coating
- Very few works were identified on the computational investigation of the tribological behavior of the composite coating

2.8 Research problem

Limited work has been reported on the use of composite coating material in tribological applications. The tribological behavior of such composite coating material is still dramatic in nature, and meticulous examination of interacting coated surfaces with such composite films under various operating conditions is still required. The present research work addresses the development of composite MoS_2-TiO_2 coating (with in-house synthesized TiO_2 having different crystallite size and with different wt. % addition) and its tribological investigation in sliding contact under different operating conditions. The developed composite MoS_2-TiO_2 coating has been tested in machining application to study its effect onto the machining performance.

2.9 Research hypothesis

It is believed that composite MoS_2-TiO_2 coating improves the tribological behavior of interacting surfaces. It is expected that the crystallite size and with different wt. % addition of TiO_2 would show a prominent effect on the output parameters like COF and wear rate of interacting surfaces. These output parameters depends on input variables like contact pressure, sliding speed, temperature and coating thickness. It is also assumed that composite MoS_2-TiO_2 coating will help to improve the machining performance.

2.10 Objectives of present research work

The above research gaps motivate the researcher quest to produce MoS_2 based new composite coating, which will be able to enhance the tribological properties at different operating conditions. In view of the aforementioned research problem, the objectives of present research work can be outlined as follows;

- Fabrication and characterization of composite MoS_2-TiO_2 coating material
- Tribological investigation of composite MoS_2-TiO_2 coating to examine the effect of different crystallite size and wt. % of TiO_2

- Parametric optimization of factors affecting the tribological behavior of composite MoS_2-TiO_2 coating using Taguchi and Artificial Neural network (ANN)
- Evaluate the performance of composite MoS_2-TiO_2 coating in machining application (i.e. milling process)

2.11 Summary

The exhaustive literature review on different solid lubricants used in machining and tribological applications is presented. The review has reported pre-treatment techniques, reinforcement materials, binding materials and coating deposition processes used in case of solid lubricant coating. The objectives of the present research work based on the research gaps identified are outlined.

The detailed procedure of fabrication and characterization of composite MoS_2-TiO_2 coating is discussed in chapter 3.

Chapter 3

Fabrication and Characterization of Composite MoS_2-TiO_2 Coating Material

This chapter addresses the materials used for coating and characterization methods to test the coating material. The present chapter also discusses the synthesis of TiO_2 material and doping of TiO_2 material with different crystallite sizes and wt. % into the MoS_2 base matrix for the development of composite MoS_2-TiO_2 coating material. The mechanical properties like hardness and scratch strength of the different coating samples are evaluated.

3.1 Materials and characterization methods

As observed from the previous chapter, molybdenum disulphide (MoS_2) is popularly used as a solid lubricant in various applications due to its superior tribological behavior. However, it possesses low hardness; poor scratch and wear resistance which requires further improvement. In the present chapter, efforts have been made to enhance the hardness and the scratch resistance of pure MoS_2 coating film by doping TiO_2 nanoparticles as a reinforcement material. The materials used for the preparation of coating material and characterization techniques to study the developed coating material are explained below.

3.1.1 Materials

The factors affecting bond strength between substrate and coating are substrate surface finish, coating thickness, binding agent and reinforcement material (Pathanatecha 2019). There is no direct relation between substrate material property (like Young's modulus, hardness) and bond strength between substrate and coating material. Therefore, in the present work a popularly used steel material i.e. AISI 52100 steel is chosen as a substrate material because of its usage in various applications such as anti-friction bearings, punches, mill rolls, taps, fasteners, dies for structural components used in the automotive and aircraft industry (Bhadeshia 2012, Guo and Liu 2001). This material possesses high hardness; excellent wear resistance and good dimensional stability. The mechanical properties of the substrate material are listed in table 3.1

Table 3.1 Mechanical properties of AISI 52100 steel material

Material properties	Magnitude
Young's modulus	210 GPa
Density	7.81 g/cm^3
Fracture toughness	15.4-18.7 MPa-m½
Bulk modulus	160 GPa
Shear modulus	80 GPa
Hardness	60-67 (Rc)

In the present work, AISI 52100 specimens were prepared with dimensions of 30 mm X 30 mm X 5 mm thick, for hardness and scratch test. The chemical composition of the substrate material is depicted in table 3.2.

Table 3.2 Chemical composition (wt. %) of steel material used for substrate

Fe	Cr	C	Mn	Si	Ni
96.75	1.50	1.00	0.30	0.25	0.20

To improve the bond strength between substrate and coating material, some pre-treatment processes were investigated by the researchers. As per the reported literature (Duszczyk et al., 2018, Rajagopal and Vasu 2000) various pre-treatment processes like salt-bath nitriding, shot peening, sand-blasting, abrasive blasting, phosphating, and micro-arc oxidation process were used. Among these, phosphating was popularly used as it creates micro-pores which help to trap the solid lubricant into the interstices between the phosphate crystals which results in enhanced bonding strength. Hence in the present work, phosphating is used as a pre-treatment process to enhance the bond strength between the steel substrate and coating material. For phosphating, the necessary chemicals like phosphoric acid (H_3PO_4), magnesium carbonate ($MgCO_3$), sodium nitrate ($NaNO_2$), and sodium hydroxide (NaOH) are used. These are procured from Sigma Aldrich Ltd., Mumbai, India.

For fabrication of pure MoS_2 coating, MoS_2 powder (with size 70-90 nm) is purchased from Sisco Research Laboratories Pvt. Ltd., Mumbai, India. Further to fabricate the composite MoS_2-TiO_2 coating, the TiO_2 has been synthesized in-house. For the synthesis of TiO_2, various chemicals are used like titanium tetra isopropoxide (TTIP), acetone, sodium hydroxide (NaOH) and methanol which are procured from S. D. Fine Chemicals Ltd., Mumbai, India.

3.1.2 Characterization methods

For synthesized TiO_2 particles and MoS_2-TiO_2 composite coated specimens the following characterization methods/equipments are used.

X-Ray diffraction analysis

X-ray diffraction analysis (XRD) is performed using Bruker D8 Advanced X-ray Diffractometer as depicted in Fig. 3.1 (Cu-Kα radiation, k = 0.154056 nm). The samples are analyzed in the continuous scanning mode in the 2θ range of 20–80º, using a scan rate of 0.001 degree/s and used for estimation of the crystallite size of the prepared TiO_2 powder (as per the standard Rutile, JCPDS No. 21-1276). By observing the XRD patterns the average crystallite sizes of the synthesized TiO_2 nanoparticles are evaluated using the Scherrer formula (Orendorz et al., 2007).

$$D = \frac{k\lambda}{\beta \cos\theta} \tag{3.1}$$

Where,

D is crystallite size in nm,

k = 0.89 shape factor constant,

β is the full width at half maximum (FWHM) in radian,

λ = 1.540598 nm wave length of the X-ray which and

θ is the Bragg's diffraction angle.

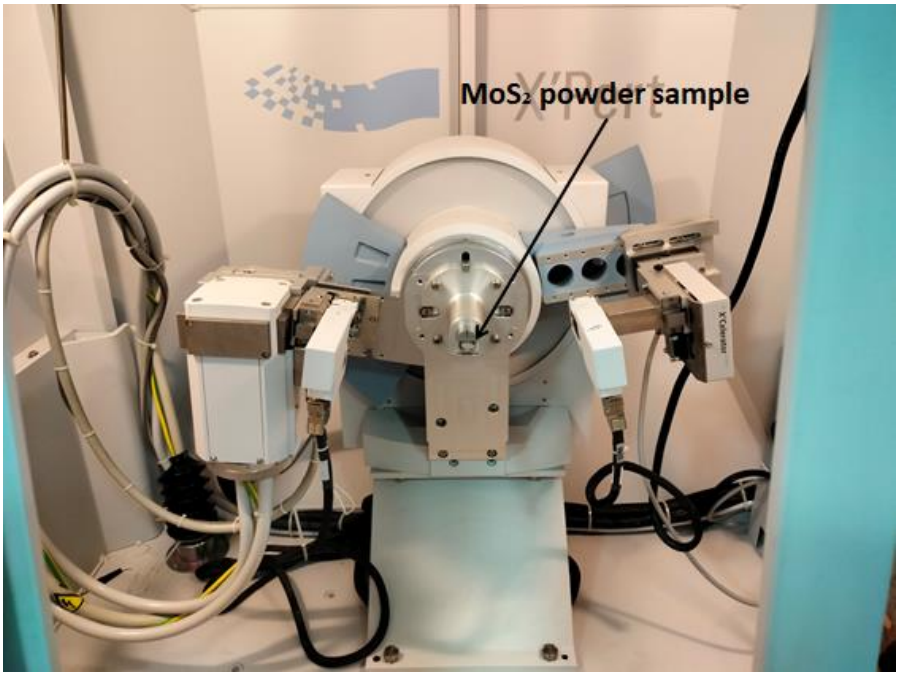

Fig. 3.1 X-ray Diffractometer

Scanning electron microscopy (SEM)

The morphological study before and after scratch test of the coated samples is performed using scanning electron microscopy (SEM) in a higher resolution field emission gun microscope, Hitachi-4800 (Tokyo, Japan), equipped with an energy dispersive x-ray analysis (EDAX) detector (Bruker, XFlash4100, Billerica, MA, USA) as shown in Fig. 3.2.

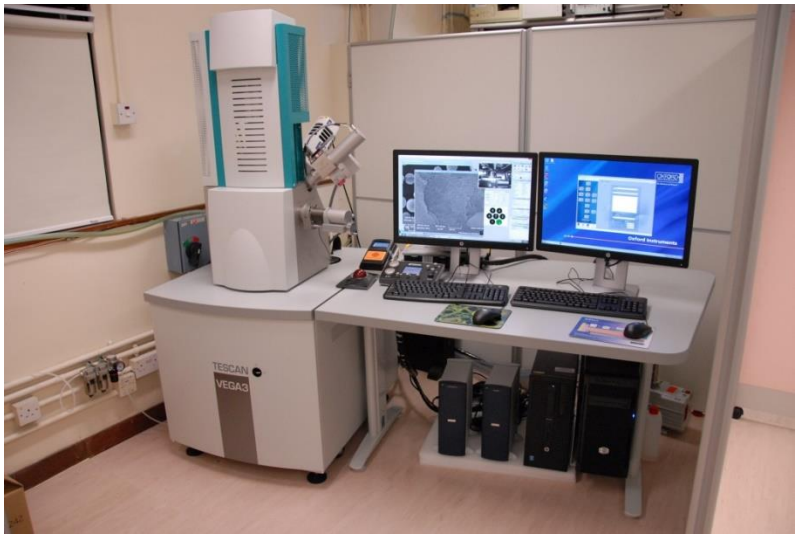

Fig. 3.2 Scanning Electron Microscope

Microhardness testing

The microhardness of the coated samples is measured (as per ASTM-D-3363) using a Vickers microhardness tester supplied by Chennai Metco Pvt. Ltd., (Chennai, India). This equipment is equipped with a testing force range of 0.0981 N to 9.81 N and an automatic loading-unloading dwell period of 50-60 sec. The maximum resolution of the equipment is 0.0625 μm. The optical microscope (Model QX-4RT) supplied by Quasmo (Haryana, India) is used for capturing the impressions produced under load by a pyramid-shaped diamond indenter on the coated specimens. The Microhardness tester used in this experimental study is shown in Fig. 3.3.

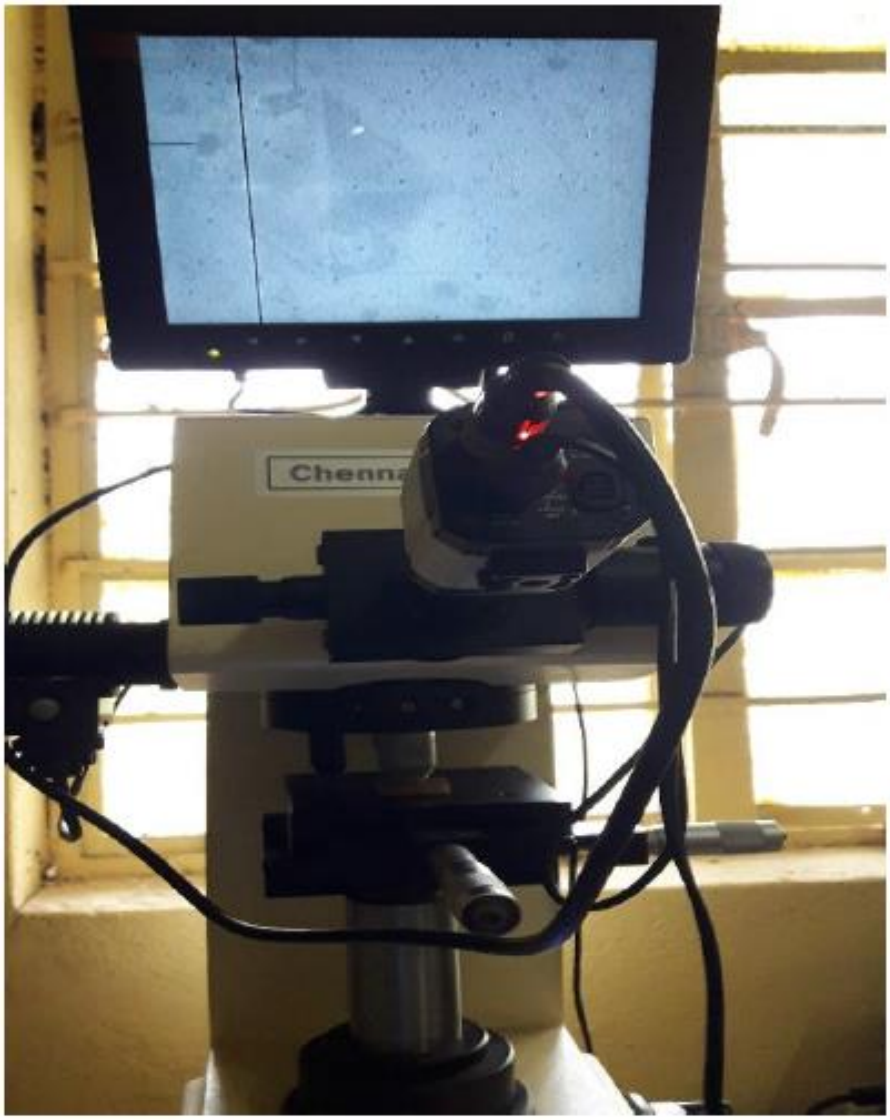

Fig. 3.3 Vickers microhardness tester

Scratch test

The adhesion strength of the substrate-coating interface of the different prepared samples is measured (as per ASTM-D-2510) using MCT setup, Anton Paar make, Austria (this facility is available at Indian Institute of Technology Kharagpur). It is equipped with a diamond Rockwell indenter having an apex angle 120° and a spherical tip of radius of 100 μm. The modulus of elasticity and Poisson's ratio of this indenter are 1140 GPa and 0.07 respectively. The instrument is having an electromagnetic load actuator equipped with a LVDT depth sensor. It is having a testing load range of 500 (mN) to 200 (N) with a resolution of 3 (mN), loading rate of 0.4 to 300 (N/m), data acquisition rate of 192 (kHz) and scratch speed ranges from 0.4 to 600 (mm/Min).

Surface topography

The surface roughness of the pin samples (before the pre-treatment process) and the counter-disc surface (before the wear test) is measured using a surface roughness tester (Taylor Hobson, Surtronic S-100) as depicted in Fig. 3.4. The measurements are done with a measuring tip having a rounding radius of 2 μm. The required surface roughness is achieved by polishing the substrate surface with different grades of silicon carbide papers.

Fig. 3.4 Surface Roughness Tester Surtronic S-100 (Taylor Hobson)

3.2 Development and application of the composite MoS_2-TiO_2 coating

To deposit MoS_2-TiO_2 coating, the required TiO_2 nano-powder is synthesized in-house using a chemical approach. The synthesis procedure is explained as follows.

3.2.1 Synthesis of TiO_2 powder

The TiO_2 exists in various phases like anatase, brookite and rutile. Among these, rutile phase is chemically stable, non-toxic, non-soluble in water and has better thermal stability. The rutile phase of TiO_2 has a melting point of 1850 ºC. It possesses high strength and excellent wear resistance. Because of these merits, the rutile phase of TiO_2 is selected as a reinforcement material to develop a composite coating material. To study the influence of TiO_2 crystallite size on the tribological performance of the composite MoS_2-TiO_2 coating, TiO_2 with different crystallite sizes have been synthesized.

The TiO_2 powder is synthesized as per the procedure reported by Hernandez et al. (2012) using an ultrasound approach which is described using a flow chart as shown in Fig. 3.5 (b). To initialize the reaction, 10 mL of titanium tetra isopropoxide (TTIP) is mixed with 2 mL of acetone and 2 mL of methanol. This TTIP solution is kept in an ultrasound reactor. The ultrasound reactor is set up for 30 min. A 50 mL NaOH solution is add-

ed drop-wise to the TTIP solution. The sonication is continued even after the complete addition of NaOH to ensure 100 % conversion of TTIP. The final product is formed in the form of white precipitate. It is then filtered, cured and calcinated at 500-700 ºC for 5 h in an electric furnace.

To compare the effect of ultrasound synthesis with a conventional approach, the same process is repeated using a magnetic stirrer. The performance of both approaches is compared in terms of obtained crystallite size of TiO_2 powder (refer Fig. 3.5 (a)).

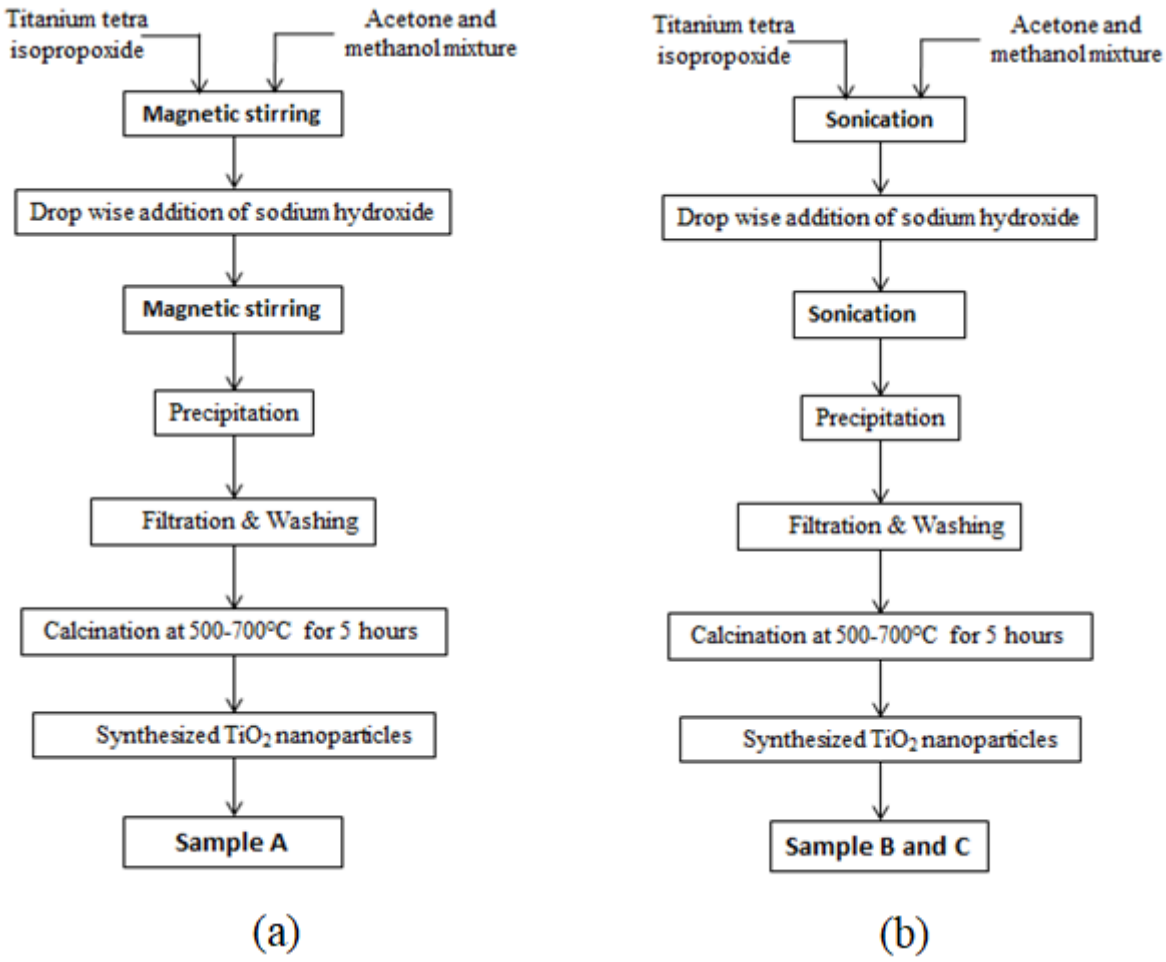

Fig. 3.5 Synthesis procedure for TiO_2 using (a) conventional magnetic stirrer, (b) ultrasound reactor

The XRD spectra of the TiO_2 powder are depicted in Fig. 3.6. According to the spectrogram of the crystal structure, the well-defined peaks of TiO_2 in the crystal structure of TiO_2 have been clearly observed. This is in compliance with the reports of the norms of the joint committee on powder diffraction standard (JCPDS card number 21-1276).

The peaks at 2θ value 25.3°, 37.8°, 47.9°, and 54.6° are assigned to (1 1 0), (1 0 1), (2 1 0) (2 1 1) planes of the TiO_2 phase. Among all the initial peaks generated at 25-30° are the prominent peaks with high intensity, which are used to evaluate the crystallite size. The average crystallite sizes of synthesized TiO_2 powders are shown in table 3.3. In this, sample A is prepared using conventional magnetic stirrer while sample B and C using an ultrasound reactor.

Table 3.3 Crystalline sizes of different TiO_2 samples prepared

TiO_2 sample	2θ	FWHM in radian	Average crystallite size (nm)
Sample A	25.4677	0.0945	90.06
Sample B	25.2763	0.1920	44.13
Sample C	25.1913	0.3072	27.69

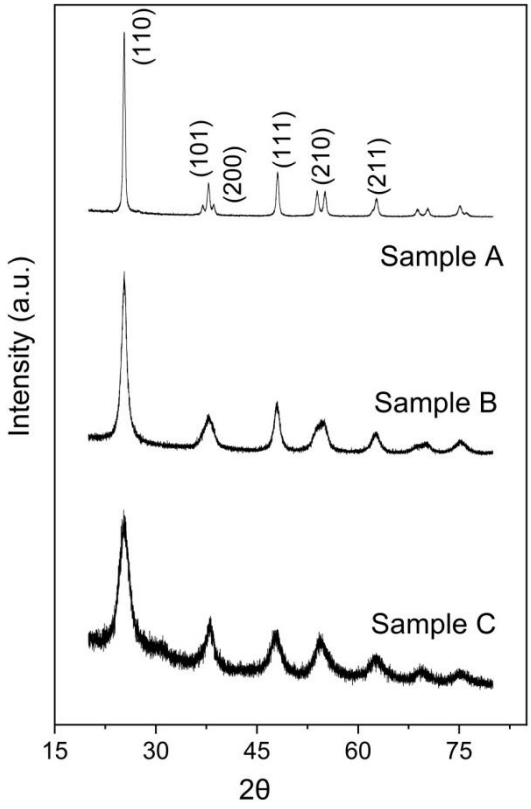

Fig. 3.6 XRD pattern for synthesized TiO_2 samples

3.2.2 Pre-treatment process

The substrate surface is polished before phosphating (pre-treatment process) with different series of polish paper grades such as 220, 600, 800 grit size. After polishing, the surface roughness is measured at various locations using (Surtronic S-100 Taylor Hobson series) surface roughness tester. The average surface roughness value (Ra) is observed to be 0.4

μm. The different steps involved in the phosphating process are degreasing, pickling, rinsing, phosphating, rinsing and drying (Sankara 2005, Quitmeyer 2006, Fouladi and Amadeh 2013, Pokorny et al., 2016). Degreasing is the first step in the phosphating process. The samples are dipped into 10 wt. % NaOH solution at 60 ºC for 5 min., then cleaned with ultra-sonication using acetone bath. Rinsing is the second step in which these samples are rinsed using acetone and distilled water to remove any leftover grease or oil from the surface. In the third step, these samples are pickled using 10 wt. % H_2SO_4 solutions at 60 ºC for 3 to 5 min to furnish an appropriate base for nucleation of the phosphate layers. Further, these samples are rinsed using deionized water. Then these samples became ready for phosphating in which the samples are dipped into 400 mL volume of magnesium phosphate bath as per the composition, described in table 3.4. These samples are immersed into a phosphating bath at 80 ºC and kept for 30 minutes. After phosphating, the samples are properly rinsed with distilled water to clean and remove any leftover acid residue, soluble salts and foreign particles. Finally, these samples are dried by heating up to 60 to 70 ºC for 30 minutes.

Table 3.4 Detailed chemical composition of phosphating bath

Bath composition	Concentration
H_3PO_4 (85 %)	23 mL\L
$MgCO_3$	8.5 g\L
$NaNO_2$	0.4 g\L
NaOH	6.8 g\L

After carrying out the phosphating process the surface roughness is measured at different locations using a surface roughness tester. The average surface roughness value (Ra) is observed to be 1.9 μm. The substrate surface before phosphating and after phosphating is observed using scanning electron microscopy (SEM) and it is shown in Fig. 3.7. In Fig. 3.7 (b) micro-pores of phosphates have been observed, which acts as a reservoir for solid lubricant as well as enhances the bond strength.

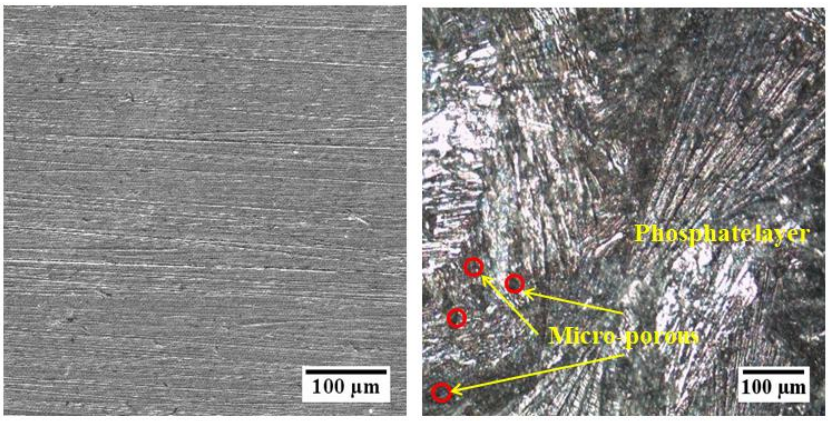

Fig. 3.7 Substrate surface (a) before phosphating and (b) after phosphating

3.2.3 Deposition of pure MoS_2 and composite (MoS_2-TiO_2) coating on substrate surface

Generally, a binder is used to hold together the materials used for coating in the form of powders onto the substrate surface. In the present study, sodium silicate (Na_2SiO_3) is used as a binder to hold together MoS_2 and TiO_2 powders onto the pre-treated AISI 52100 steel substrate surface. While preparing a mixture of coating powders and binder, it is noticed that less amount of Na_2SiO_3 fails to absorb the powders, whereas excess amount causes poor adhesion. After many trials, optimum proportions of wt. % 1 : 2.2 of MoS_2 and Na_2SiO_3 for pure MoS_2 coating have been observed. In the case of composite coating the wt. % of TiO_2 varied from 5 to 25 % into the MoS_2 matrix and accordingly the proportion of Na_2SiO_3 is varied. This prepared coating is deposited onto the pre-treated substrate surface by bonding technique as explained in Shankara et al. (2008). These coated samples are dried and cured at 160 ˚C for two hours in an electric furnace.

The steps in the preparation of the samples are shown in Fig. 3.8.

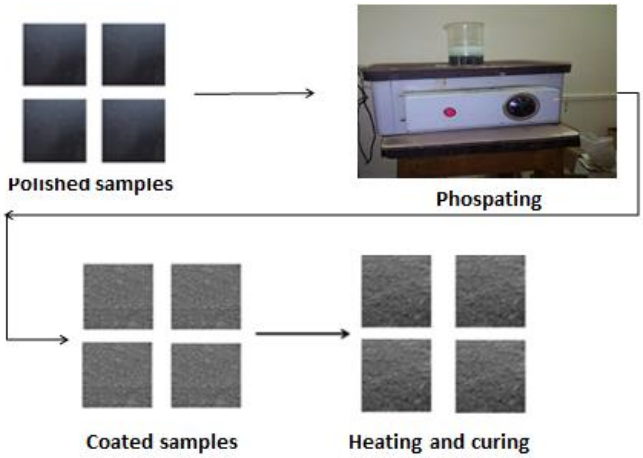

Fig. 3.8 Steps in sample preparation for investigating hardness and scratch test

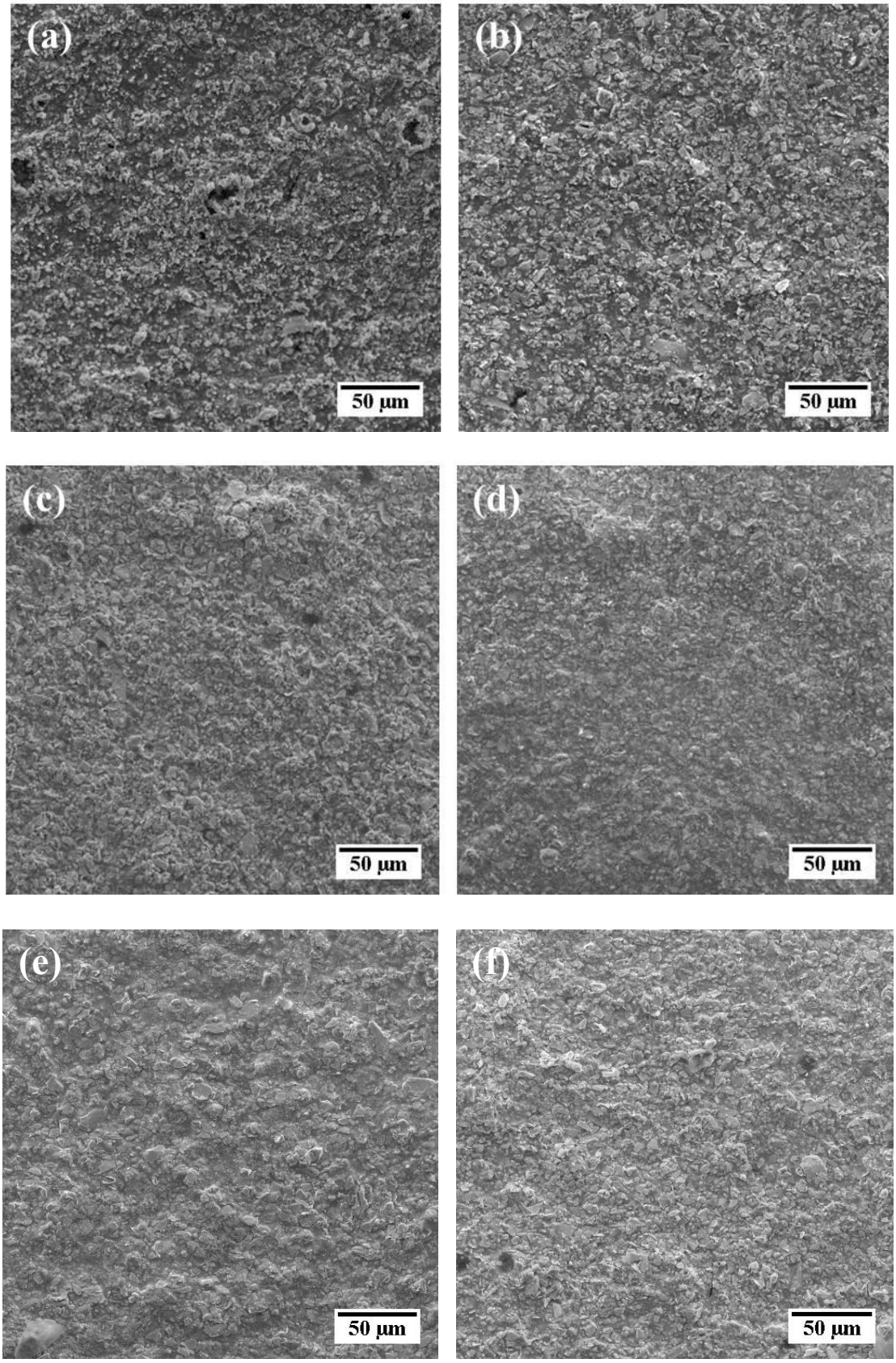

Fig.3.9 (a) Pure MoS_2 coating, Composite MoS_2-TiO_2 coating (b) 5 wt. % TiO_2, (c) 10 wt. % TiO_2, (d) 15 wt. % TiO_2, (e) 20 wt. % TiO_2, (f) 25 wt. % TiO_2

The morphology of pure MoS_2 and composite MoS_2-TiO_2 coating with different wt. % addition of TiO_2 particles is characterized by SEM, as depicted in Fig. 3.9. In pure MoS_2 coating some voids have been observed (refer Fig. 3.9(a)). In case of composite MoS_2-TiO_2 coating, with increase in wt. % addition of TiO_2 the microstructure becomes dense, as greater number of TiO_2 particles entrapped into MoS_2 base matrix (refer Fig. 3.9 (b to f)). After deposition of pure MoS_2 and composite MoS_2-TiO_2 coating, the roughness of the surface is assessed at three different locations using a surface roughness tester. The measured average surface roughness (Ra) is reported in table 3.5.

Table 3.5 Surface roughness values for pure MoS_2 and composite MoS_2-TiO_2 coating material films

Surface roughness measured at three different locations	Pure MoS_2 coating	Composite MoS_2-TiO_2 coating with different wt. % of TiO_2				
		5 %	10 %	15 %	20 %	25 %
1	1	1.6	1.4	1.6	1.2	1.7
2	0.9	1.1	0.9	1.3	1.4	1.5
3	1.3	1.2	1	1.1	1	1.2
Average surface roughness Ra (μm)	1.07	1.3	1.1	1.33	1.2	1.47

3.3. Experimental Investigation

The developed coating material has been tested for mechanical properties such as hardness of the coating film and adhesion strength between substrate and coating. The experimental test details are explained below.

3.3.1 Microhardness test

The coating microhardness is measured using a Vickers micro-hardness tester. The hardness of the prepared specimens is measured in this test with the application of a 4 N load. After hardness measurement, the indentations impressions are captured using an optical microscope to analyse the effect of the addition of TiO_2 onto the hardness of composite MoS_2-TiO_2 coated samples. The indentation impressions after the microhardness test are shown in Fig. 3.10. It is noticed that with increasing wt. % of TiO_2 the coating film hardness increases. With the increase in the amount of TiO_2, the greater number of particles is entrapped into the MoS_2 matrix which in turn enhances the hardness of the coating film (Shang et al., 2018). Eventually, this results in improvement in the wear resistance. However beyond 15 wt. % addition of TiO_2 the coating film becomes brittle. The indentation

impressions represented in Fig. 3.10 (e, f) depict that the coating film becomes brittle and ruptures which results in failure of the coating.

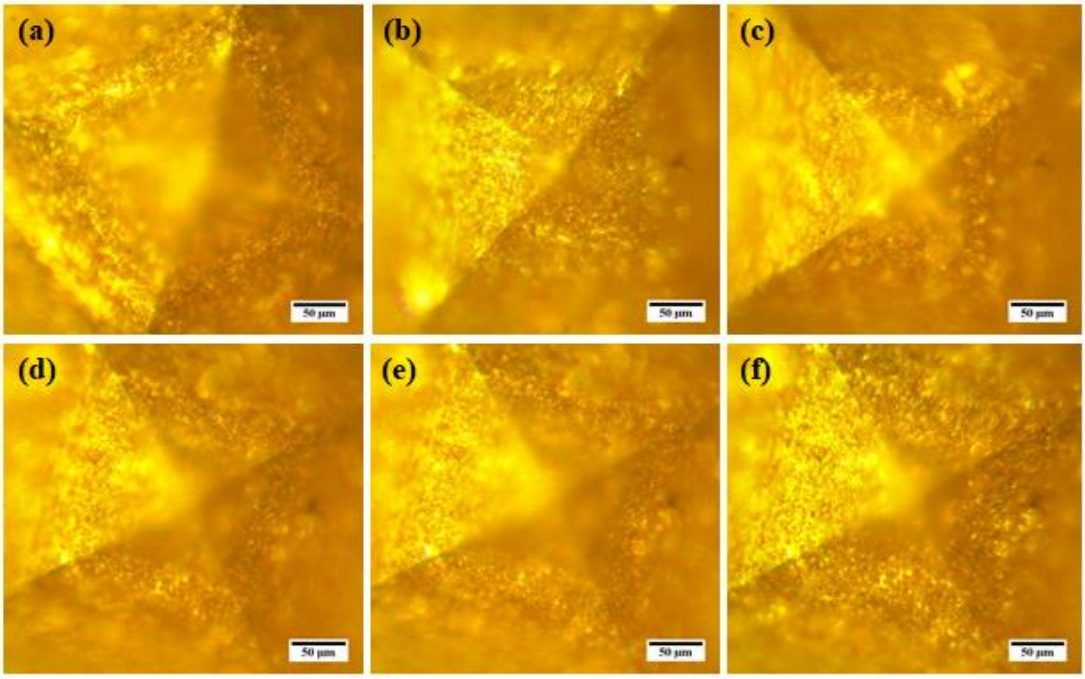

Fig. 3.10 Indentation impressions after micro-hardness test (a) pure MoS_2, Composite MoS_2-TiO_2 coating (b) 5%, (c) 10%, (d) 15 %, (e) 20% and (f) 25% wt. of TiO_2 into MoS_2 base matrix

The hardness values of pure MoS_2 and composite MoS_2-TiO_2 coating with wt. % variation of TiO_2 are mentioned in table 3.6. To achieve the reliable data, the indentations of each coating specimen are repeated thrice and the average value is considered.

Table 3.6 Micro-hardness values of coated samples

Vickers Micro-hardness in HV					
Pure MoS_2	5%	10%	15%	20%	25%
13.4 ± 4.2	19.3 ± 5.4	26.8 ± 6.9	30.5 ± 5.7	35.3 ± 3.7	47.2 ± 4.6

3.3.2 Scratch test

A progressive scratch test is a faster one than other tests since in a single stroke it covers the entire load range. Hence mostly this test has been used for rapid analysis of thin films and coatings (Bull and Berasetegui 2006). Therefore in the present work progressive scratch test is used to analyse the scratch strength between substrate and coating. The experimental and schematic setup for a progressive load scratch test is shown in Fig. 3.11. It consists of a stylus which is moved across the coated sample surface with a linearly incre-

mental load up to the fracture point. During the test, a normal load (Fz) and a lateral load (Fx) are recorded with respect to the scratch distance and test time. Apart from these parameters, the acoustic emission (AE) values have also been recorded. The AE values are critical for the accurate determination of sub-surface failure and interface failure. The critical load which causes to generate micro-fracture is identified by an increase in acoustic emission. The primary factors which are influenced the critical load includes the adhesion strength between coating and substrate, the loading rate (N.s), the radius of the indenter and the mechanical properties of coating as well as substrate. Similarly the secondary factors which are influenced the critical load includes internal stress within the coating, defects at the interface of coating and substrate, coating thickness, COF between indenter and coating. SEM analysis is performed to determine the mode of coating failure after the scratch test.

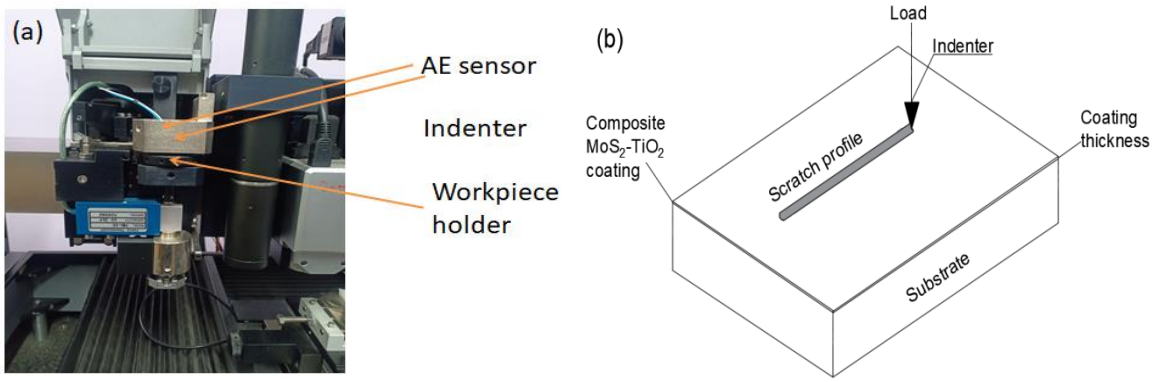

Fig. 3.11 (a) Experimental and (b) Schematic set up of a scratch test

In the progressive load scratch test, the pure MoS_2 and composite MoS_2-TiO_2 coated specimens are scratched for a single scratch line by setting a 5 mm scratch distance. Initially, the tip of the indenter is brought into contact with the coated samples at a comparatively low normal load of 500 mN to maintain the tip steady on the coated sample surface. Once the contact took place, the sample is scratched with a constant normal load which is amplified gradually from 500 mN to 80 N to investigate the critical force causes for failure of the coating. As reported previously by Arslan et al. (2008), the critical force is termed as the applied force, where the coating fails and the substrate surface gets exposed. To get reliable data, the scratch test for the same progressive loading, is repeated for three times.
After performing the scratch test at different loads for pure MoS_2 and composite MoS_2-TiO_2 coating (with different wt. % of TiO_2 from 5 % to 25 %), the SEM analysis is performed and the results are represented in Fig. 3.12. Overall with the increase in normal

load from 20 N to 80 N, the scratch depth is found to be increased and widened. In the case of pure MoS_2 coating, with an increase in normal load, the coating delaminates from the substrate surface due to poor bond strength as shown in Fig. 3.12 (c, d)) (Tran et al., 2018). As the TiO_2 is added as a reinforcement material into the MoS_2 base matrix, improvement in the scratch resistance of composite MoS_2-TiO_2 coating has been observed, as depicted in Fig. 3.12 (e to p)). In the case of composite MoS_2-TiO_2 coating, with 15 wt. % TiO_2, the shorter width and depth of scratch is observed even at higher loading condition (refer Fig. 3.12 (m to p)). However, with an increase in the amount of reinforcement material beyond 15 wt. % TiO_2, leads to improper mixing between additive and base matrix which results in poor bonding and eventually leads to lower scratch resistance (Shankara et al., 2008). In the case of composite MoS_2-TiO_2 coating, with 25 wt. % TiO_2, the coating founds to be highly brittle, as the major cracks have been developed (refer Fig 3.12 (q to x)).

The elemental composition analysis of the coated surface and scratched area at 20N and 80 N loads is performed using the energy dispersive analysis of the X-ray (EDAX) technique. As SEM coupled EDAX microprobe analysis is semi-quantitative, several spots on the considered area have been analyzed and eventually an average value is considered. Table 3.7 represents EDAX spectra for pure MoS_2 and composite MoS_2-TiO_2 coated samples. For the pure MoS_2 coating at 20N load different elements like C, O, Na, Si, P, S and Mo signals have been observed with Mo and S as the principal elements. Whereas at higher load 80 N, due to poor bond strength of pure MoS_2 coating, coating worn out from the substrate surface and Fe signal is observed along with other reported elements. For the composite MoS_2-TiO_2 coating, the Ti signals have been clearly observed with the other reported elements. As the TiO_2 was added as a reinforcement material into the MoS_2 base matrix, improvement in the wear resistance of composite MoS_2-TiO_2 coating has been observed. From the EDAX analysis it has been observed upto 15 wt. % addition of TiO_2, the scratch resistance of coating improves significantly as even at higher loads the coating remains present on the substrate surface. However, beyond 15 wt. % addition of TiO_2, the coating becomes brittle. As the coating becomes brittle, at higher load 80 N, the indenter causes to delaminate the coating from both edges of the scratch channel and touches the substrate surface. Due to which, in case of composite MoS_2-TiO_2 coating with 20 wt. % and 25 wt. % addition of TiO_2, due to contact between indenter and substrate, Fe signal is observed along with other reported elements.

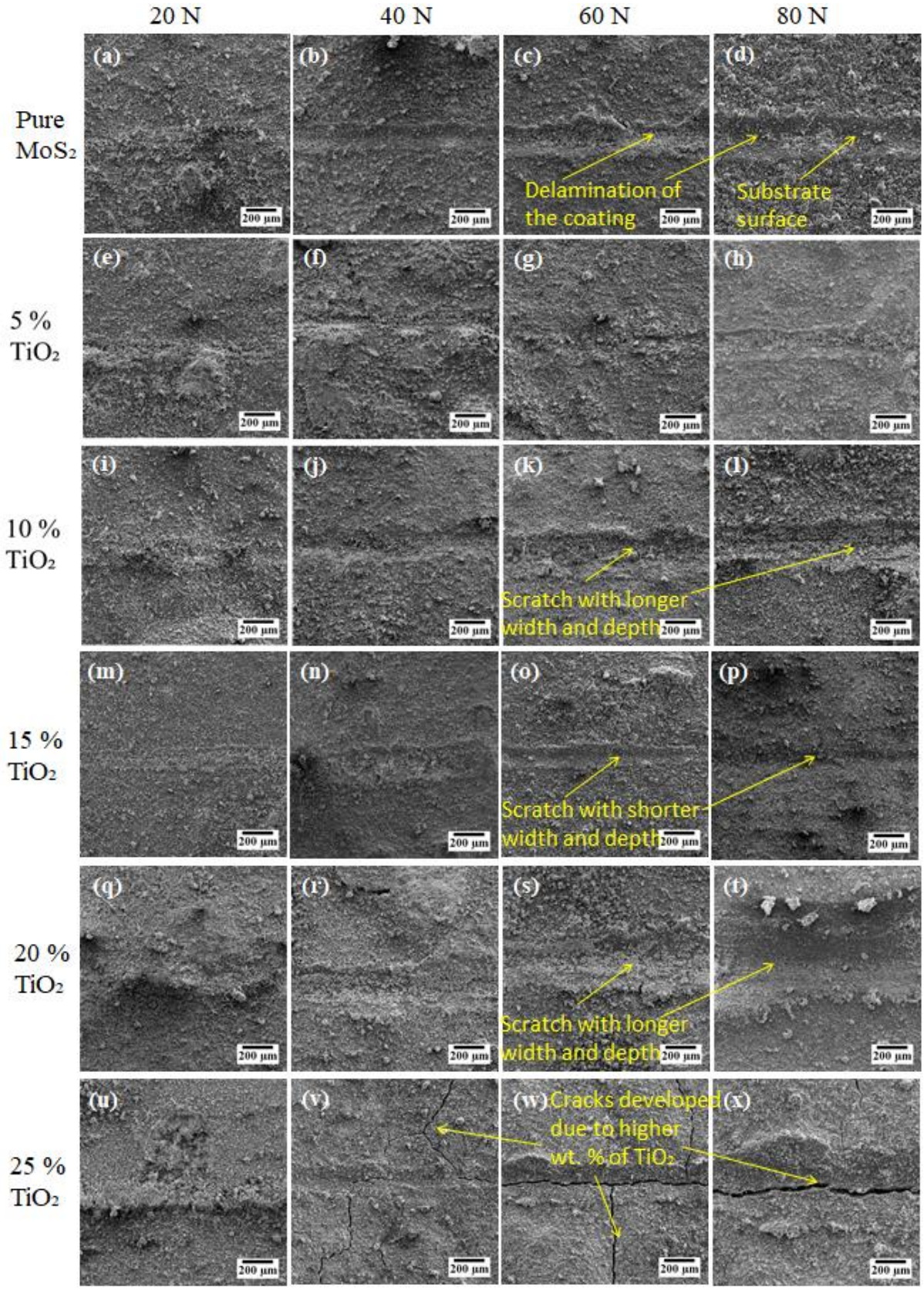

Fig. 3.12 Scratch test results pure MoS_2 (a to d), Composite MoS_2-TiO_2 coating with TiO_2 wt. % addition 5 % (e to h), 10 % (i to l), 15 % (m to p), 20 % (q to t) and 25 % (u to x) at different normal loads 20 N, 40 N, 60 N and 80 N

Table 3.7 EDAX mapping analysis of (a) pure MoS_2 and composite MoS_2-TiO_2 coating with TiO_2 wt. (b) 5%, (c) 10%, (d) 15%, (e) 20% and (f) 25%

(a) pure MoS_2			(b) 5 wt. % of TiO_2			(c) 10 wt. % of TiO_2		
	20 N	80 N		20 N	80 N		20 N	80 N
Element	Ato. %	Ato. %	Element	Ato. %	Ato. %	Element	Ato. %	Ato. %
C	16.60	18.63	C	16.63	15.57	C	20.42	17.41
O	61.86	60.36	O	57.12	59.28	O	60.09	61.25
Na	13.59	13.6	Na	14.37	12.03	Na	13.97	15.09
Si	2.75	1.87	Si	2.82	2.46	Si	1.58	1.29
P	0.09	0.05	P	0.07	0.06	P	0.06	0.09
S	2.87	3.24	S	6.46	5.75	S	1.95	2.26
Fe	---	0.37	Ti	0.15	0.21	Ti	0.11	0.16
Mo	2.24	1.88	Mo	2.38	4.64	Mo	1.82	2.44

(d) 15 wt. % of TiO_2			(e) 25 wt. % of TiO_2			(f) 25 wt. % of TiO_2		
	20 N	80 N		20 N	80 N		20 N	80 N
Element	Ato. %	Ato. %	Element	Ato. %	Ato. %	Element	Ato. %	Ato. %
C	17.26	0	C	16.43	16.56	C	17.84	15.47
O	61.33	64.63	O	61.28	59.36	O	61.88	54.60
Na	14.61	6.93	Na	15.40	10.59	Na	15.73	7.21
Si	1.46	11.27	Si	1.38	4.18	Si	1.20	6.89
P	0.07	0.04	P	0.09	0.13	P	1.66	0.45
S	3.36	9.31	S	3.58	5.49	S	0.10	10.00
Ti	0.12	2.42	Ti	0.19	0.63	Ti	0.08	---
Mo	1.79	5.40	Fe	---	0.22	Fe	---	0.30
			Mo	1.65	2.85	Mo	1.51	5.08

The progressive scratch test performed for pure MoS_2 coating and composite MoS_2-TiO_2 coating and the results are shown in Fig. 3.13. It has been observed that due to poor wear resistance, the pure MoS_2 coating detached from the substrate surface at lower normal loads exhibiting lower values of critical loads L_{C1} and L_{C2}, compared to all composite MoS_2-TiO_2 coated samples. In case of composite MoS_2-TiO_2 coated samples, with increase in TiO_2 wt. % the samples sustain even at higher critical loads due to improved

scratch resistance. However, beyond 15 wt. % addition of TiO_2, due to increase in brittleness of the coating, decrease in critical load L_{C2} has been observed as shown in Fig. 3.13.

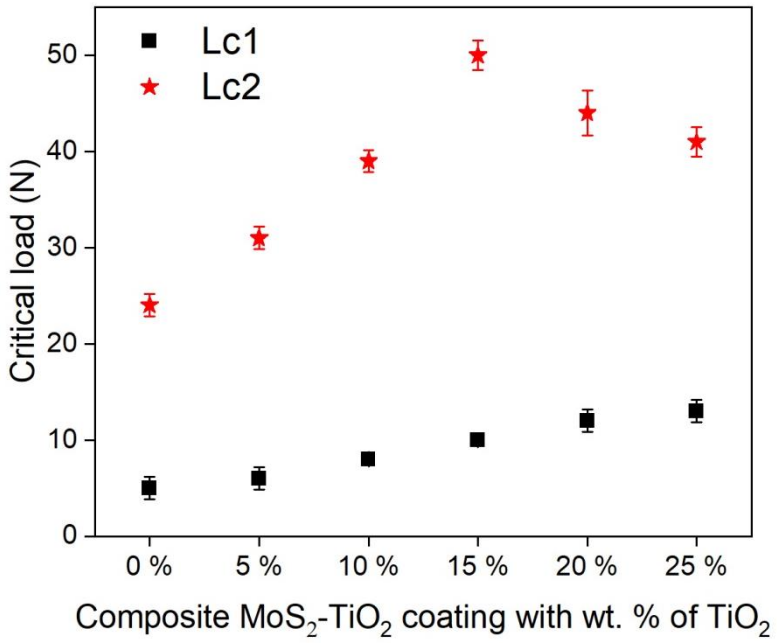

Fig. 3.13 Critical loads L_{C1} and L_{C2} obtained for the pure MoS_2 coating and composite MoS_2-TiO_2 coating with TiO_2 wt. 5 % to 25 %

As the composite MoS_2-TiO_2 coating with 15 wt. % of TiO_2 exhibits higher scratch resistance, its corresponding normal load (F_n) and lateral load (F_t) along with acoustic emission (AE) are outlined in Fig. 3.14. The critical load which leads to coating failure has been observed with the rise of acoustic emission. As depicted in Fig. 3.14, the change in AE corresponding to a load of 10 N is noted as the first L_{C1}. The pre-critical load causes flaking of coating film at the scratch channel edge. The indenter pressed against the coating film in contact with substrate further causes the delamination of the coating from both the edges of scratch channel. The critical load which leads to coating failure has been observed with a sudden rise in acoustic emission. As depicted in Fig. 3.14, the change in AE corresponding to a load of 50 N was noted as the first L_{C2}. A similar kind of failure mode was pointed out by Mroz et al., (2016).

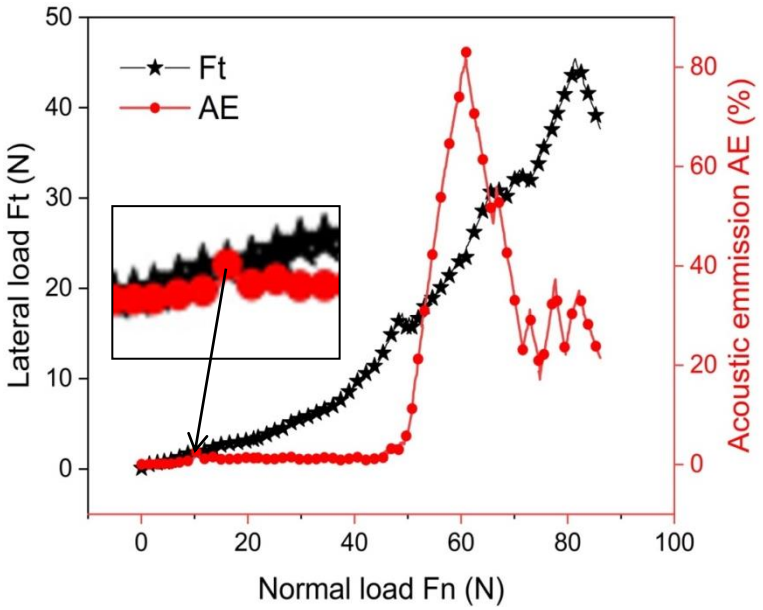

Fig. 3.14 Lateral load and AE signals of the composite MoS_2-TiO_2 coating (with 15% wt. TiO_2) during scratch testing under increasing normal load

The test is performed for the scratch length of 5 mm and the scratch speed employed during each test is twice the scratch length i.e. 10 mm/min. The variation in COF along the scratch length for the composite MoS_2-TiO_2 coating with 15% wt. TiO_2 at 80 N load is depicted in Fig. 3.15.

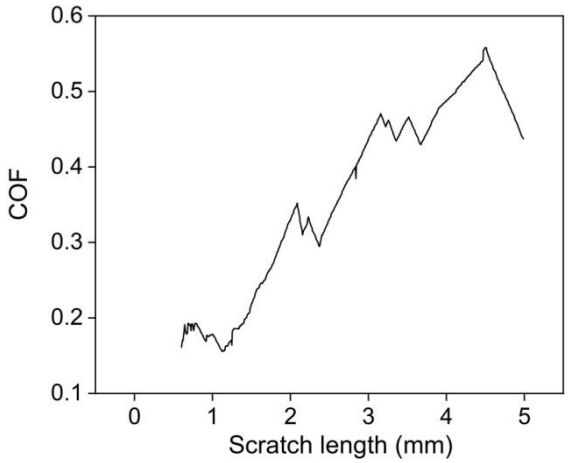

Fig. 3.15 Variation in COF along the scratch length for the composite MoS_2-TiO_2 coating with 15% wt. TiO_2 at 80 N load

The average COF is estimated by taking the values of COF obtained during the entire scratch test. To get reliable data, the test is repeated thrice and the average value is considered. The average COF is obtained after completion of the scratch test for pure

MoS_2 and composite MoS_2-TiO_2 coating (with different wt. % TiO_2) at different normal loads 20 N, 40 N, 60 N and 80 N and these are depicted in Fig. 3.16. The test results reveal that with an increase in applied normal load, the COF tends to increase. The wt. % of TiO_2 also shows a significant effect on the COF. The pure MoS_2 coating (designated with 0 wt. % of TiO_2) exhibits a higher value of COF in comparison with composite MoS_2-TiO_2 coated samples. This is due to the poor adhesion between coating and substrate (refer Fig. 3.12 (d)). This is in agreement with the previous literature (Shankara et al., 2008 and Shang et al., 2018). The addition of TiO_2 into the MoS_2 base matrix leads to enhance the adhesion between coating and substrate. Due to which a reduction in COF values has been observed. The COF value is reduced up to 15 wt. % addition of TiO_2 beyond which a reverse trend is observed due to improper mixing of dopant and base matrix material (Ding et al., 2010). Eventually, this resulted in poor adhesion which causes a rise in COF values as depicted in Fig. 3.16.

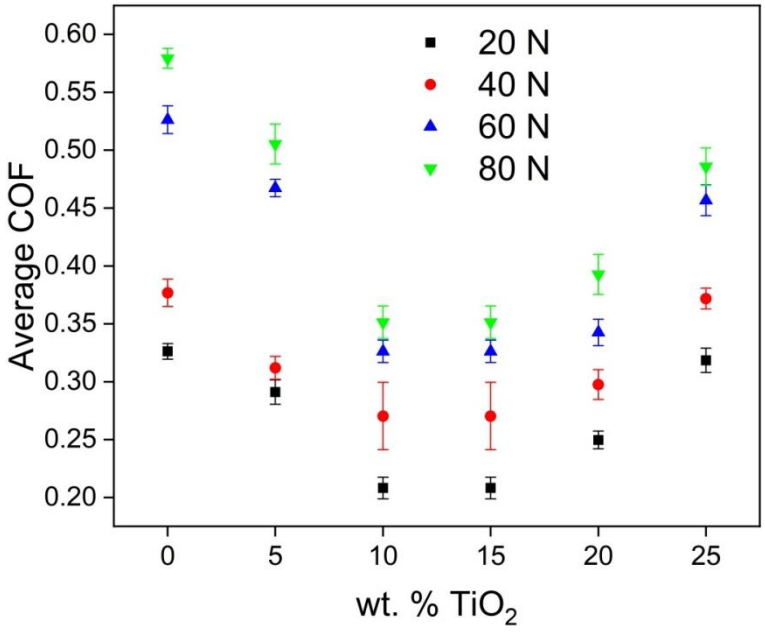

Fig. 3.16 Average COF for pure MoS_2 and composite MoS_2-TiO_2 coating (with different wt. % TiO_2) at different normal loads 20 N, 40 N, 60 N and 80 N

3.4 Summary

The composite MoS_2-TiO_2 coating has been successfully developed. The important mechanical properties like hardness and scratch strength of the developed composite MoS_2-TiO_2 coating are evaluated. It is observed that the coating has a dense microstructure and the Vickers microhardness test results shows that doping of TiO_2 increases the film hard-

ness. Among pure MoS_2 and composite MoS_2-TiO_2 coating, coating with 15 wt. % TiO_2 exhibits superior hardness and bond strength. The critical load causes to the failure of a coating film, which is evaluated using a variation of acoustic emission is observed to be 10 N as the first L_{C1} and 50 N as first L_{C2}. The COF is observed to be higher for pure MoS_2 coating at all applied normal loads. The addition of reinforcement material TiO_2 into the MoS_2 base matrix help to improve the scratch strength in turns resulted in a reduction of COF values. The composite MoS_2-TiO_2 coating with 15 wt. % addition of TiO_2 represents the lowest values of COF at all applied normal loads.

The interacting surfaces are subjected to friction and wear, finally causes to failure of the tribological systems. To mitigate the frictional and wear losses, advancement in modern tribology has facilitated the use of solid lubricant based composite coatings in various tribological applications. But the performance of these composite coatings affected by various operating parameters like contact pressure, sliding speed, temperature and coating thickness. Therefore in Chapter 4 a detailed tribological investigation of developed composite MoS_2-TiO_2 coating is performed using pin-on-disc friction and wear test rig under different operating conditions.

Chapter 4

Tribological Investigation of Composite MoS_2-TiO_2 Coating Material

In the previous chapter, the fabrication process of pure MoS_2 and composite MoS_2-TiO_2 coating is described in detail. In the present chapter, a detailed tribological investigation of developed composite MoS_2-TiO_2 coated samples is carried out.

4.1 Sample preparation

The same substrate material reported in previous chapter AISI 52100 steel is taken as a substrate material for pin. The pin is having a flat end with 12mm diameter and 25mm length. The pin sample is coated as per the procedure described in the chapter 3 section 3.2. The steps involved in the preparation of the samples are shown in Fig. 4.1. After deposition of the composite MoS_2-TiO_2 coating, the surface roughness of the coated surface is measured using a surface roughness tester. The average surface roughness value (Ra) is observed to be 1.2 μm. Figure 4.2 (a) and (b) depicts the EDX spectrum and mapping analysis for different elements present in pure MoS_2 and composite MoS_2-TiO_2 coating (with 25 wt. % of TiO_2 sample C). The initial spectrum (a) represents various elements that constitute MoS_2 coatings such as Mo, S, Na, Si, O, while the other spectrum (b) shows traces of Ti along with above mentioned elements.

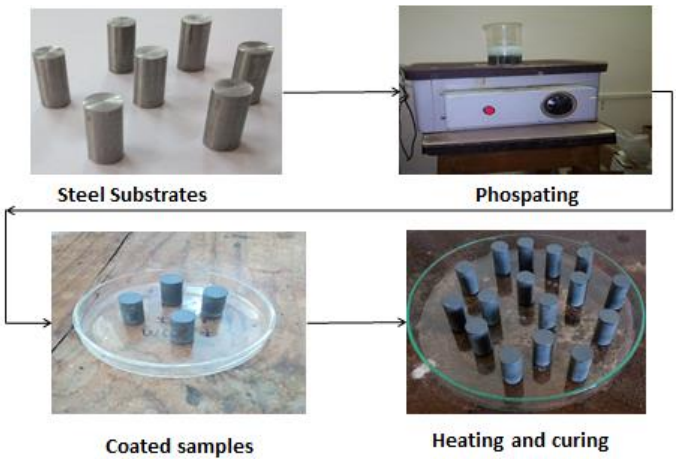

Fig. 4.1 Steps in sample preparation for tribological investigation

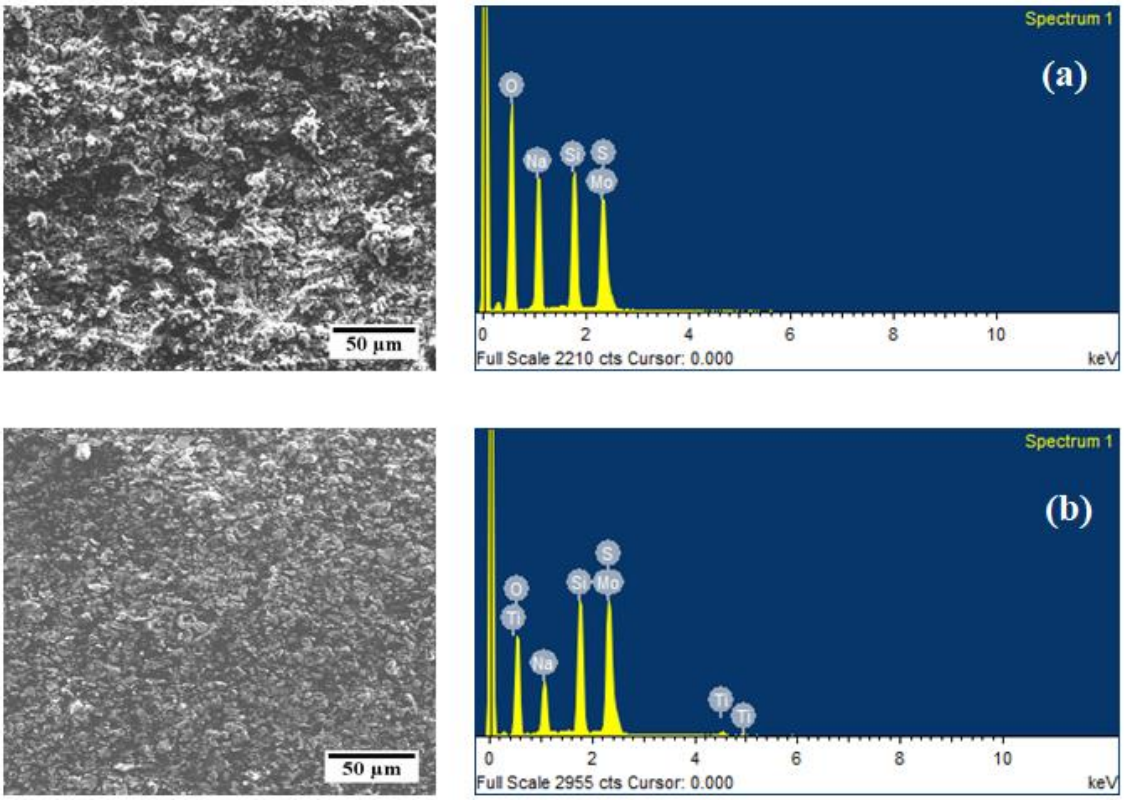

Fig. 4.2 EDX spectrum and mapping analysis for different elements constituted into (a) Pure MoS_2 coating and (b) composite MoS_2-TiO_2 coating (25 wt. % TiO_2 sample C)

4.2 Experimental investigation on the tribological performance of composite MoS_2-TiO_2 coating

In general, the solid lubricants are used in machining and tribological applications for controlling friction and wear between the interacting surfaces. The endurance life of the coating plays a significant role in improving the overall tribological performance. In machining application due to direct contact between tool-chip interface higher friction and temperature is attained. Eventually, this leads to higher tool wear and poor machining performance. These conditions are quite common in machining operations such as turning drilling, milling etc. In order to overcome these drawbacks one of the solutions is applying coating material on to the tool surface. Therefore, in the present work, a fundamental study on the developed composite MoS_2-TiO_2 coating is performed under laboratory conditions to achieve the beneficial effects in terms of friction and wear reduction, enhanced machining performance and tool life. The experiments are carried out using pin on disc friction and wear test rig provided by Magnum, India referring to (ASTM Standard G99-17, 2017). An experimental setup of the pin-on-disk friction and wear test rig is shown in Fig. 4.3.

The counterbody disk was of EN-31 steel material (165 mm diameter and thickness of 8 mm).

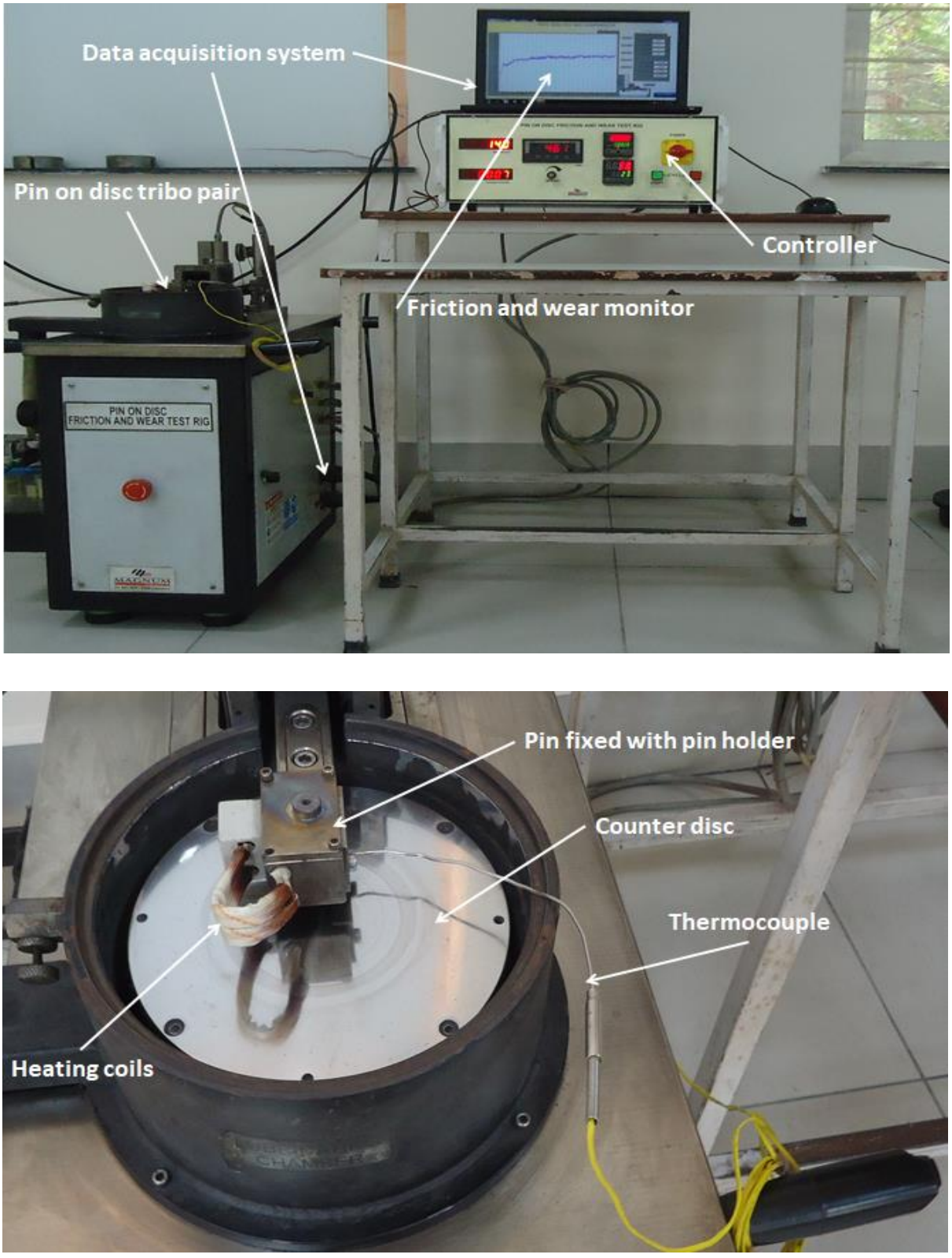

Fig. 4.3 Pin-on-disc tribological testing setup used in tribological tests

4.2.1 Experimental conditions

The experimental conditions are adopted from the machining application i.e. milling process; where severe friction and tool wear occurs at the tool-chip interface. In a typical milling process, the cutting speed is in a range of 200 rpm to 700 rpm (Reddy et al., 2006). In the present work, three values of cutting speeds have been considered i.e., 238 rpm, 477 rpm, and 714 rpm and its corresponding sliding velocities are obtained as 1 m/s, 2m/s and 3 m/s respectively, based on a track radius of 40 mm. The spindle torque observed to be in the range of 0.5 to 1 Nm in milling process (Reddy et al., 2010). In the present work, three values of frictional torques have been considered i.e., 0.24 Nm, 0.6 Nm, and 0.96 Nm and its corresponding contact pressures for the considered pin surface area are obtained as 176 kPa, 442 kPa and 707 kPa respectively. The detailed test parameters and the operating conditions are mentioned in table 4.1.

Table 4.1 Test parameters and ranges

Sr. No.	Parameters	Operating Conditions
1	Contact pressure	176, 442, 707 kPa
2	Sliding speed	1, 2, 3 m/sec
3	Track radius	40 mm
4	Sliding distance	3000 m
5	Temperature	RT, 100, 200, 300, 400 ºC

Before carrying out each test, the disc surface is cleaned with acetone and then dried thoroughly. After the wear test, the pin surface is analyzed using an optical microscope (Model QX-4RT) which is equipped with different magnification lens (4X, 10X, 20X, 40X, 100X) to analyse the surface morphology. The weight loss i.e. the difference between initial weight and the final weight is used to estimate the wear rate of the coating. In order to get reliable data, each experiment is repeated three times. The COF and wear rate are estimated using the following equations (Essa et al., 2017).

$$COF = \frac{F_f}{F_n} \tag{4.1}$$

$$WR = \frac{\Delta W}{\rho \times d_s} \tag{4.2}$$

Where, F_f is friction force in N, F_n is the normal load in N, ΔW is weight loss of the coated pin in g, ρ is density of the coated sample in g/mm and d_s is sliding distance in m, which was calculated from sliding velocity v (m/min) and sliding time t (min).

4.3 Tribological test results

The effect of various parameters such as crystallite size and different wt. % of TiO_2, coating thickness and operating conditions such as contact pressure, sliding speed and temperature on tribological properties of composite MoS_2-TiO_2 coating is explained as below.

4.3.1 Effect of crystallite size and different wt. % of TiO_2 on COF and wear rate

The effect of crystallite size and wt. % addition of TiO_2 on COF and wear rate at different contact pressures i.e. 176 kPa, 442 kPa, 707 kPa with sliding speeds 1m/s, 2m/s and 3m/s are represented in Figs. 4.4, 4.5 and 4.6. It is observed that the crystallite size of TiO_2 has a marginal effect on the magnitude of COF and wear rate. Whereas wt. % addition of TiO_2, contact pressure and sliding speed shows a significant effect on the magnitude of COF and wear rate. The composite MoS_2-TiO_2 coating with 15 wt. % of TiO_2 exhibits excellent tribological performance. Among different crystallite sizes, the lower crystallite size (i.e. 27.69 nm) of TiO_2 depicts the lowest COF and wear rate. The experimental results have shown that at low contact pressure and low speed (i.e. 176 kPa and 1 m/s) condition, composite MoS_2-TiO_2 coating (TiO_2 with lower crystallite size) demonstrates 24% and 36% reduction in COF and wear rate; whereas, at high contact pressure and high speed (707 kPa and 3 m/s) (TiO_2 with lower crystallite size) demonstrates 55% and 58% reduction in COF and wear rate compared with pure MoS_2 coating.

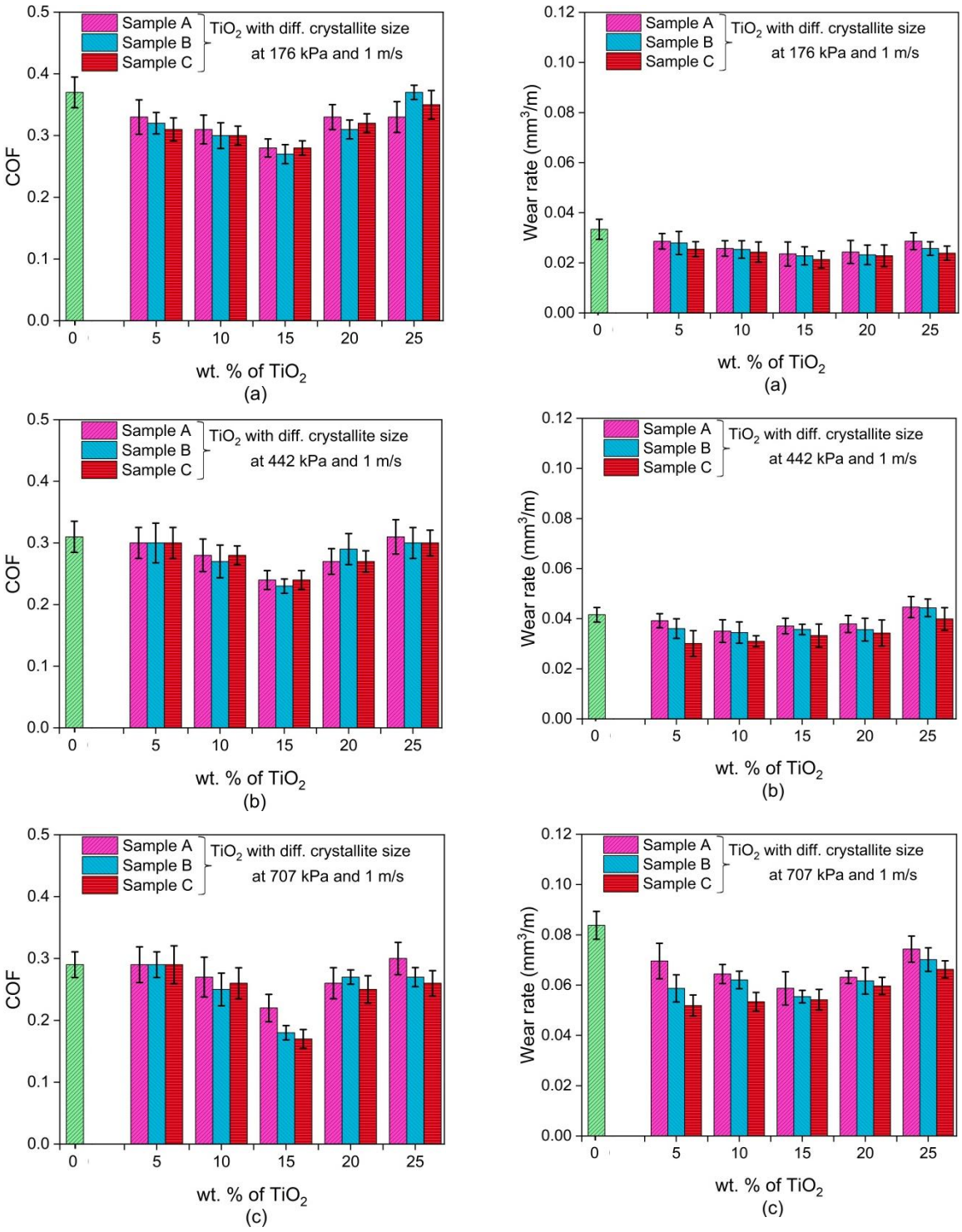

Fig.4.4 Effect of addition of different wt. % TiO_2 on COF and wear rate at (a) 176 kPa, (b) 442 kPa, (c) 707 kPa contact pressure with 1m/sec sliding speed

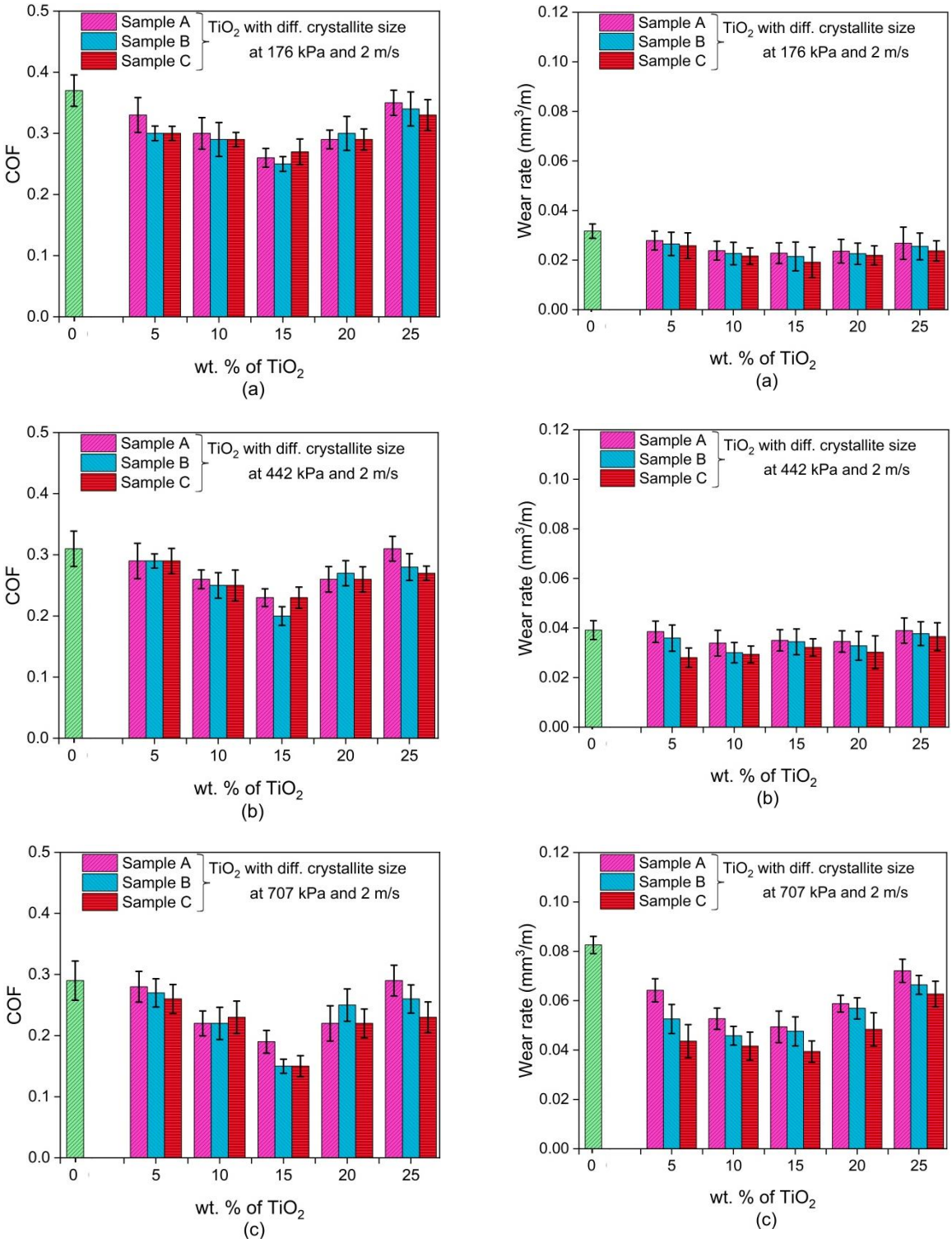

Fig.4.5 Effect of addition of different wt. % TiO_2 on COF and wear rate at (a) 176 kPa, (b) 442 kPa, (c) 707 kPa contact pressure with 2m/sec sliding speed

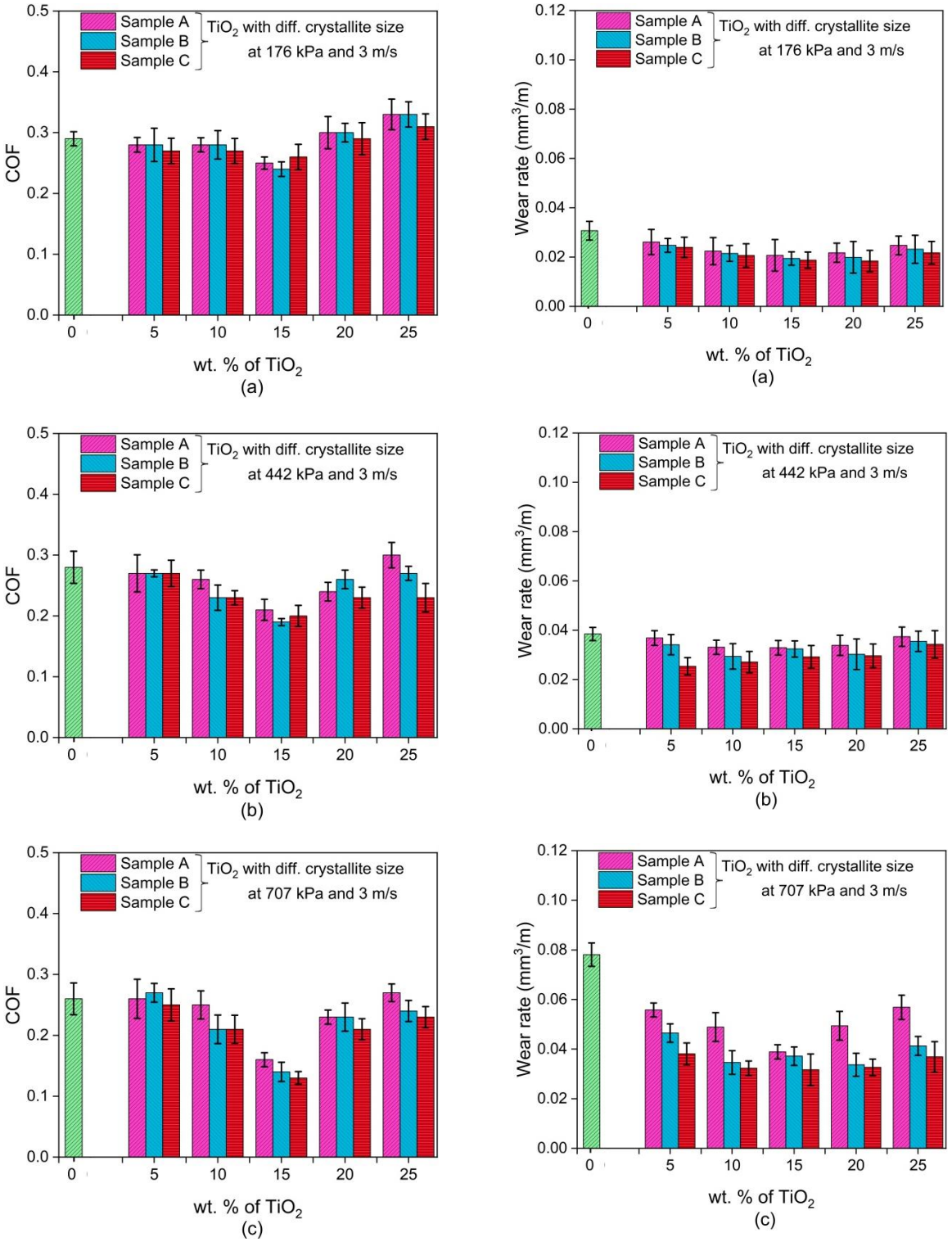

Fig.4.6 Effect of addition of different wt. % TiO_2 on COF and wear rate at (a) 176 kPa, (b) 442 kPa, (c) 707 kPa contact pressure with 3m/sec sliding speed

The pure MoS_2 coating (denoted by 0 wt. % of TiO_2) exhibits higher values of wear rate and COF as compared to other samples due to poor bonding between the substrate and coating, the coating worn out at a faster rate from the substrate as depicted in

Fig. 4.7 (a). This is in agreement with the previous literature (Shankara et al., 2008 and Shang et al., 2018), where they reported that pure MoS_2 coating possesses low wear resistance due to which it exhibits a higher wear rate. The addition of TiO_2 into the MoS_2 base matrix improves the tribological performance of coated sliding contact. However, the higher concentration of reinforcement material leads to improper mixing between the reinforcement and base matrix which results in poor bonding due to which a reverse trend in the tribological properties is observed (Ding et al., 2010).

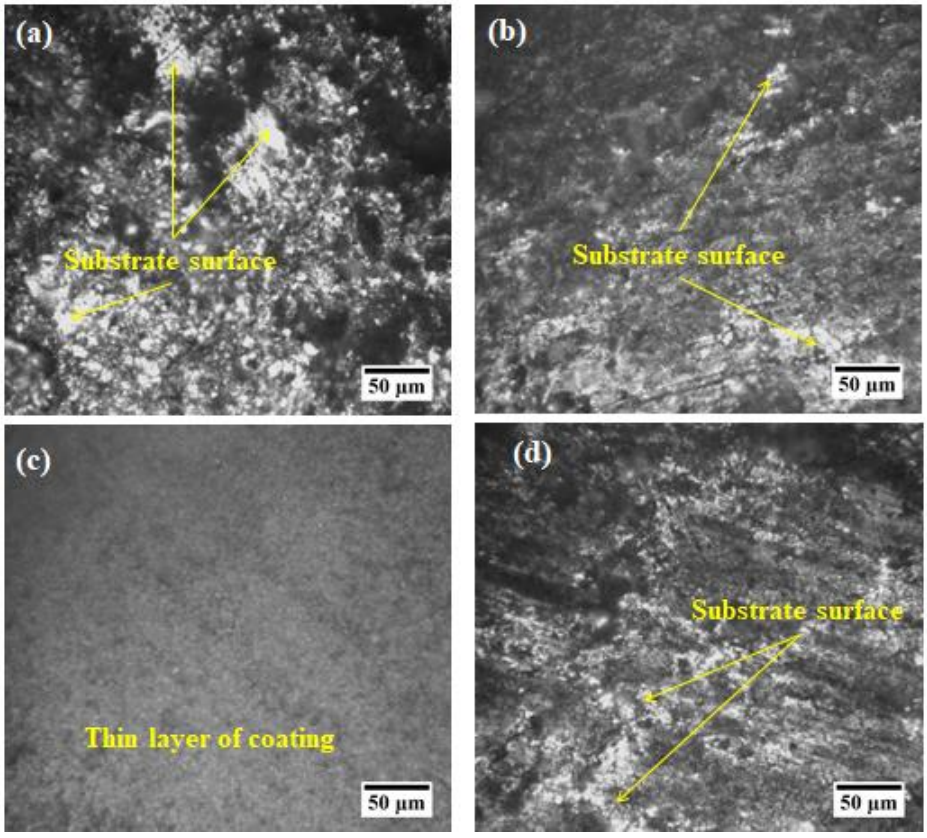

Fig.4.7 Pin surface after wear test (a) pure MoS_2, and composite MoS_2-TiO_2 coating (b) 5 wt. % TiO_2, (c) 15 wt. % TiO_2, (d) 25 wt. % TiO_2 (with TiO_2 sample C)

Figure 4.7 represents the pin surfaces after a tribological test performed on pure MoS_2 and composite coating of MoS_2 with different wt. % of TiO_2 (Sample C). In composite coating with the addition of TiO_2 up to 15 wt. %, the coating still remains present on the pin surfaces. The coating strongly adheres to the substrate surfaces as depicted in Fig. 4.7 (b) and (c) which resulted in lower values of COF. As the wt. % of TiO_2 increases beyond 15%, the excess TiO_2 particles are not well mixed into the MoS_2 matrix which may lead to poor bonding between them. Due to this, coating worn out at a faster rate from the substrate as shown in Fig. 4.7 (d) and leads to an increase in COF and wear rate. Further-

more, to understand the reason behind the increased wear rate, a microhardness test is performed. From the micro-hardness test, it is observed that with increase in wt. % of TiO_2 the hardness of the coating increases. As the wt. % of TiO_2 increases, more number of particles entrapped into MoS_2 matrix which results in improved hardness (Borgaonkar and Syed 2021, Bulbul and Efeoglu 2010). This helps to improve the wear resistance. However, as the wt. % of TiO_2 increased beyond 15%, it starts deteriorating the tribological performance, because beyond 15 wt. % of TiO_2 even though the hardness is increasing, at the same time the coating becomes brittle and ruptures which leads to deteriorating the performance of the coating. As from the obtained results, composite MoS_2-TiO_2 coating with 15 wt. % of TiO_2 and lower crystallite size 27.69 nm (i.e. sample C) depicts the lowest COF and wear rate. Hence for further analysis coating, this composition is taken into consideration to study the influence of temperature as well as coating thickness on the tribological characteristics.

4.3.2 Influence of temperature on COF and wear rate

The influence of temperature on the tribological performance of the composite MoS_2-TiO_2 coating is depicted in Fig. 4.8. From the experimental results it is observed that up to 100°C, the rate of change of COF is higher as compared to the rate of change of wear rate. Therefore, it is recommended to use the coating up to 100°C, beyond which the rate of change of wear rate is higher as compared to a rate of change of COF.

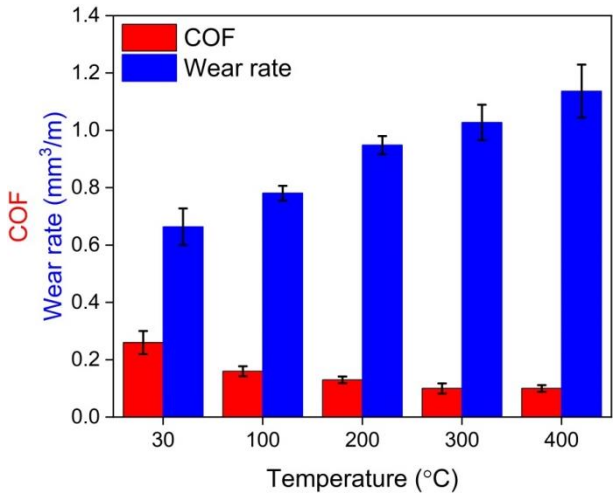

Fig.4.8 Influence of temperature on COF and wear rate at 707 kPa contact pressure and 3m/sec sliding speed

The microscopic analysis of the surfaces is shown in Fig. 4.9. It depicts that when solid lubricant operated at higher temperatures, more amount of coating layer transferred

from the pin surface to the counter disc surface. This worn-out material from the pin surface helps to form a tribolayer onto the track which results in lower COF values. On the other hand, since more amount of coating layer transferred to the counter disc surface results in an increase in wear rate which is depicted in Fig. 4.9. The wear rate increases with temperature could be due to oxidation, as at high temperature there is a chance of formation of harder MoO_3 film which favours for asperity contact and removal of the coating due to ploughing (Donnet and Erdemir (a) 2004, Chhowalla 2013, Borgaonkar and Syed (b) 2020). For better tribological performance, the developed composite MoS_2-TiO_2 coating can be used up to an operating temperature of 100 ºC, after which in comparison with COF the wear rate increases at a higher rate.

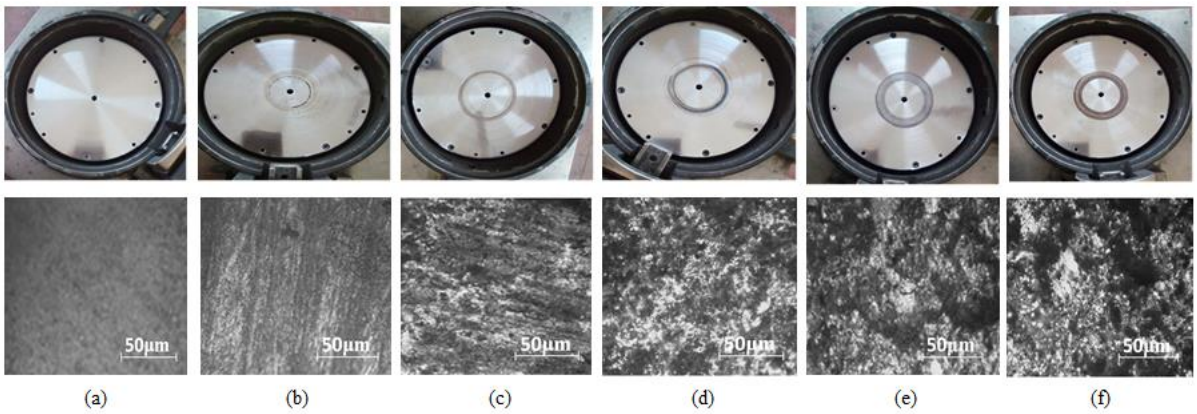

Fig.4.9 Disc and pin surface (a) before test and after wear test (b) RT, (c) 100, (d) 200, (e) 300 and (f) 400˚C at constant contact pressure 707kPa and 3m/sec sliding speed at different temperatures

4.3.3 Influence of coating thickness on COF and wear rate

The effect of coating film thickness on COF and wear rate is shown in Fig. 4.10. The rate of change of wear rate is significant with the coating film thickness as compared to the rate of change of COF. Therefore, a lower film thickness is recommended where COF is a significant parameter in comparison with the wear rate and vice-versa. These findings are in line with previous studies (Shankara et al., 2008, Lara et al., 2015, Borgaonkar and Syed (a) 2020). The EDX analysis is performed to understand the behavior of coating film thickness on the tribological properties.

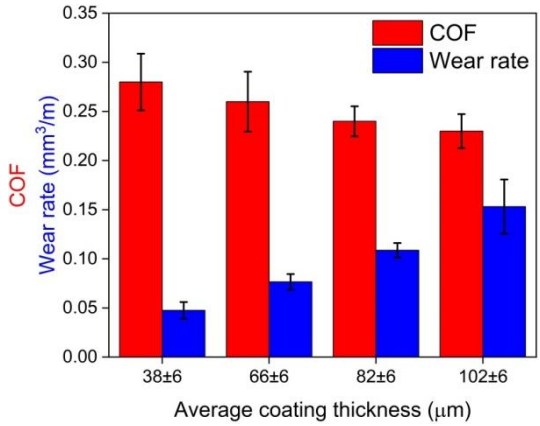

Fig.4.10 Influence of coating thickness on COF and wear rate at 707kPa contact pressure and 3m/sec sliding speed

Figure 4.11 shows the EDX spectrum and mapping analysis for different elements present in the composite MoS_2-TiO_2 coating (15 wt. % of TiO_2) of both 38 and 102 μm thickness respectively.

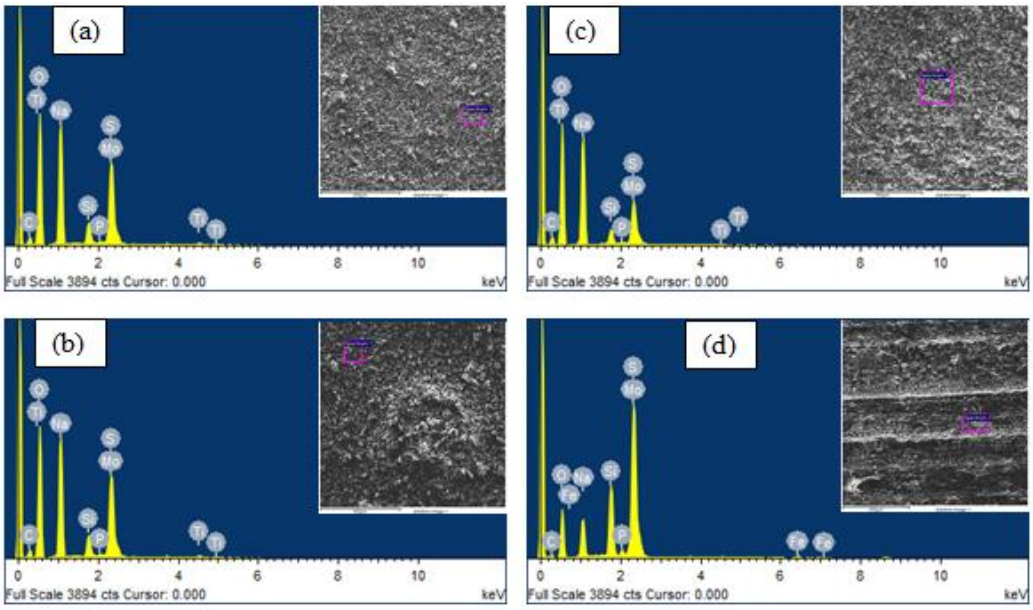

Fig.4.11 EDX analysis for different elements constituted into composite MoS_2-TiO_2 coating (15 wt. % of TiO_2) 1) 38±6 μm (a) before wear test, (b) after wear test 2) 102±6 μm (c) before wear test, (d) after wear test

The EDX analysis is carried out before and after the wear test of a coated sample. The initial spectrum Fig. 4.11 (a) and (c) for the coated speciments with different thicknesses (i.e. 38 and 102 μm), before wear test depicts different elements that constitute coatings like Mo, S, Ti, Na, Si, O, P and C. In case of coating with lower thickness, the

coating found to be still remain present on the substrate surface even after the wear test is shown in Fig. 4.11 (c) having the same elemental composition. Whereas, in case of coating with higher thickness after wear test shows some traces of Fe along with the above mentioned elements (refer Fig. 4.11.(d)). The EDX analysis clearly depicts that in the case of higher coating thickness the coating worn out at a faster rate due to poor bond strength. After worn out of the coating, asperity contact between the contacting surfaces take place which can be confirmed with the traces of Fe along with the other elements.

4.3 Summary

The tribological properties of the developed composite MoS_2-TiO_2 coating material with different wt. % of TiO_2 and crystallite size at different contact pressure, sliding speed, temperature and coating thickness have been investigated. The test results reveal that in comparison with the application of pure MoS_2 coating, the composite MoS_2-TiO_2 coating exhibits excellent tribological performance in all considered operating conditions due to the synergistic effect of both MoS_2 and TiO_2. At ambient conditions, the introduction of TiO_2 into the MoS_2 matrix helps to improve the bond strength without spoiling the lubricating property of MoS_2 and in turns lead to enhance the endurance life of the coating. The crystallite size of TiO_2 is not influential on COF and wear rate as compared to wt. % addition of TiO_2. Overall the composite MoS_2-TiO_2 coating (TiO_2 with 27.69 nm crystallite size) with 15% wt. depicts the lowest COF and wear rate. In addition, a positive effect on COF and a negative effect on wear rate have been observed with the increase in the temperature of the coated pin surface. A similar trend is also observed with the increase in coating thickness.

From the tribological investigation of the composite MoS_2-TiO_2 coating it has been observed that wear and frictional characteristics are significantly affected by the factors such as wt. % addition of TiO_2, contact pressure, sliding speed and temperature. The influencing factors among these parameters on the tribological performance of the composite MoS_2-TiO_2 coating is studied using Taguchi and ANN approach and it is discussed in Chapter 5.

Chapter 5

Parametric Optimization of Factors Affecting the Tribological Behavior of Composite MoS_2-TiO_2 Coating Using DOE Techniques

In the previous chapter, tribological investigation of composite MoS_2-TiO_2 coating material is carried out considering various factors such as wt. % addition of TiO_2, contact pressure, sliding speed and temperature. In the present chapter, parametric optimization of these factors has been carried out using DOE techniques such as Taguchi and artificial neural network (ANN). The Taguchi approach is employed with standard L27 orthogonal array. The developed model is validated through the Analysis of variance (ANOVA) technique. The artificial neural network (ANN) tool is also implemented for predicting the output tribological responses.

5.1 Taguchi approach

Generally, Taguchi design of experiment (DOE) is the most popular and potential analytical tool employed to optimize the design parameters. Compared to the conventional experimental approach, Taguchi's DOE approach helps to reduce the number of experiments substantially. This results in a great reduction of cost and time (Kumar and Chauhan 2012). The conventional practice (experimental approach) involves considering one- factor-at-a- time, which requires a change in one variable at a time while others are constant. The major limitation in this approach is that it may omit some of the possible interactions between the defined set of parameters. Another limitation of this practice is that it fails to consider all the factors in a single experiment and govern their main effects. To overcome these drawbacks Taguchi technique was developed. The Taguchi approach considers the output as the mean value of the response function at a particular parameter level (Montgomery 2017). With the change in the level of the factor, the overall mean response deviates from the initial value. The Taguchi approach is formulated to identify the process and

optimize the best feasible combinations of the factors, for producing best output responses (Sahoo and Pal 2007).

5.1.1 Design of experiment (DOE)

The experimental results in terms of COF and wear rate of composite MoS_2-TiO_2 coating material obtained at various operating parameters such as wt. % addition of TiO_2, contact pressure, sliding speed and temperature using the pin-on-disc friction and wear test rig as reported in the chapter 4 is considered for optimization.

In the case of Taguchi method, experimental findings are converted into a signal-to-noise (S/N) ratio. There are lot many S/N ratios that exist according to the type of characteristics. In the current study, a smaller-the-better S/N ratio for both coefficient of friction (COF) and wear rate (WR) is employed. The S/N ratio is estimated with a logarithmic transformation of the loss function (Kumar and Manisekar 2014).

$$\frac{S}{N} = -10\log\frac{1}{n}\left(y^2\right)$$

(5.1)

where y - observed data and n - number of observations.

The four different process parameters with their three different levels are listed in table 5.1.

Table 5.1 Process parameters with their different levels

Process parameters	Level I	Level II	Level III
A: TiO_2 wt. % addition	5	15	25
B: Contact pressure (KPa)	176	442	707
C: Sliding speed (m/sec)	1	2	3
D: Temperature (°C)	27	200	400

All sets of experiments are performed as per the conditions represented in table 5.2. Mean response characteristic curves are plotted with the help of Minitab-17 software and the % contribution of the test parameters is examined using ANOVA analysis (Minitab User Manual 2016).

Table 5.2 Design of experiment with L27 (2^{13}) orthogonal array

L27 (2^{13})	A (wt. % of TiO_2)	B Contact Pressure (kPa)	C Sliding speed (m/s)	D Temp (°C)	Avg. COF	S/ N Ratio (dB)	Avg. WR (mm^3/m)	S/ N Ratio (dB)
1	0*	176	1	27	0.37	8.6360	0.033	29.6297

2	0*	176	2	200	0.15	16.4782	0.0595	24.5097
3	0*	176	3	400	0.11	19.1721	0.0742	22.5919
4	0*	442	1	200	0.13	17.7211	0.0683	23.3116
5	0*	442	2	400	0.1	20.0000	0.0896	20.9538
6	0*	442	3	27	0.28	11.0568	0.0488	26.2316
7	0*	707	1	400	0.07	23.0980	0.159	15.9721
8	0*	707	2	27	0.23	12.7654	0.084	21.5144
9	0*	707	3	200	0.09	20.9151	0.126	17.9926
10	15	176	1	200	0.14	17.0774	0.054	25.3521
11	15	176	2	400	0.11	19.1721	0.0677	23.3882
12	15	176	3	27	0.26	11.7005	0.028	31.0568
13	15	442	1	400	0.08	21.9382	0.0764	22.3381
14	15	442	2	27	0.24	12.3958	0.0392	28.1343
15	15	442	3	200	0.12	18.4164	0.0695	23.1603
16	15	707	1	27	0.17	15.3910	0.054	25.3521
17	15	707	2	200	0.1	20.0000	0.0862	21.2899
18	15	707	3	400	0.07	23.0980	0.114	18.8619
19	25	176	1	400	0.13	17.7211	0.0593	24.5389
20	25	176	2	27	0.33	9.6297	0.024	32.3958
21	25	176	3	200	0.16	15.9176	0.0724	22.8052
22	25	442	1	27	0.32	9.8970	0.0421	27.5144
23	25	442	2	200	0.14	17.0774	0.0793	22.0145
24	25	442	3	400	0.12	18.4164	0.0858	21.3303
25	25	707	1	200	0.11	19.1721	0.0713	22.9382
26	25	707	2	400	0.09	20.9151	0.0987	20.1137
27	25	707	3	27	0.23	12.7654	0.0737	22.6507

0* indicates Pure MoS_2 coating i.e. without addition of TiO_2

5.1.2 ANOVA Analysis

The data obtained using DOE L27 (2^{13}) orthogonal array for output responses i.e. COF and WR are converted into S/N ratios as depicted in table 5.2. An ANOVA table is developed to discover the rank of significant factors and their interactions. Table 5.3 and 5.4 represent the ANOVA result of the MoS_2-TiO_2 composite coating in terms of COF and WR respectively.

Table 5.3 ANOVA results for COF

Source	DOF	Adj SS	Adj MS	F-Value	P-Value	Percentage of contribution
A	2	0.006785	0.003393	17.62	0.003	3.54
B	2	0.020363	0.010181	52.87	0.000	10.62
C	2	0.000363	0.000181	0.94	0.441	0.19
D	2	0.153119	0.076559	397.52	0.000	79.88
A*B	4	0.000793	0.000198	1.03	0.463	0.41
A*D	4	0.004637	0.001159	6.02	0.027	2.42
B *D	4	0.004459	0.001115	5.79	0.029	2.33
Error	6	0.001156	0.000193			0.60
Total	26	0.191674				

Table 5.4 ANOVA results for WR

Source	DOF	Adj SS	Adj MS	F-Value	P-Value	Percentage of contribution
A	2	0.001566	0.000783	8.69	0.017	6.76
B	2	0.009027	0.004514	50.11	0.000	38.98
C	2	0.000365	0.000183	2.03	0.212	1.57
D	2	0.009069	0.004535	50.34	0.000	39.16
A*B	4	0.001811	0.000453	5.03	0.040	7.81
A*D	4	0.000291	0.000073	0.81	0.563	1.26
B *D	4	0.000490	0.000123	1.36	0.350	2.11
Error	6	0.000540	0.00009			2.33
Total	26	0.023160				

From the ANOVA analysis, it has been observed that in case of COF, the temperature has the biggest influence (p = 79. 88%), followed by contact pressure (p = 10.62%), wt. % of TiO_2 (p = 3.54%), and sliding speed (p = 0.19%). The sliding speed displays the least significant contribution to COF. The interaction of A*D (p = 2.42%) and B*D (p = 2.33%) displays a comparatively more substantial contribution to the COF, while the remaining interaction A*B had less significant contribution to the COF. The main effect plots and interaction plots are considered to evaluate the individual parameter effect and their interaction effects on COF, as depicted in Fig. 5.1. The R_{-Sq} 99.40 % and R^2_{adj} 97.39 % values of the model are in the acceptable range of variability in predicting COF values. Regression analysis is performed using the (S/N) ratio value. The analysis demonstrates whether the factors are significantly in relation with data response. The coefficients of regression equation based on their significant p-values for COF are listed in table 5.5.

Table 5.5 Coefficients of regression analysis for COF

Term	Coefficient	P value
Constant	0.16481	0.000
A (wt. % TiO_2)		
15	-0.02148	0.001
B Contact pressure (KPa)		
176	0.03074	0.000
D Temperature (°C)		
27	0.10519	0.000
A* D		
15 wt. % TiO_2 and 27°C	-0.02519	0.003
B *D		
176 KPa Contact pressure	0.01926	0.011

The equation of regression for the COF is as follows:

COF = 0.16481 - 0.02148 A + 0.03074 B + 0.10519 D - 0.02519 A*D + 0.01926 B*D (5.2)

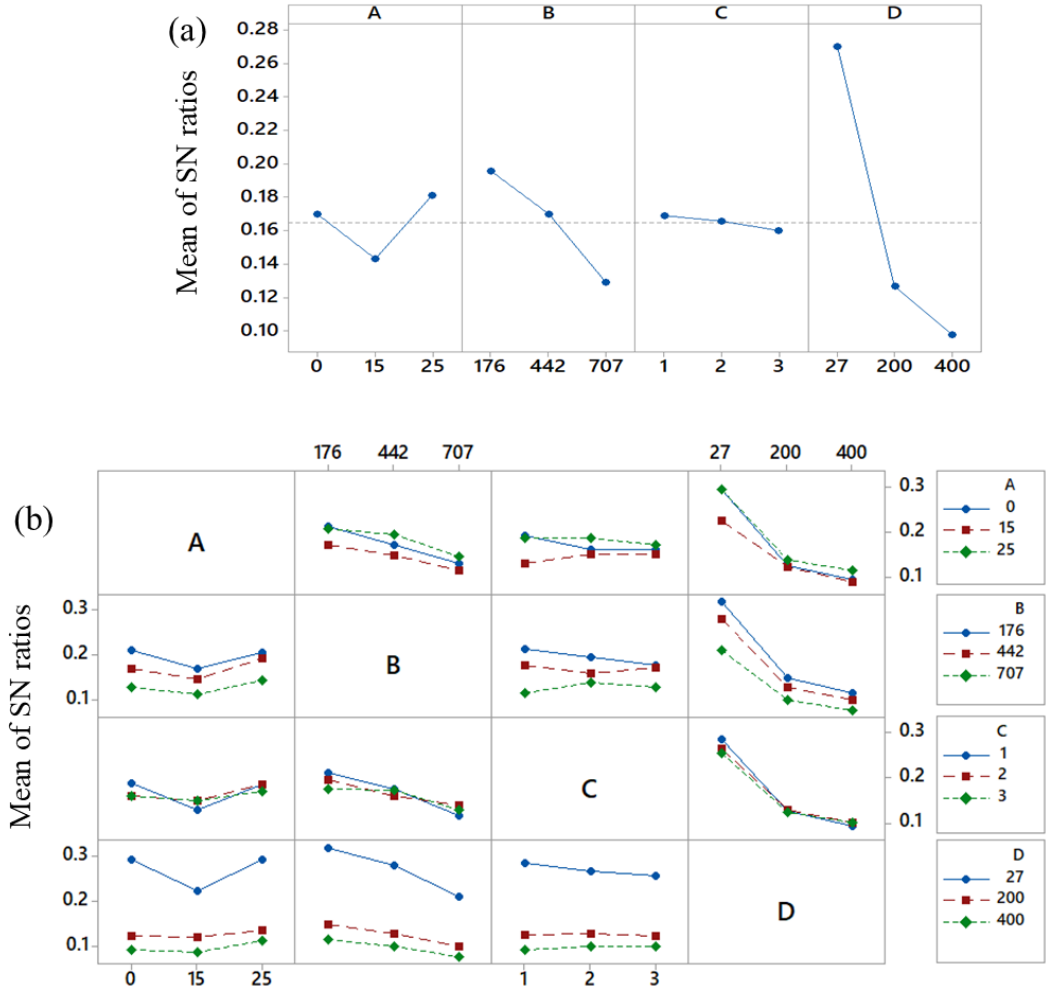

Fig. 5.1 COF (a) Main effect plot of factors (b) Interaction plots for composite MoS_2-TiO_2 coating

Similarly in case of WR, temperature has highest influence (p = 39. 16%), followed by contact pressure (p = 38.98%), wt. % of TiO_2 (p = 6.76%), and sliding speed (p = 1.57%). The sliding speed displays the least significant contribution to WR. The interaction of A*B (p = 7.81%) and B*D (p = 2.11%) represents a comparatively more substantial contribution to the WR, while the remaining interaction A*D has a less significant contribution to the WR. Therefore temperature is observed to be the highly influential parameter on both COF and WR. The main effect plots and interaction plots are considered to evaluate the individual parameter effect and their interaction effects on WR, as depicted in Fig. 5.2.

The R_{-Sq} 97.67 % and R^2_{adj} 95.83 % values of the model are in the acceptable range of variability in predicting WR values.

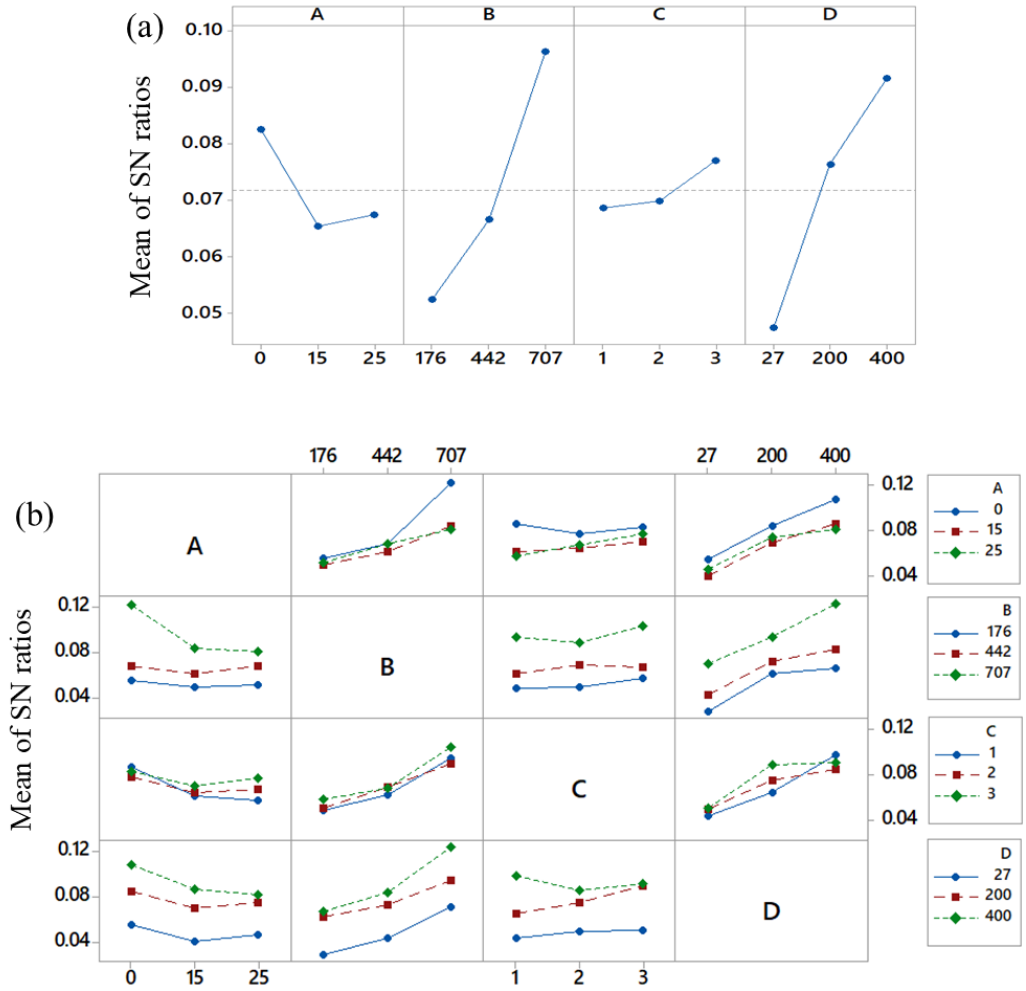

Fig. 5.2 Wear rate (a) Main effect plot of factors (b) Interaction plots for composite MoS_2-TiO_2 coating

Regression analysis is performed using the (S/N) ratio value. The analysis demonstrates whether the factors are significantly in relation with data response. The coefficients of regression equation based on their significant p-values for WR are listed in table 5.6.

Table 5.6 Coefficients of regression analysis for WR

Term	Coefficient	P value
Constant	0.07178	0.000
A (wt. % TiO_2)		
15	0.01071	0.006
B Contact pressure		
176	-0.01932	0.000
D Temperature		
27	-0.02436	0.000

The equation of regression for the WR is as follows:

Wear rate (mm^3/min) = 0.07178 + 0.01071 A - 0.01932 B - 0.02436 D (5.3)

5.1.3 Statistical analysis employing Taguchi approach

The S/N ratio proved to be the significant criterion in the Taguchi approach for studying the experiments. The S/N ratio must possess a maximum value to acquire optimum test conditions, as per the Taguchi approach. The responses in terms of S/N ratios for COF and WR are presented in table 5.7. The ranking for the process parameters (affecting the output i.e. COF and WR) with their various levels are mentioned in table 5.7. The ranks obtained for the process parameters based upon the delta statistics correlates the relative magnitude of effects (Kumar and Chauhan 2012).

Table 5.7 Responses obtained in S/N ratios

	COF					WR (mm^3/m)			
Level	A	B	C	D	Level	A	B	C	D
1	16.65	15.06	16.74	11.58	1	22.52	26.25	24.11	27.16
2	17.69	16.32	16.49	18.09	2	24.33	23.89	23.81	22.6
3	15.72	18.68	16.83	20.39	3	24.03	20.74	22.96	21.12
Delta	1.96	3.62	0.34	8.81	Delta	1.8	5.51	1.14	6.04
Rank	3	2	4	1	Rank	3	2	4	1

5.1.4 Confirmation tests

The confirmation of experiments is the last step involved in the DOE methodology (Kumar and Chauhan 2012). The output responses i.e. COF and WR, are predicted for the combining the factors that are different from the existing set. The experiment was carried out for the same combination of the factors. The comparison between the predicted and experimental results for COF and WR is represented in table 5.8. An error of 2.68 % for COF and 1.2 % for WR (S/N ratios) was observed. There was close agreement observed between the results obtained by both methods.

Table 5.8 Confirmation test results

	Initial parameter combination	Prediction	Experimental result	Improvement in S/N ratio
Level	A1B1C1D1	A1B1C3D3		
COF	0.2815	0.1053	0.11	
SN ratio (dB)	11.0085	19.7004	19.1721	8.1636
Level	A1B3C1D3	A3B2C3D3		
Wear rate (mm^3/m)	0.12056	0.09087	0.0858	
SN ratio (dB)	18.3759	21.0736	21.3303	2.9544

Taguchi approach has good reproduction of results; however, it is concerned only with the individual effects of process parameters. Whereas, Artificial Neural Network (ANN) having the ability to learn and find multi-dimensional dependencies between process parameters (Ripa and Frangu 2004, Rudnicki and Figiel 2002). However, the data for teaching the ANN need to be carefully selected, and a wide range of data needs to be trained. Hence in the present study, the data required for teaching the ANN is selected from the designed data set that has been used in the Taguchi approach.

5.2 Artificial neural network (ANN)

ANN is one of the best popular modelling techniques, which could be employed to resolve problems that are complex in nature for human beings or traditional computers. The data processing procedure in ANN is evolved from the biological nervous systems and operation of the human brain. The architecture of ANN is divided into three layers like input, hidden and output layer. While operation, all the nodes of consequent layers are interconnected with each other and the number of neurons present within the hidden layer can be changed (Kumar and Chauhan 2012). From the available experimental data, information is provided to an input layer. Further, this input data is assigned with specific weights for interconnecting with the adjacent hidden layer. At this stage, the multiplication between provided data and assigned weights has been done and eventually, the addition of the individual product data has been carried out. This obtained data further executed by the transfer function, in this way, the signal reaches to an output layer (Velten et al., 2000). This learning approach helps the neural network to achieve the desired responses for the provided input variables (Hassan and Mohammed 2016). The ANN helps to develop a well performed network that predicts the correlation between input and output parameters. This

helps substantially to reduce a large amount of time involved in tedious experimental work. These advantages make it an adaptable, popular and promising modelling technique from the past few decades in many engineering fields, such as aviation, industrial production, material science, robotics, electronics and telecommunications.

5.2.1 ANN data processing procedure with employed topology and structure

In the present work, to evaluate COF and WR, the data obtained through experimental trials and used to train the ANN. A Back propagation (BP) neural network is employed for the evaluation of COF and WR. The Levenberg-Marquart neural network is intentionally implemented due to its fast learning capability (Zhao et al., 2010). The performance of each developed and trained neural network is analyzed with regard to minimum values of mean square error (MSE) and the iterations needed to train the network. The learning function LEARNGD and performance function MSE are adapted among the developed neural networks. In the present work, the ANN optimization is performed with the 'nnfit' wizard of MATLAB R2015a software. The procedure employed to find an optimum neural network model is shown with a flow chart as depicted in Fig. 5.3.

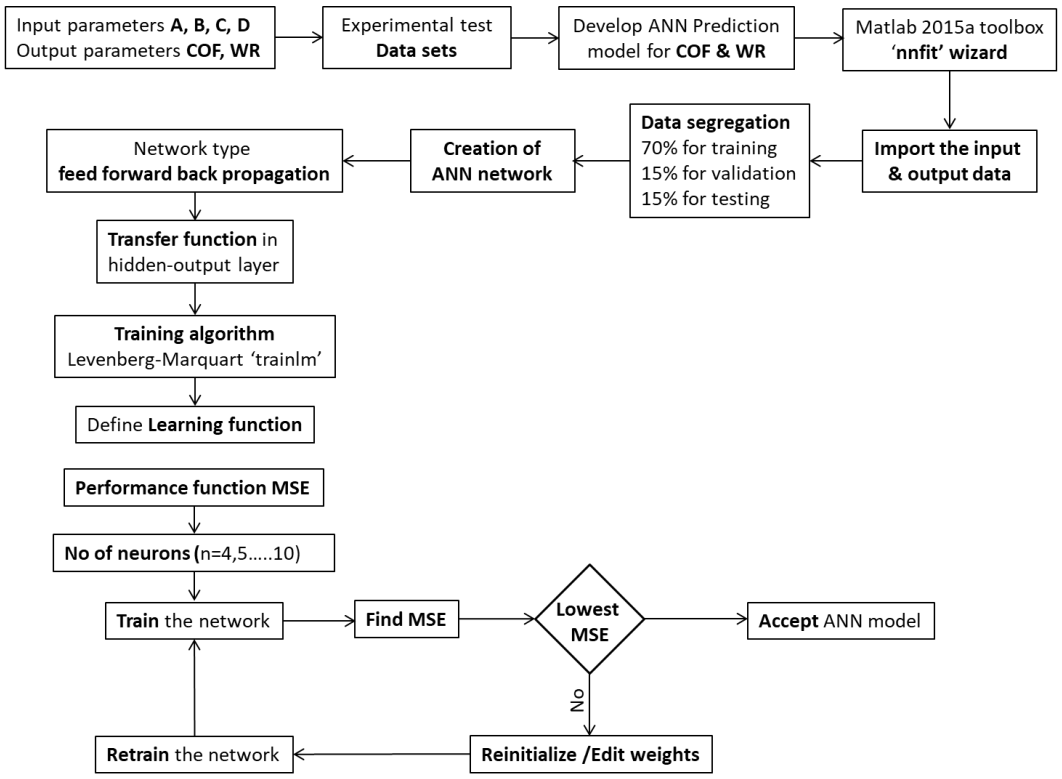

Fig. 5.3 Stepwise procedure for finding optimum neural network

The topology and structure implemented in this study for ANN are shown in Fig. 5.4. The four different independent input parameters such as A, B, C and D are comprising the input layer, whereas COF and WR have been taken into account in the output layer of the ANN model (mentioned in table 5.2). In the present work, two types of architectures were studied namely, 4-n-1 and 4-n-2 architectures. The 4-n-1 architecture is depicted in Fig. 5.4 (a) and (b) in which four neurons present in the input layer (i.e., A, B, C, D), 'n' designate neurons considered in the hidden layer while 1 designate neurons considered in the output layer (i.e., COF or WR). The 4-n-2 architecture is represented in Fig. 5.4 (c) is quite identical to 4-n-1 besides the neurons considered in the output layer. In this topology two neurons were available in the output layer (i.e., both COF and WR).

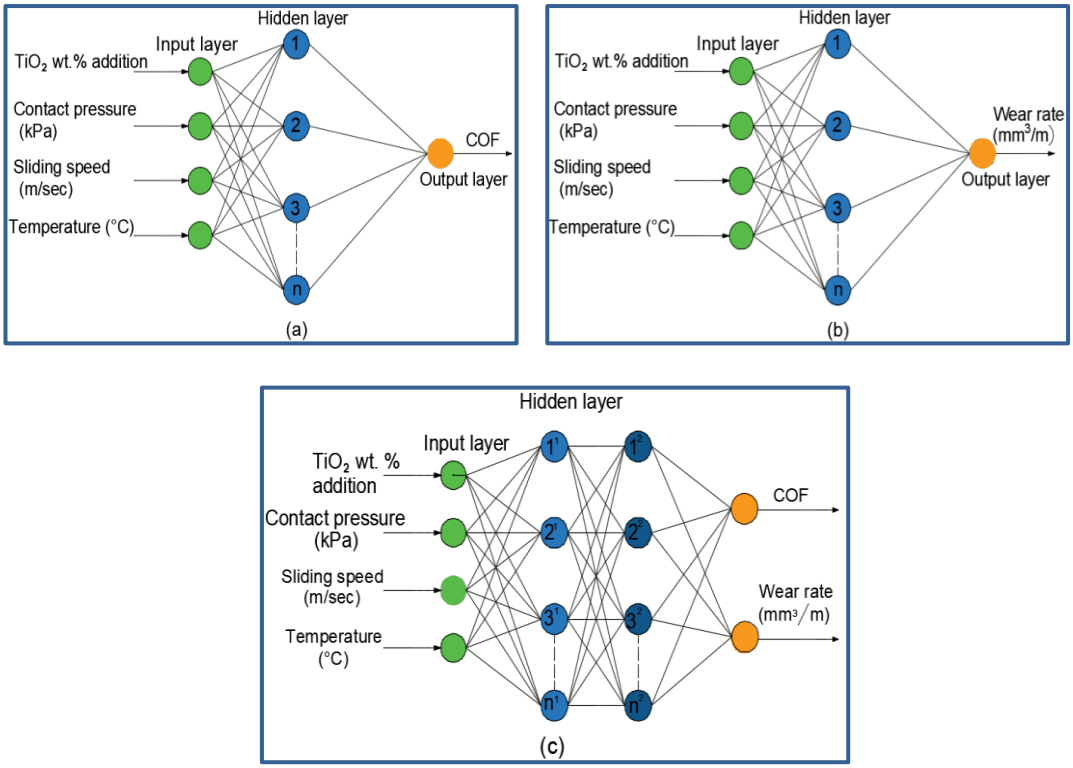

Fig. 5.4 ANN with 4-n-1 topology for (a) COF, (b) WR and (c) ANN with 4-n-2 topology for COF and WR

5.2.2 ANN training and prediction

Eventually, the optimal ANN architecture is determined using the trial and error method by varying the number of neurons and hidden layers. While training the ANN, 27 data samples are considered, from which 70 % considered for training and the remaining 15 % each considered for validation and testing. In view of the performance of the training process substantially relies on the sampling of data and initialization of the interconnection

weights. To precise prediction, each network was trained five times. The predicted results were compared with the target values by utilizing a fresh input data set for training. Based on the R^2 value close to unity and least MSE value, the ANN model finalized and predicted the output responses.

As discussed in the previous section 5.1.3, the different ANN models are developed to predict the experimental results (i.e. COF and WR). The ANN is constructed with four input parameters, namely wt. % of TiO_2, contact pressure, sliding speed and temperature. In the present work, a trial and error method is employed to optimize the number of neurons and hidden layers.

ANN model for predicting individual response (COF or Wear rate)

The ANN model has been developed, which correlates the input process parameters and output responses for the tribological characteristics of composite MoS_2-TiO_2 coatings. The eight different ANN models are designed by employing different neuron numbers with various combinations of transfer functions. Based on the R^2 value and least MSE value, the best ANN model to predict (COF and WR) was finalized. Table 5.9 illustrates the R^2 values and MSE for different ANN models developed to predict COF.

Table 5.9 Summarized results for 4-n-1 ANN model to predict COF

Network Structure	**Transfer function**			**R^2 values**				**MSE**
	Layer 1	Layer 2	Layer 3	Training	Validation	Testing	All	COF
	TRANSIG	PURELIN	----					
4-4-1				0.9738	0.9695	0.9289	0.9625	0.003252
4-5-1				**0.9811**	**0.9805**	**0.9935**	**0.9879**	**0.000051**
4-6-1				0.9558	0.9443	0.9669	0.9563	0.000645
4-7-1				0.9665	0.9651	0.9805	0.9629	0.001404
4-8-1				0.9496	0.9931	0.9611	0.9611	0.001792
4-9-1				0.9749	0.9228	0.9811	0.9602	0.008641
4-10-1				0.9235	0.9564	0.9716	0.9409	0.00051
	LOGSIG	PURELIN	----					
4-4-1				0.9592	0.9627	0.9746	0.9603	0.001692
4-5-1				0.9559	0.9589	0.9876	0.9601	0.000371
4-6-1				0.9575	0.9861	0.9631	0.9634	0.000697
4-7-1				0.9509	0.9522	0.9795	0.9569	0.00248
4-8-1				0.9566	0.9776	0.9735	0.9614	0.000623
4-9-1				0.9565	0.9779	0.9832	0.9623	0.000115
4-10-1				0.9585	0.9376	0.9638	0.9575	0.002552
	PURELIN	PURELIN	----					
4-4-1				0.8706	0.8866	0.8779	0.8511	0.004449
4-5-1				0.8349	0.8713	0.9153	0.8506	0.003979
4-6-1				0.8132	0.8715	0.9597	0.8452	0.001028
4-7-1				0.8701	0.7573	0.8585	0.8521	0.003363

4-8-1				0.8288	0.9092	0.9505	0.8508	0.001698
4-9-1				0.8526	0.8761	0.8623	0.8506	0.00526
4-10-1				0.8527	0.9084	0.8688	0.8511	0.002465
	TRANSIG	TRANSIG	PURELIN					
4-5-4-1				0.9782	0.9421	0.9817	0.9631	0.003994
4-6-5-1				0.9684	0.9492	0.9762	0.9634	0.00184
4-6-6-1				0.9691	0.9559	0.9533	0.9639	0.002531
4-7-6-1				0.9775	0.9226	0.9604	0.9613	0.004289
4-8-7-1				0.9668	0.9638	0.9859	0.9651	0.000237
4-9-8-1				0.9595	0.9762	0.9688	0.9603	0.001553
	TRANSIG	PURELIN	PURELIN					
4-5-4-1				0.9325	0.9886	0.9436	0.9417	0.000822
4-6-5-1				0.9605	0.9684	0.9776	0.9608	0.000341
4-6-6-1				0.9512	0.9849	0.9786	0.9618	0.000257
4-7-6-1				0.9601	0.9221	0.9878	0.9522	0.000381
4-8-7-1				0.9656	0.9239	0.9801	0.9572	0.002443
4-9-8-1				0.9703	0.9575	0.9571	0.9654	0.001117
	LOGSIG	LOGSIG	PURELIN					
4-5-4-1				0.9646	0.9659	0.9671	0.9641	0.000145
4-6-5-1				0.9575	0.9948	0.9628	0.9625	0.001894
4-6-6-1				0.9643	0.9802	0.9519	0.9629	0.001242
4-7-6-1				0.9315	0.9723	0.9473	0.9416	0.002499
4-8-7-1				0.9438	0.9742	0.9864	0.9514	0.001085
4-9-8-1				0.9657	0.9901	0.9329	0.9647	0.001249
	LOGSIG	PURELIN	PURELIN					
4-5-4-1				0.9651	0.9626	0.9728	0.9645	0.001238
4-6-5-1				0.9566	0.9868	0.9498	0.9533	0.001646
4-6-6-1				0.9577	0.9729	0.9633	0.9605	0.000571
4-7-6-1				0.9799	0.9206	0.9254	0.9615	0.000412
4-8-7-1				0.9646	0.9707	0.9653	0.9651	0.000127
4-9-8-1				0.9596	0.9748	0.9762	0.9627	0.002443
	PURELIN	PURELIN	PURELIN					
4-5-4-1				0.8559	0.9078	0.8869	0.8521	0.004512
4-6-5-1				0.8463	0.9058	0.8152	0.8517	0.00562
4-6-6-1				0.8463	0.8148	0.9337	0.8511	0.001472
4-7-6-1				0.8349	0.8963	0.9248	0.8488	0.007596
4-8-7-1				0.8334	0.8896	0.9312	0.8508	0.004757
4-9-8-1				0.8329	0.8403	0.9599	0.8498	0.001943

The results listed in table 5.9 show that, the ANN model 4-5-1 i.e. 5 neurons in hidden layer with transig-purelin transfer functions, exhibits the highest R^2 value of 0.9879 with MSE of 0.000051. This developed ANN model helps to predict COF closer to the target value. The predicted results demonstrated that MAPE is about 4.38 %. Hence, the developed ANN model is adequately precise to predict the responses for unknown input process parameters.

In the same fashion table 5.10 represents the R^2 value and MSE obtained for the prediction of WR. The ANN model 4-7-1 i.e. 7 neurons in hidden layer with transig-purelin transfer functions, exhibits the highest R^2 with 0.9822 with MSE about 0.000014.

The predicted results demonstrated that MAPE is about 5.21 %. Hence, the developed ANN model is adequately precise to predict the responses for unknown input process parameters.

Table 5.10 Summarized results for 4-n-1 ANN model to predict WR

Network Structure	**Transfer function**			**R^2 values**				**MSE**
	Layer 1	Layer 2	Layer 3	Training	Validation	Testing	All	Wear rate
	TRANSIG	PURELIN	----					
4-4-1				0.9561	0.9784	0.9828	0.9614	0.000464
4-5-1				0.9585	0.9778	0.9756	0.9634	0.000499
4-6-1				0.9553	0.9537	0.9693	0.9578	0.000198
4-7-1				**0.9856**	**0.9909**	**0.9845**	**0.9822**	**0.000014**
4-8-1				0.9649	0.9771	0.9629	0.9619	0.000032
4-9-1				0.9727	0.9562	0.9646	0.9632	0.000299
4-10-1				0.9675	0.9703	0.9722	0.9669	0.000448
	LOGSIG	PURELIN	----					
4-4-1				0.9459	0.9778	0.9839	0.956	0.000672
4-5-1				0.9616	0.9889	0.9585	0.9588	0.000615
4-6-1				0.9562	0.9554	0.9801	0.9588	0.000106
4-7-1				0.9516	0.9819	0.9589	0.9574	0.001251
4-8-1				0.9629	0.9839	0.9734	0.9656	0.000148
4-9-1				0.9608	0.9869	0.9609	0.9636	0.000733
4-10-1				0.9725	0.9794	0.9779	0.9673	0.000019
	PURELIN	PURELIN	----					
4-4-1				0.8653	0.8696	0.9583	0.8716	0.000393
4-5-1				0.8494	0.9817	0.8889	0.8724	0.000453
4-6-1				0.8533	0.9213	0.8888	0.8613	0.001329
4-7-1				0.8523	0.9388	0.9714	0.8714	0.002663
4-8-1				0.8414	0.8952	0.9358	0.8698	0.000115
4-9-1				0.8592	0.9644	0.9074	0.8726	0.001031
4-10-1				0.8652	0.9084	0.9102	0.8716	0.000824
	TRANSIG	TRANSIG	PURELIN					
4-5-4-1				0.9416	0.986	0.9604	0.9527	0.000609
4-6-5-1				0.9756	0.9807	0.9545	0.9669	0.001166
4-6-6-1				0.9612	0.9839	0.9514	0.9625	0.000501
4-7-6-1				0.935	0.9642	0.9814	0.9446	0.000175
4-8-7-1				0.9671	0.9871	0.9319	0.9596	0.000523
4-9-8-1				0.9564	0.9789	0.9758	0.9636	0.000046
	TRANSIG	PURELIN	PURELIN					
4-5-4-1				0.9711	0.9742	0.9685	0.9676	0.000725
4-6-5-1				0.9509	0.9139	0.9718	0.9502	0.000283
4-6-6-1				0.9607	0.9839	0.9529	0.9623	0.000351
4-7-6-1				0.9676	0.9798	0.9692	0.9647	0.001212
4-8-7-1				0.9549	0.9756	0.9928	0.9626	0.001109
4-9-8-1				0.9479	0.9706	0.9719	0.9556	0.000479
	LOGSIG	LOGSIG	PURELIN					
4-5-4-1				0.9626	0.9774	0.9839	0.9647	0.000511
4-6-5-1				0.9543	0.9597	0.9869	0.9584	0.000031
4-6-6-1				0.9214	0.9628	0.9717	0.9344	0.000374

4-7-6-1			0.9646	0.9689	0.9779	0.9618	0.000424
4-8-7-1			0.9698	0.9487	0.9776	0.9657	0.000031
4-9-8-1			0.9599	0.9882	0.9686	0.9648	0.000151
	LOGSIG	PURELIN PURELIN					
4-5-4-1			0.9708	0.9729	0.9403	0.9626	0.000605
4-6-5-1			0.9582	0.9729	0.9732	0.9641	0.000164
4-6-6-1			0.9697	0.9779	0.9441	0.9621	0.00107
4-7-6-1			0.9634	0.9736	0.9799	0.9671	0.000959
4-8-7-1			0.9559	0.9519	0.9694	0.9525	0.001095
4-9-8-1			0.9523	0.9669	0.9871	0.9599	0.00081
	PURELIN	PURELIN PURELIN					
4-5-4-1			0.8895	0.8857	0.8695	0.8681	0.002036
4-6-5-1			0.8812	0.8614	0.8615	0.8725	0.000101
4-6-6-1			0.8924	0.8492	0.8843	0.8696	0.001323
4-7-6-1			0.8557	0.9027	0.89	0.8703	0.000718
4-8-7-1			0.8901	0.8756	0.8903	0.8666	0.001754
4-9-8-1			0.8908	0.8395	0.9349	0.8694	0.000129

ANN model for predicting dual responses in the output layer (COF and WR)

Further to check the capability of the 4-n-2 ANN model for predicting combined response for COF and WR together, ANN models developed with combinations of different transfer functions. The obtained results in terms of R^2 and MSE are listed in table 5.11. The result shows that the network 4-7-2 i.e. 7 neurons in the hidden layer with transig-purelin transfer functions exhibits the highest R^2 value of 0.9822 with MSE value of 0.00005. The predicted results demonstrated that MAPE is about 8.03 % for COF and 8.48 % for WR. Hence, the developed ANN model is adequately precise to predict the responses for unknown input process parameters.

Table 5.11 Summarized results for 4-n-2 ANN model to predict COF and WR simultaneously

Network Structure	**Transfer function**			**R^2 values**				**MSE**	
	Layer 1	Layer 2	Layer 3	Training	Validation	Testing	All	COF	WR
	TRANSIG	PURELIN	----						
4-4-2				0.9773	0.9662	0.9689	0.9695	0.00209	0.00049
4-5-2				0.9752	0.9677	0.9899	0.9735	0.00202	0.00028
4-6-2				0.9749	0.9828	0.9752	0.9754	0.00039	0.00063
4-7-2				**0.9683**	**0.9932**	**0.9969**	**0.9765**	**0.00002**	**0.00005**
4-8-2				0.9778	0.9837	0.9821	0.9775	0.0012	0.00131
4-9-2				0.9734	0.9921	0.9785	0.9755	0.00045	0.00045
4-10-2				0.9703	0.9912	0.9898	0.9776	0.00163	0.00059
	LOGSIG	PURELIN	----						
4-4-2				0.9679	0.9414	0.972	0.9652	0.00084	0.00028
4-5-2				0.9721	0.9713	0.9825	0.9727	0.00099	0.00048
4-6-2				0.9725	0.9664	0.9848	0.9753	0.00022	0.00023
4-7-2				0.9638	0.9732	0.9757	0.9649	0.00338	0.00051

4-8-2				0.9694	0.9838	0.9865	0.9739	0.00068	0.00092
4-9-2				0.9743	0.9701	0.9836	0.9713	0.00318	0.00084
4-10-2				0.9767	0.9755	0.9805	0.9758	0.00111	0.00039
	PURELIN	PURELIN	----						
4-4-2				0.8999	0.9232	0.9269	0.9042	0.00213	0.00028
4-5-2				0.9024	0.9525	0.8931	0.9065	0.00344	0.00179
4-6-2				0.9013	0.8922	0.9588	0.9067	0.00167	0.00009
4-7-2				0.9182	0.8744	0.9002	0.9056	0.00063	0.00068
4-8-2				0.9097	0.9043	0.9094	0.9065	0.00268	0.00054
4-9-2				0.9028	0.9241	0.9221	0.9047	0.00145	0.00166
4-10-2				0.9064	0.8988	0.9159	0.9066	0.00041	0.00043
	TRANSIG	TRANSIG	PURELIN						
4-5-4-2				0.9701	0.9682	0.9808	0.9697	0.00279	0.00109
4-6-5-2				0.9755	0.9793	0.9782	0.9756	0.00223	0.00114
4-6-6-2				0.9596	0.9716	0.9926	0.9674	0.00002	0.00252
4-7-6-2				0.9781	0.9718	0.9719	0.9754	0.00096	0.00284
4-8-7-2				0.9662	0.994	0.9824	0.9722	0.00125	0.00041
4-9-8-2				0.9762	0.9769	0.9686	0.9722	0.00392	0.00014
	TRANSIG	PURELIN	PURELIN						
4-5-4-2				0.9541	0.9605	0.9805	0.9604	0.00007	0.00031
4-6-5-2				0.9759	0.9657	0.9867	0.9759	0.00081	0.00041
4-6-6-2				0.9772	0.9761	0.9746	0.9767	0.00031	0.00084
4-7-6-2				0.9711	0.9821	0.9898	0.9739	0.00047	0.00059
4-8-7-2				0.9825	0.9465	0.9623	0.9742	0.00411	0.00123
4-9-8-2				0.9777	0.9751	0.9787	0.9771	0.00129	0.00097
	LOGSIG	LOGSIG	PURELIN						
4-5-4-2				0.9759	0.9831	0.9753	0.9756	0.00116	0.00053
4-6-5-2				0.9604	0.9811	0.9774	0.9673	0.00005	0.00234
4-6-6-2				0.9759	0.9533	0.9899	0.9725	0.00096	0.0001
4-7-6-2				0.9751	0.9813	0.9825	0.9759	0.00062	0.00014
4-8-7-2				0.9665	0.9548	0.9889	0.9691	0.00112	0.00093
4-9-8-2				0.9665	0.9841	0.9784	0.9688	0.00281	0.0005
	LOGSIG	PURELIN	PURELIN						
4-5-4-2				0.9604	0.9759	0.9886	0.9674	0.00023	0.00091
4-6-5-2				0.9763	0.9748	0.9777	0.9753	0.00104	0.00056
4-6-6-2				0.9753	0.9609	0.9721	0.9733	0.00099	0.00141
4-7-6-2				0.9709	0.9812	0.9898	0.9737	0.00007	0.00045
4-8-7-2				0.9671	0.9851	0.9848	0.9709	0.00115	0.00019
4-9-8-2				0.9744	0.9746	0.9768	0.9744	0.00054	0.00102
	PURELIN	PURELIN	PURELIN						
4-5-4-2				0.9138	0.9032	0.8978	0.9068	0.00212	0.00056
4-6-5-2				0.9146	0.9162	0.8713	0.9043	0.00682	0.00137
4-6-6-2				0.9064	0.9365	0.8843	0.9068	0.00139	0.00088
4-7-6-2				0.9071	0.8874	0.9115	0.9033	0.00149	0.00048
4-8-7-2				0.9041	0.9004	0.9192	0.9054	0.00131	0.00181
4-9-8-2				0.9052	0.9109	0.9091	0.9062	0.00039	0.00195

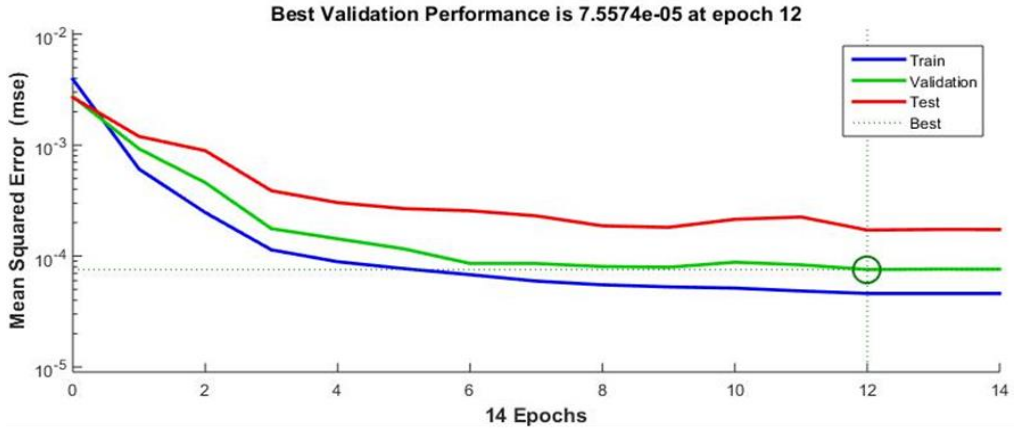

(a)

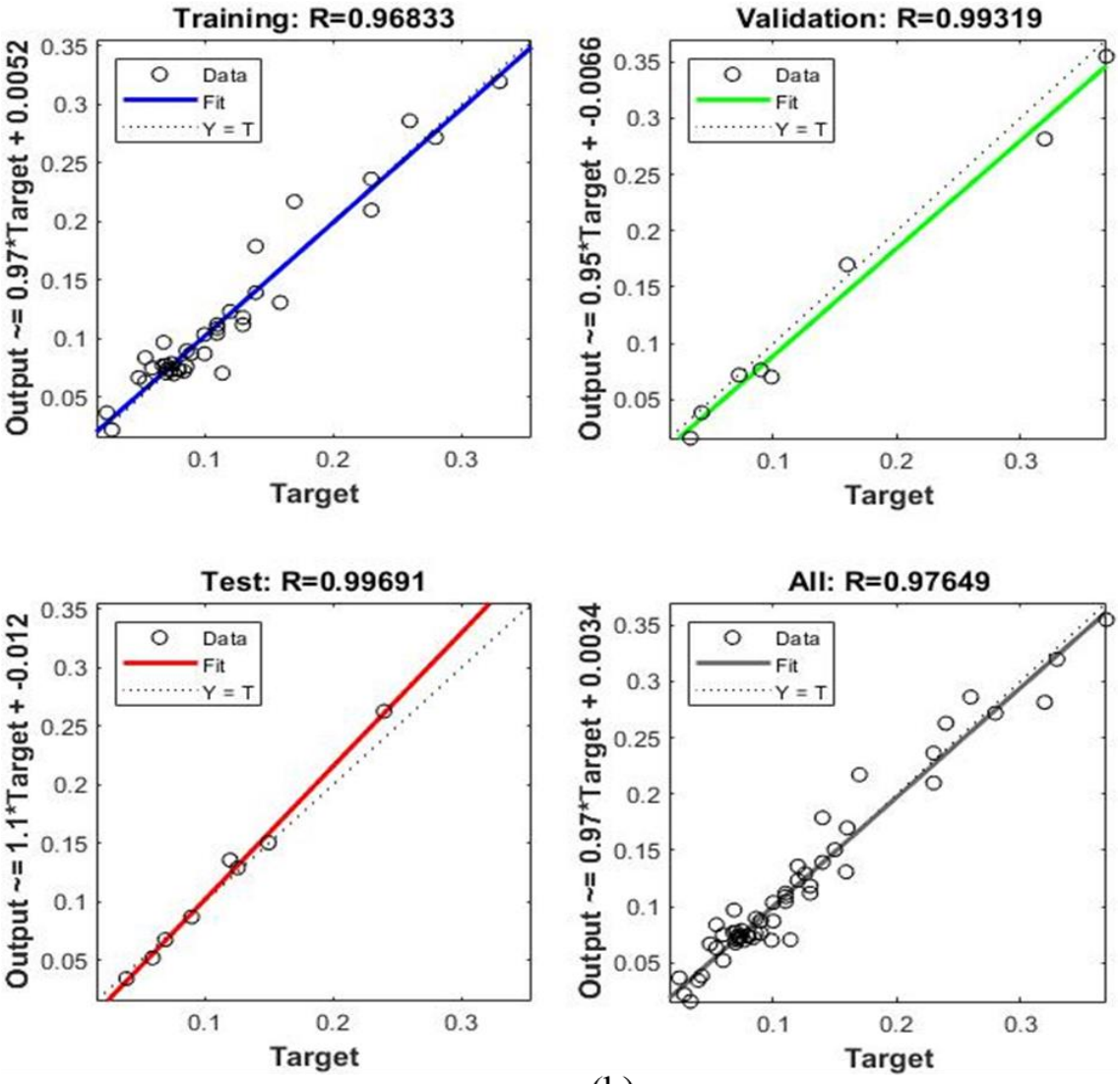

(b)

Fig. 5.5 (a) Performance and (b) Regression plot for 4-7-2 (transig-purelin) network model

It has been observed that the ANN network 4-5-1 and 4-7-1 with transig-purelin transfer functions are found to be appropriate for predicting COF and WR respectively. Moreover, the 4-7-2 model with transig-purelin transfer functions is observed to be appropriate for predicting COF and WR simultaneously. Fig. 5.5 (a) and (b) depict the performance and regression plot for the 4-7-2 ANN model.

5.3 Comparative analysis

The comparison of individual predicted responses (i.e. COF or WR) as well as simultaneous predicted responses (i.e. COF and WR) using Taguchi and ANN is shown in Fig. 5.6 and Fig. 5.7 respectively.

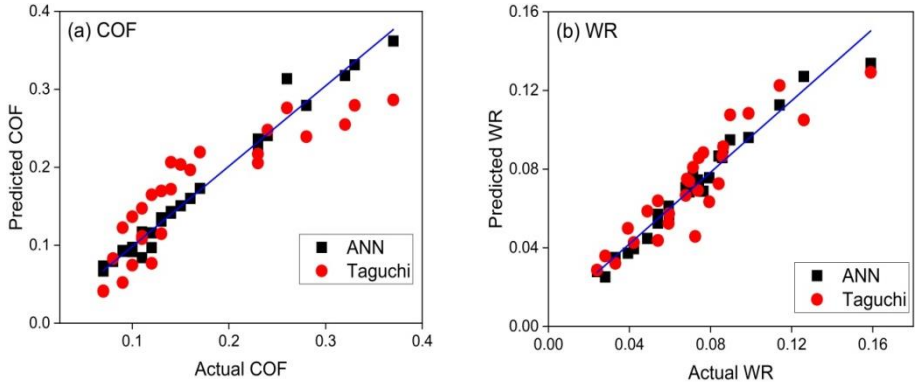

Fig. 5.6 Actual and predicted responses 4-n-1 model (a) COF and (b) WR

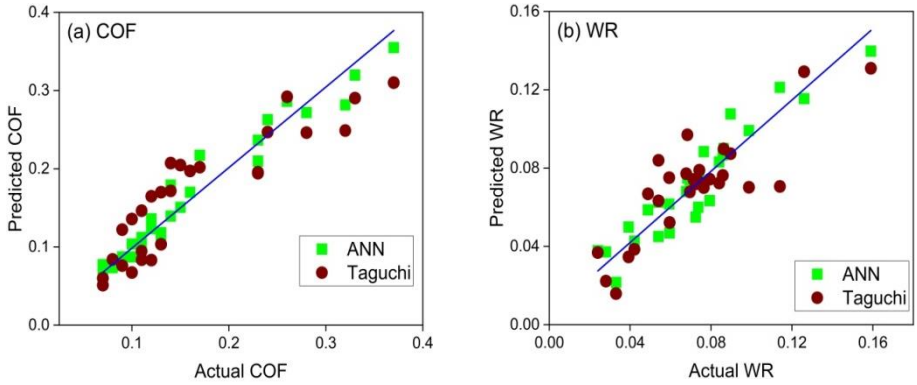

Fig. 5.7 Actual and predicted responses 4-n-2 model (a) COF and (b) WR

The comparison of results obtained using both the approaches shows that, the ANN predicted results in close agreement with the experimental results. Hence the ANN model is superior over the Taguchi model. In addition, the ANN approach helps to predict precisely the interactive effects of the input process parameters (i.e. wt. % of TiO_2, contact pressure, sliding speed and temperature) on the output responses (i.e. COF and WR).

5.4 Summary

The tribological behavior of the composite of MoS_2-TiO_2 coating material with different influential parameters such as wt. % of TiO_2, contact pressure, sliding speed and temperature have been studied. Taguchi design of experiment (DOE) and artificial neural network (ANN) tools have been implemented for developing a better correlation between above mentioned input parameters and output tribological responses such as COF and WR. The number of investigations based upon the Taguchi and ANN approach following conclusions has been drawn.

1. Taguchi's approach demonstrates that temperature is a highly significant parameter followed by contact pressure, wt. % of TiO_2 and sliding speed affecting both COF as well as wear rate. In case of individual factor despite the other factors, sliding speed affects less; but it displays significant effect in case of interaction with the other factors.
2. ANN with 4-n-1 topology model exhibits more precise prediction as compared to ANN with 4-n-2 topology model. In addition, ANN also exhibits a more precise prediction of the output responses as compared to Taguchi prediction.

Overall, the ANN tool proved to be an effective tool for predicting COF and wear rate for composite MoS_2-TiO_2 coating. This could benefit industries, particularly at the initial research and development stage where cut down in time and money is a primary objective.

The application of coated tool machining is an effective alternative, as it is environment friendly clean technology to improve the machining performance and tool life. The machining performance is evaluated on the basis of output responses such as cutting forces, surface roughness, cutting temperature at the tool-chip interface, specific energy and tool life. In Chapter 6, the performance of developed composite MoS_2-TiO_2 coating in machining application (i.e. milling operation) is evaluated.

Chapter 6

Performance of Composite MoS_2-TiO_2 Coating in Machining Application

Machining is one of the most basic and imperative processes in the manufacturing industry. The machining responses such as cutting forces, surface roughness, cutting temperature, specific energy and tool life decisively plays an important role to evaluate the machining performance. In the traditional approach, cutting fluids are extensively used to dissipate the heat generated during machining; their usage causes harm to nature and affects the health of human beings. Hence, there is a necessity to discover environment friendly alternatives to traditional cutting fluids. The field of advanced tribology has promoted the use of solid lubricants. In the present study, to improve the machining performance of milling process, both pure MoS_2 and composite MoS_2-TiO_2 coating materials have been employed.

6.1 Experimental investigation

The materials and equipment used for machining are described in the following subsection.

6.1.1 Materials

The workpiece material AISI 52100 steel plate having dimensions 200 mm X 100 mm X 15 mm thick is procured from Gayatri Chemicals, Warangal, Telangana, India. The high-speed parallel shank end mill cutter is used for milling procured from Addison and Co. Ltd., Kanchipuram, Tamilnadu, India.

6.1.2 Experimental test details

The experimental test details considered in the present work have been shown in table 6.1.

Table 6.1 Experimental test details

Cutting tools	HSS parallel shank end mill cutter (Addison make)
Cutter diameter	20 mm
Overall length	108 mm
Flute length	38 mm
No. of flutes	6
Helix angle	30°
Relief angle	6°
Density	14.5 g/cm^3
Hardness	1570 HV
Transverse rupture strength	3800 N/mm^2
Process parameters	
Cutting speed (S)	8, 22, 45 m/min
Depth of cut (h)	0.5, 1, 1.5 mm
Feed rate (f)	50 mm/min
Environments	A] Dry machining with conventional tool B] Conventional tool with MoS_2 powder as lubricant (third body) C] Dry machining with MoS_2 coated tool D] Dry machining with composite MoS_2-TiO_2 coated tool E] MoS_2 coated tool with MoS_2 powder as lubricant (third body) F] Composite MoS_2-TiO_2 coated tool with composite MoS_2-TiO_2 powder as lubricant (third body)

The experimental setup used for milling operation is depicted in Fig. 6.1. The machining is performed on vertical milling machine Bharat Fritz Werner make, Bangalore, Karnataka, India. The cutting zone temperature is measured during machining using a non-contacting type Kiray-300 infrared camera supplied by Kimo instruments, Canada. After milling operation at individual operating conditions, the surface roughness is measured using the Surtronic S-100 (Taylor Hobson) Series Surface Roughness Tester. A three-component Kistler dynamometer of type 5697A and a recorder (Graphtec-4 channel thermal array corder) AG Winterthur Switzerland make is used force measurements.

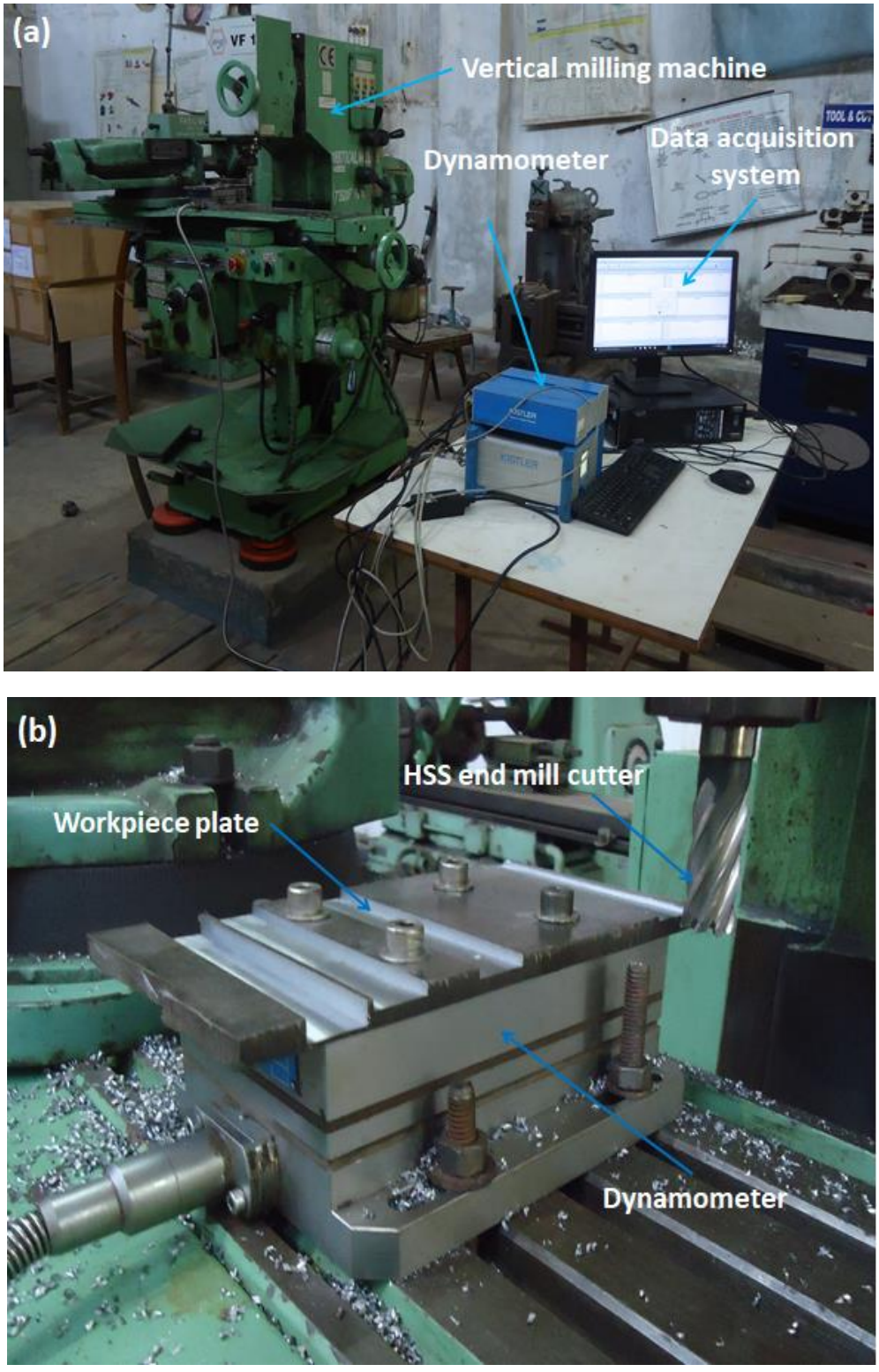

Fig. 6.1 Experimental set-up used for machining

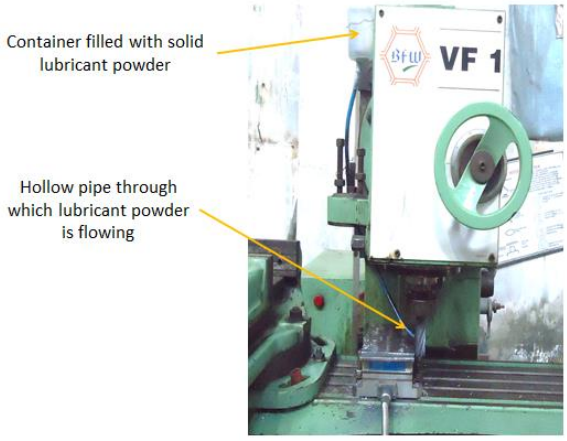

Fig. 6.2 Solid lubricant feeder

Usage of Pure MoS_2 and composite MoS_2-TiO_2 lubricants

The dry machining is carried out using conventional end mill cutter. The solid lubricant assisted machining is performed using the solid lubricants i.e. pure MoS_2 and composite MoS_2-TiO_2 powder as lubricant (third body) as well as in the form of coatings. The solid lubricant powder is supplied onto the cutting zone at the atmospheric pressure using machine vibrations at the spindle. The cylindrical container containing solid lubricant powder is attached to the machine, as depicted in Fig. 6.2. The average supply of the solid lubricant powder is observed to be from 10 gm/min to 15 gm/min. Besides, the end mill cutter is coated with pure MoS_2 and composite MoS_2-TiO_2 coating. These coatings are deposited as per the procedure explained in chapter 3, section 3.2. The conventional end mill cutter, pure MoS_2 coated and composite MoS_2-TiO_2 coated end mill cutters are shown in Fig. 6.3.

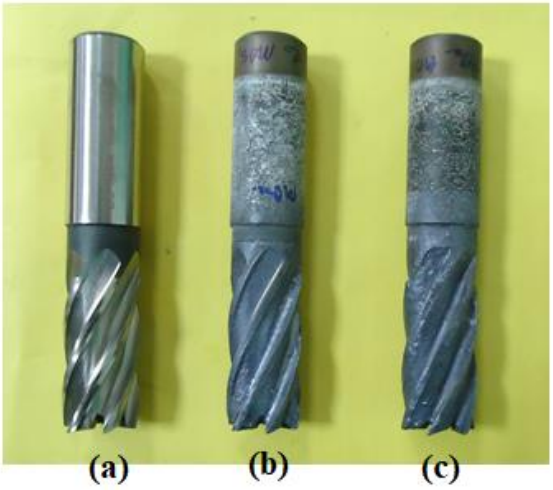

Fig. 6.3 HSS end mill cutters (a) conventional, (b) pure MoS_2 coated and (c) composite MoS_2-TiO_2 coated

6.2 Machining responses

The machining responses like cutting forces, surface roughness, cutting temperature, specific energy and tool life have been evaluated from the experimental tests and described in the below subsections.

6.2.1 Cutting forces and surface roughness

Generally, in machining lower cutting forces and surface roughness is desirable. Therefore in the present study, the machining is performed at various environmental conditions as mentioned in table 6.1. From the experimental tests, it is observed that the cutting force and surface roughness are the functions of cutting speed and depth of cut (as depicted in Figs 6.4, 6.5). The reduction in cutting force and surface roughness are observed with higher and lower values of cutting speed and depth of cut respectively, and vice-versa. These results are in-line with the previously reported literature (Vamsi et al., 2010, Vamsi et al., 2011, Reddy et al., 2010). Among the considered environmental conditions, highest cutting force and surface roughness values are observed in dry machining with conventional tool. For the rest of other environmental conditions, reduction in cutting force and surface roughness have been observed due to reduced friction at the contacting faces between end mill cutter and workpiece. This is attributed due to introduction of solid lubricant (Deng et al., 2011, Jianxin et al., 2012 and Ilie and Tita 2012). In comparison with all considered environmental conditions, MoS_2-TiO_2 coated tool with MoS_2-TiO_2 powder as lubricant (third body) exhibits a significant decrement in cutting forces and surface roughness parameters.

At 0.5 mm depth of cut with cutting speed of 8 (m/min), 22 (m/min) and 45(m/min), the improvement in the cutting force of MoS_2-TiO_2 coated tool with MoS_2-TiO_2 powder as lubricant (third body) in comparison with dry machining is observed to be 59%, 64% and 63% respectively. In the similar way with 1 and 1.5 mm depth of cut, the improvement in the cutting force is observed to be 43%, 43%, 31 % and 43%, 40%, 27%, respectively.

In case of surface roughness, MoS_2-TiO_2 coated tool with MoS_2-TiO_2 powder as lubricant (third body) exhibits an improved surface roughness of 60 %, 63 % and 68 % as compared to dry machining at 0.5 mm depth of cut with cutting speed of 8 (m/min), 22 (m/min) and 45(m/min) respectively. In the similar way with 1 and 1.5 mm depth of cut, the improvement in the surface roughness is observed to be 64 %, 69 %, 71 % and 60 %, 61 %, 63 %, respectively.

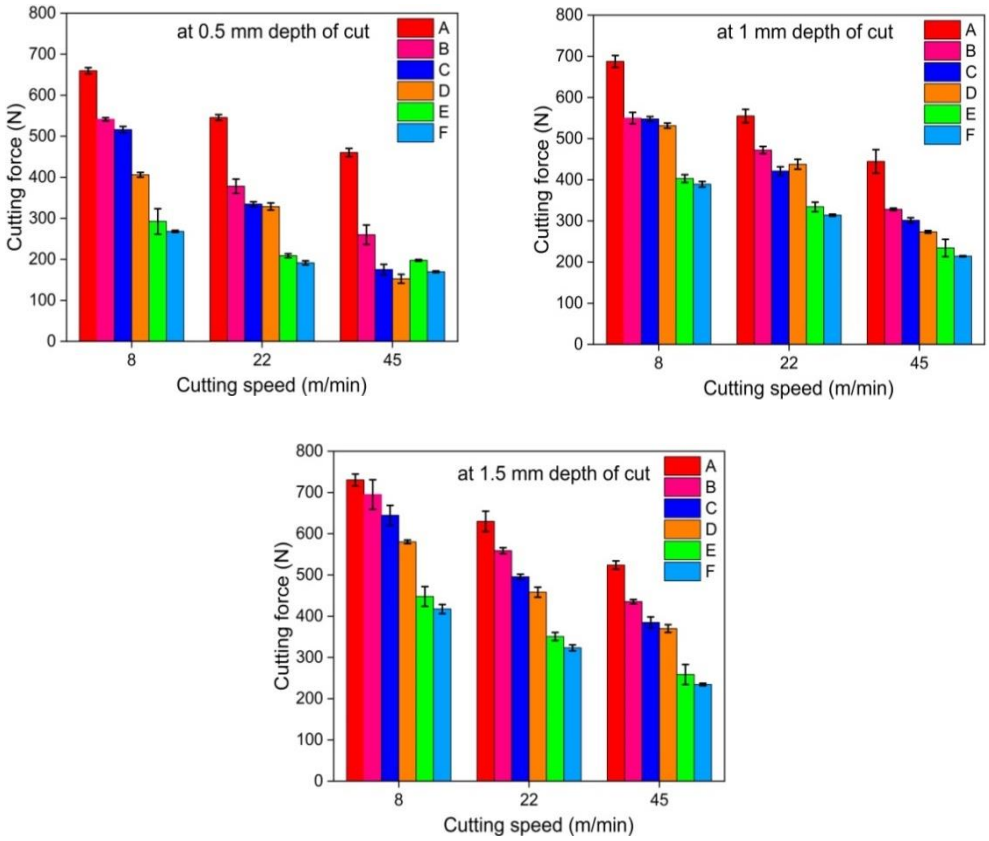

Fig. 6.4 Variation of cutting force with cutting speed at various levels of depth of cut

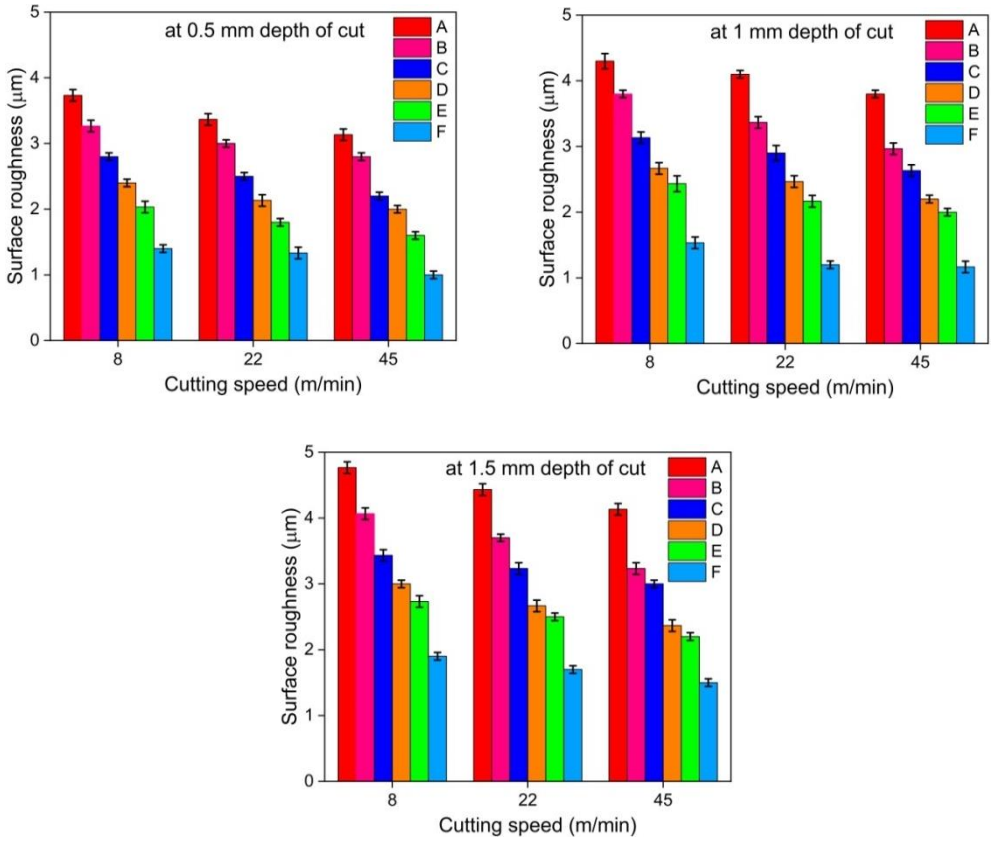

Fig. 6.5 Variation of surface roughness with cutting speed at various levels of depth of cut

6.2.2 Cutting temperatures

In machining, heat is generated at the contact zone between the tool and workpiece, which leads to increase the cutting temperature. Generally in machining, lower cutting temperature is desirable at the tool-chip interface as it affects the tool life. Hence in the present study, to reduce the cutting temperature solid lubricant is introduced in the form of powder as lubricant (third body) as well as in the form of coating. During machining operation, the cutting temperature at the tool-chip interface at different operating conditions measured at 10, 20 and 30 sec using an infrared thermography camera are depicted in Fig. 6.6. It is observed that the cutting temperature is the function of cutting speed and depth of cut. It is noted that the highest cutting temperature is observed to be 139.7 °C at 8 (m/min) and 1.5 mm depth of cut under dry machining condition with conventional tool. Whereas lowest cutting temperature is observed to be 44.3 °C at 8 (m/min) and 0.5 mm depth of cut under MoS_2-TiO_2 coated tool with MoS_2-TiO_2 powder as lubricant (third body). This is attributed to the lubricating action of the MoS_2, which eventually results into reduction in the tool wear (Teer 2001).

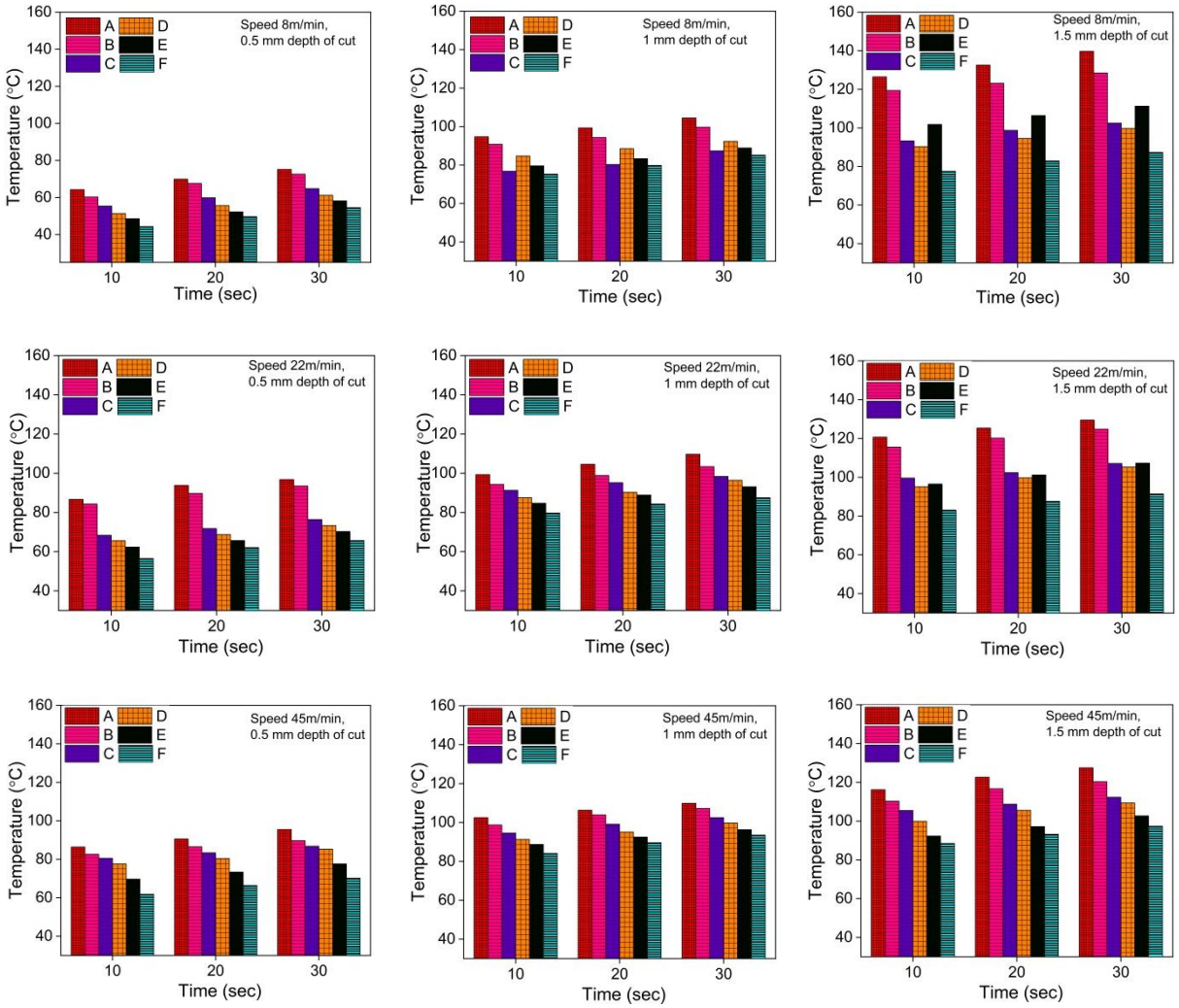

Fig. 6.6 Variation of temperature with cutting speed and depth of cut

6.2.3 Specific energy

In general, lowest specific energy is desirable in machining application. In the present work, specific energy obtained in dry machining with conventional tool is compared with different environmental conditions (where solid lubricant introduced in the form of powder as lubricant (third body) or in the form of coating) as mentioned in the table 6.1. From the Fig. 6.7, it is observed that specific energy is a function of cutting speed and depth of cut. From the experimental results, highest specific energy is observed in case of dry machining with a conventional tool, whereas lowest specific energy is observed in case of composite MoS_2-TiO_2 coated tool with composite MoS_2-TiO_2 powder as lubricant (third body).

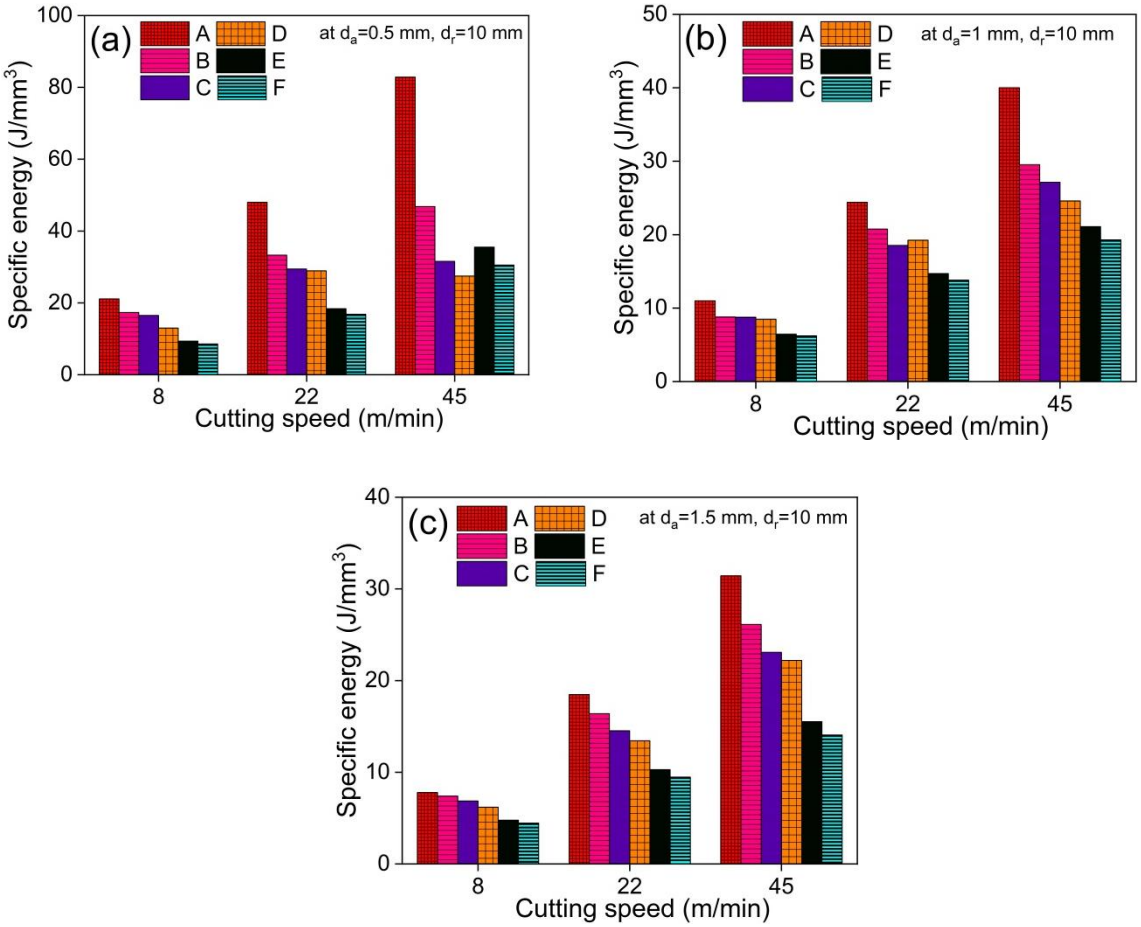

Fig. 6.7 Variation of specific energy with cutting speed at various levels of depth of cut

6.2.4 Tool life

Tool life is a measure of the span of time until a tool will cut the material effectively. Generally in machining application, higher tool life is desirable. The tool life obtained for various operating conditions is shown in Fig. 6.8. With the introduction of the solid lubricant in the form of coating or powder as lubricant (third body), improvement in tool life has been observed. The use of composite MoS_2-TiO_2 coated tool with composite MoS_2-TiO_2 powder as lubricant (third body) exhibit almost 1.5 times increase in tool life as compared to dry machining with conventional tool.

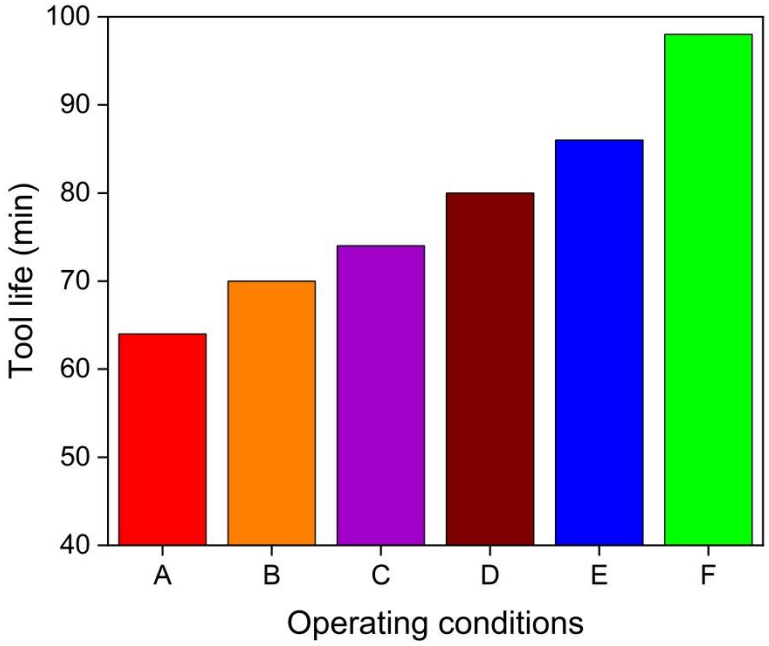

Fig. 6.8 Tool life at various operating conditions

6.3 Summary

The findings of the present study demonstrate that with the use of the MoS_2-TiO_2 coated tool with MoS_2-TiO_2 powder as lubricant (third body) depicts a significant improvement in machining performance as compared to dry machining with conventional tool in terms of cutting force, surface roughness, cutting temperature, specific energy and tool life. With this environmental condition almost 1.5 times increase in tool life is observed as compared to dry machining with conventional tool. The use of pure MoS_2 and composite MoS_2-TiO_2 lubricant in manufacturing industry can also improve productivity, as it causes an overall improvement in the machining performance. The pure MoS_2 and composite MoS_2-TiO_2 lubricant assisted machining technique may arise as a viable green alternative to dry machining.

The overall conclusion of the study and scope for the future work is reported in Chapter 7.

Chapter 7

Conclusion and Future Scope

The present dissertation focused on the development of composite MoS_2-TiO_2 coating material and its tribological behavior in dry sliding contact. The characterization of the developed composite MoS_2-TiO_2 coating is performed to investigate its hardness and adhesion strength. The parametric optimization for the tribological performance of the coating material is investigated using Taguchi and ANN approach. Furthermore, the composite MoS_2-TiO_2 coating is deposited onto the end mill cutters to study the improvement in the machining performance.

7.1 Conclusions

- A composite MoS_2-TiO_2 coating material is successfully developed (with different crystallite size and wt. % of TiO_2). As compared to pure MoS_2 coating material, the developed composite MoS_2-TiO_2 coating material exhibits excellent mechanical and tribological properties.
- The characterization study of composite MoS_2-TiO_2 coating shows that with higher doping percentage of TiO_2 exhibits dense microstructure and increase in the film hardness. Coating with 15 wt. % TiO_2 exhibits superior hardness, bond strength and scratch resistance in comparison with pure MoS_2 coating and other percentages of MoS_2-TiO_2 coating material.
- The tribological test results reveals that composite MoS_2-TiO_2 coating exhibits excellent tribological performance in all considered operating conditions due to the synergistic effect of both MoS_2 and TiO_2. At ambient conditions, the introduction of TiO_2 into the MoS_2 matrix helps to improve the bond strength without spoiling the lubricating property of MoS_2 and in turns lead to enhance the endurance life of the coating.
- The crystallite size of TiO_2 has less dominance on Coefficient of Friction (COF) and wear rate as compared to wt. % addition of TiO_2. At higher contact pressure and sliding speed, the composite MoS_2-TiO_2 coating with lower crys-

tallite size (i.e. 27.69 nm) with 15% wt. of TiO_2 depicts the lowest COF and wear rate.

- With increase in coating thickness and temperature, a reduction in COF is observed and vice-versa for wear rate.
- Taguchi approach demonstrates that temperature is highly significant parameter followed by contact pressure, wt. % of TiO_2 and sliding speed, affecting both COF as well as wear rate. In case of individual factor, sliding speed affects less; but in case of interaction with the other factors it displays significant effect.
- ANN with 4-n-1 topology model exhibits more precise prediction as compared to ANN with 4-n-2 topology model. In addition, ANN exhibit more precise prediction of the output responses as compared to Taguchi prediction.
- The application of composite MoS_2-TiO_2 coated tool with composite MoS_2-TiO_2 powder as lubricant (third body) in machining (i.e. milling) process depicts the larger reduction in cutting forces, specific energy, cutting temperature at tool–chip interface and improvement in surface finish and tool life as compared to dry machining with conventional tool.

7.2 Recommendations and future scope

Based on the conclusion drawn in this chapter following recommendations have been made for future work.

- The tribological performance of the developed composite MoS_2-TiO_2 coating material in combination with surface texturing can be studied.
- Computational study of the developed composite MoS_2-TiO_2 coating material can be performed for validating the experimental results.
- The corrosion resistance of the developed composite MoS_2-TiO_2 coating material can be studied.

References

Abou Gharam, A., Lukitsch, M.J., Balogh, M.P. and Alpas, A.T., 2010. High temperature tribological behaviour of carbon based (B_4C and DLC) coatings in sliding contact with aluminum. Thin Solid Films, 519(5), pp. 1611-1617.

Agarwal, S. and Venkateswara Rao, P., 2007. Performance improvement of SiC grinding using solid lubricants. Machining science and technology, 11(1), pp. 61-79.

Agarwal, V. and Agarwal, S., 2021. Performance profiling of solid lubricant for eco-friendly sustainable manufacturing. Journal of Manufacturing Processes, 64, pp. 294-305.

Aouadi, S.M., Luster, B., Kohli, P., Muratore, C. and Voevodin, A.A., (a) 2009. Progress in the development of adaptive nitride-based coatings for high temperature tribological applications. Surface and Coatings Technology, 204(6-7), pp. 962-968.

Aouadi, S.M., Paudel, Y., Simonson, W.J., Ge, Q., Kohli, P., Muratore, C. and Voevodin, A.A., (b) 2009. Tribological investigation of adaptive $Mo_2N/MoS_2/Ag$ coatings with high sulfur content. Surface and Coatings Technology, 203(10-11), pp. 1304-1309.

Arslan, E., Baran, O., Efeoglu, I. and Totik, Y., 2008. Evaluation of adhesion and fatigue of MoS_2-Nb solid-lubricant films deposited by pulsed-dc magnetron sputtering. Surface and Coatings Technology, 202(11), pp. 2344-2348.

Asmoro, G., Surojo, E., Ariawan, D., Muhayat, N. and Raharjo, W.W., 2018. Role of solid lubricant (MoS_2 and graphite) variations on characteristics of brake lining composite. Materials Science and Engineering 420(1), pp. 1-8.

ASTM D2510-94, 2017, Standard Test Method for Adhesion of Solid Film Lubricants, ASTM International, West Conshohocken, PA.

ASTM D3363-20, 2020, Standard Test Method for Film Hardness by Pencil Test, ASTM International, West Conshohocken, PA.

ASTM G99-17, 2017. Standard Test Method for Wear Testing with a Pin-on-Disk Apparatus, ASTM International, West Conshohocken, PA.

Azhaarudeen, S., Faruck A.A. ,and Nevosad, A., 2018. Tribological behaviour and wear mechanisms of manganese phosphate coatings under dry reciprocating sliding contact conditions, Tribology International 122, pp. 189-199.

Baker, C.C., Chromik, R.R., Wahl, K.J., Hu, J.J. and Voevodin, A.A., 2007. Preparation of chameleon coatings for space and ambient environments. Thin Solid Films, 515(17), pp. 6737-6743.

Bhadeshia, H. K. D. H., 2012. Steels for Bearings, Progress in Materials Science, 57, pp. 268-435.

Bhushan, B., 2000.Modern Tribology Handbook, CRC Press, New York.

Borgaonkar, A. and Syed, I., 2021. Friction and wear behaviour of composite MoS_2-TiO_2 coating material in dry sliding contact. Journal of the Brazilian Society of Mechanical Sciences and Engineering, 43(1), pp. 1-13.

Borgaonkar, A.V. and Syed, I., (a) 2020. Effect of coatings on rolling contact fatigue and tribological parameters of rolling/sliding contacts under dry/lubricated conditions: a review. Sādhanā, 45(1), pp. 1-16.

Borgaonkar, A.V. and Syed, I., (b) 2020. Effect of temperature on the tribological performance of MoS_2-TiO_2 coating material. In: Voruganti H., Kumar K., Krishna P., Jin X. (eds) Advances in Applied Mechanical Engineering. Lecture Notes in Mechanical Engineering, Singapore Springer pp. 611-618,

Bruce, R.W. ed., 2012. Handbook of lubrication and tribology, theory and design, Vol. 2. CRC press.

Bulbul, F. and Efeoglu, İ., 2010. MoS_2-Ti composite films having (002) orientation and low Ti content. Crystallography Reports, 55(7), pp. 1177-1182.

Bull, S.J. and Berasetegui, E.G., 2006. An overview of the potential of quantitative coating adhesion measurement by scratch testing. Tribology International, 39(2), pp. 99-114.

Bunshah, R. and Weissmantel, C., 2000. Handbook of hard coatings.

Burke, D. Sherrington, I. Roberts, E. W., 2001.The influence of counter-face surface finish on the performance of bonded solid lubricant films. Proceedings of the 2nd World Tribology Congress.

Burke, D., 2005. The Sliding Friction of Bonded Solid Lubricants (Doctoral dissertation, University of Central Lancashire)

Carrera, S., Salas, O., Moore, J.J., Woolverton, A. and Sutter, E., 2003. Performance of CrN/MoS_2 (Ti) coatings for high wear low friction applications. Surface and Coatings Technology, 167(1), pp. 25-32.

Chan, T.Y., Hu, Y., Gharbi, M.M., Politis, D.J. and Wang, L., 2016. The friction coefficient evolution of a MoS_2/WC multi-layer coating system during sliding wear. In Journal of Physics, 734, pp. 1-5.

Chen, F., Feng, Y., Shao, H., Zhang, X., Chen, J., Chen, N., 2012. Friction and Wear Behaviors of Ag/MoS_2/G Composite in Di_erent Atmospheres and at Di_erent Temperatures. Tribol. Lett. 47, pp. 139–148.

Chen, J. and Bull, S.J., 2010. Approaches to investigate delamination and interfacial toughness in coated systems: an overview. Journal of Physics D: Applied Physics, 44(3), pp. 1-19.

Chen, L., Wang, S.Q., Zhou, S.Z., Li, J. and Zhang, Y.Z., 2008. Microstructure and mechanical properties of Ti (C,N) and TiN/Ti (C,N) multilayer PVD coatings. International Journal of Refractory Metals and Hard Materials, 26(5), pp. 456-460.

Chen, W., Gao, Y., Chen, C. and Xing, J., 2010. Tribological characteristics of Si_3N_4–hBN ceramic materials sliding against stainless steel without lubrication. Wear, 269(3-4), pp. 241-248.

Chhowalla, M., Shin, H.S., Eda, G., Li, L.J., Loh, K.P. and Zhang, H., 2013. The chemistry of two-dimensional layered transition metal dichalcogenide nanosheets. Nature chemistry, 5(4), pp. 263-275.

Cho, M.H., Ju, J., Kim, S.J. and Jang, H., 2006. Tribological properties of solid lubricants (graphite, Sb_2S_3, MoS_2) for automotive brake friction materials. Wear, 260(7-8), pp. 855-860.

Clausing, R.E., Horton, L.L., Angus, J.C. and Koidl, P. eds., 2012. Diamond and diamond-like films and coatings, Vol. 266, Springer Science & Business Media.

Clauss, F.J. ed., 2012. Solid lubricants and self-lubricating solids. Elsevier.

Cuong, P.D., Ahn, H.S., Yoon, E.S. and Shin, K.H., 2006. Effects of relative humidity on tribological properties of boron carbide coating against steel. Surface and Coatings Technology, 201(7), pp. 4230-4235.

DellaCorte, C., Zaldana, A.R. and Radil, K.C., 2004. A systems approach to the solid lubrication of foil air bearings for oil-free turbomachinery. J. Trib., 126(1), pp. 200-207.

Deng, J., Song, W., Zhang, H., Yan, P. and Liu, A., 2011. Friction and wear behaviors of the carbide tools embedded with solid lubricants in sliding wear tests and in dry cutting processes. Wear, 270(9-10), pp. 666-674.

Deshmukh, P., Lovell, M., Sawyer, W.G. and Mobley, A., 2006. On the friction and wear performance of boric acid lubricant combinations in extended duration operations. Wear, 260(11-12), pp. 1295-1304.

Dilbag, S. and Rao, P.V., 2008. Performance improvement of hard turning with solid lubricants. The International Journal of Advanced Manufacturing Technology, 38(5-6), pp. 529-535.

Ding, X.Z., Zeng, X.T., He, X.Y. and Chen, Z., 2010. Tribological properties of Cr-and Ti-doped MoS2 composite coatings under different humidity atmosphere. surface and coatings Technology, 205(1), pp. 224-231.

Dominguez-Meister, S., Rojas, T.C., Brizuela, M. and Sánchez-López, J.C., 2017. Solid lubricant behavior of MoS_2 and WSe_2-based nanocomposite coatings. Science and Technology of advanced MaTerialS, 18(1), pp. 122-133.

Donnet, C. and Erdemir, A., A-2004. Historical developments and new trends in tribological and solid lubricant coatings. Surface and coatings technology, 180, pp. 76-84.

Donnet, C. and Erdemir, A., B-2004. Solid lubricant coatings: recent developments and future trends. Tribology Letters, 17(3), pp.Bu 389-397.

Duszczyk, J., Siuzdak, K., Klimczuk, T., Strychalska-Nowak, J. and Zaleska-Medynska, A., 2018. Manganese phosphatizing coatings: the effects of preparation conditions on surface properties. Materials, 11(12), pp. 1-22.

Ebnesajjad, S., 2010. Handbook of adhesives and surface preparation: technology, applications and manufacturing. Oxford, UK, pp. 15-17

Efeoglu, I., Baran, O., Yetim, F. and Altıntaş, S., 2008. Tribological characteristics of MoS_2-Nb solid lubricant film in different tribo-test conditions. Surface and Coatings Technology, 203(5-7), pp. 766-770.

Erdemir, A. 2000. Solid lubricants and self-lubricating films. In Bhushan B, editor. Modern Tribology Handbook. CRC Press, pp. 817-856

Erdemir, A., 2001. Solid lubricants and self-lubricating films. Modern tribology handbook, 2, pp. 787-818.

Essa, F.A., Zhang, Q., Huang, X., Ali, M.K., Elagouz, A. and Abdelkareem, M.A., 2017. Effects of ZnO and MoS_2 solid lubricants on mechanical and tribological properties of M50-steel-based composites at high temperatures: experimental and simulation study, Tribology Letters. 65, pp. 1-29.

Fatah, S.K., 2017. Investigate the Friction and wear behavior of MoS_2 nanoparticles in solid state lubrication. Journal of Garmin University.1, pp. 200-228

Fleischauer, P.D., Lince, J.R. and Didziulis, S.V., 2002. Chemical effects on MoS_2 lubricant transfer film formation; wear life implications. Handbook of tribology and lubrication, 10, pp. 30-33.

Fouladi, M. and Amadeh, A., 2013. Effect of phosphating time and temperature on microstructure and corrosion behavior of magnesium phosphate coating. Electrochimica Acta, 106, pp. 1-12.

Fu, Y., Wei, J. and Batchelor, A.W., 2000. Some considerations on the mitigation of fretting damage by the application of surface-modification technologies. Journal of Materials Processing Technology, 99(1-3), pp. 231-245.

G.E. Totten, Solid lubricants. ASM Handbook, ASM International, US, 2017, pp. 191-206.

George E. Totten (2017) Solid lubricants ASM Handbook, ASM International, US, pp. 191-206.

Gradt, T. and Schneider, T., 2016. Tribological performance of MoS_2 coatings in various environments. Lubricants, 4(3), pp. 1-13.

Guo, Y. B., and Liu, C. R., 2001. Mechanical Properties of Hardened AISI 52100 Steel in Hard Machining Processes . ASME. J. Manuf. Sci. Eng. 124(1), pp. 1-9.

Haider, J. and Hashmi, M.S.J., 2011. New generation of MoSx based solid lubricant coatings: recent developments and applications. In AIP conference proceedings, 1315(1), pp. 1365-1370.

Hassan, A.K.F., Mohammed, S., 2016. Artificial neural network model for estimation of wear and temperature in pin-disc contact. Universal Journal of Mechanical Engineering. 4, pp. 39-49

Hernández-Perez, I., Maubert, A.M., Rendón, L., Santiago, P., Herrera-Hernández, H., Díaz-Barriga Arceo, L., Garibay Febles, V., Palacios Gonzalez, E. and González-Reyes, L., 2012. Ultrasonic synthesis: structural, optical and electrical correlation of TiO_2 nanoparticles. Int. J. Electrochem. Sci, 7, pp. 8832-8847.

Heshmat, H., Hryniewicz, P., Walton Ii, J.F., Willis, J.P., Jahanmir, S. and DellaCorte, C., 2005. Low-friction wear-resistant coatings for high-temperature foil bearings. Tribology International, 38(11-12), pp. 1059-1075.

Holmberg, K. and Matthews, A., 2009. Coatings tribology: properties, mechanisms, techniques and applications in surface engineering. Elsevier.

Hu, S., Muhammad, M., Wang, M., Ma, R., Du, A., Fan, Y., Cao, X. and Zhao, X., 2020. Corrosion resistance performance of nano-MoS_2-containing zinc phosphate coating on Q235 steel. Materials Letters, 265, p. 127256.

Hu, X.G., Hu, S.L. and Zhao, Y.S., 2005. Synthesis of nanometric molybdenum disulphide particles and evaluation of friction and wear properties. Lubrication Science, 17(3), pp. 295-308.

Ilie, F. and Tita, C., 2012. Modelling and experimentation of solid lubrification with powder MoS_2 through self-repairing and self-replenishing. In Advanced Materials Research. 463, pp. 1120-1124.

Jia, Y., Wan, H., Chen, L., Zhou, H. and Chen, J., 2017. Effects of phosphate binder on the lubricity and wear resistance of graphite coating at elevated temperatures. Surface and Coatings Technology, 315, pp. 490-497.

Jianxin, D., Wenlong, S., Hui, Z. and Jinlong, Z., 2008. Performance of PVD MoS_2/Zr-coated carbide in cutting processes. International Journal of Machine Tools and Manufacture, 48(14), pp. 1546-1552.

Jianxin, D., Ze, W., Yunsong, L., Ting, Q. and Jie, C., 2012. Performance of carbide tools with textured rake-face filled with solid lubricants in dry cutting processes. International Journal of Refractory Metals and Hard Materials, 30(1), pp. 164-172.

Kavimani, V., & Prakash, K. S. (2017). Tribological behaviour predictions of r-GO reinforced Mg composite using ANN coupled Taguchi approach. Journal of Physics and Chemistry of Solids, 110, 409-419.

Kiliçay, K. and Ulutan, M., 2016. Investigation of the solid lubrication effect of commercial boron-based compounds in end milling. International Journal of Precision Engineering and Manufacturing, 17(4), pp. 517-524.

Korsunsky, A. M., & Kim, K. (2010). Dissipated energy and friction coefficient evolution during fretting wear of solid lubricant coatings. Tribology international, 43(5-6), 861-867.

Krishna, P.V. and Rao, D.N., 2008. Performance evaluation of solid lubricants in terms of machining parameters in turning. International Journal of Machine Tools and Manufacture, 48(10), pp. 1131-1137.

Krishna, V.P., Rao, D.N. and Srikant, R.R., 2009. Predictive modelling of surface roughness and tool wear in solid lubricant assisted turning of AISI 1040 steel. Proceedings of the Institution of Mechanical Engineers, Part J: Journal of Engineering Tribology, 223(6), pp. 929-934.

Kumar, P.S., Manisekar, K., 2014. Prediction of effect of MoS_2 content on wear behavior of sintered Cu-Sn composite using Taguchi analysis and artificial neural network. Indian Journal of Engineering and Material Sciences. 21, pp. 657-671

Kumar, S., Chauhan, S.R., 2012. Mechanical and Dry Sliding Wear Behavior of Particulate Fillers $CaCO_3$ and $CaSO_4$ Filled Vinyl Ester Composites. International Journal of Composite Materials. 2, pp. 101-114

Lara, L.C., Costa, H. and de Mello, J.D.B., 2015. Influence of layer thickness on sliding wear of multifunctional tribological coatings. Industrial Lubrication and Tribology. 67, pp. 460-467.

Li, C., Duan, L., Tan, S., Zhang, W. and Pan, B., 2018. Effect of CaF_2 and hBN on the mechanical and tribological properties of Fe-based impregnated diamond bit matrix. International Journal of Refractory Metals and Hard Materials, 75, pp. 118-125.

Li, G., Niu, L., Lian, J. and Jiang, Z., 2004. A black phosphate coating for C1008 steel. Surface and Coatings Technology, 176(2), pp. 215-221.

Liang J., 2013. Bonded Solid Lubrication Coatings, Process, and Applications. In: Wang Q.J., Chung YW. (eds) Encyclopedia of Tribology. Springer, Boston, pp. 242-247.

Lince, J.R., 2020. Effective Application of Solid Lubricants in Spacecraft Mechanisms. Lubricants, 8(7), pp. 1-57.

Lince, J.R., Pluntze, A.M., Jackson, S.A., Radhakrishnan, G. and Adams, P.M., 2014. Tribochemistry of MoS3 nanoparticle coatings. Tribology Letters, 53(3), pp. 543-554.

Liu, C., Chen, L., Zhou, J., Zhou, H. and Chen, J., 2014. Tribological properties of adaptive phosphate composite coatings with addition of silver and molybdenum disulfide. Applied surface science, 300, pp. 111-116.

Lovell, M., Higgs, C.F., Deshmukh, P. and Mobley, A., 2006. Increasing formability in sheet metal stamping operations using environmentally friendly lubricants. Journal of materials processing technology, 177(1-3), pp. 87-90.

Luo, D.B., Fridrici, V. and Kapsa, P., (a) 2011. Evaluating and predicting durability of bonded solid lubricant coatings under fretting conditions. Tribology international, 44(11), pp. 1577-1582.

Luo, J., Cai, Z.B., Mo, J.L., Peng, J.F. and Zhu, M.H., 2015. Torsional fretting wear behavior of bonded MoS_2 solid lubricant coatings. Tribology Transactions, 58(6), pp. 1124-1130.

Luo, J., Zhu, M.H., Wang, Y.D., Zheng, J.F. and Mo, J.L., (b) 2011. Study on rotational fretting wear of bonded MoS2 solid lubricant coating prepared on medium carbon steel. Tribology International, 44(11), pp. 1565-1570.

Ma, G., Xu, B., Wang, H., Wang, X., Li, G. and Zhang, S., 2013. Research on the microstructure and space tribology properties of electric-brush plated Ni/MoS_2–C composite coating. Surface and Coatings Technology, 221, pp. 142-149.

Ma, Y., Chen, L., Ye, Y., Wan, H., Zhou, H. and Chen, J., 2019. Preparation and tribological behaviors of a novel organic-inorganic hybrid resin bonded solid lubricating coating cured by ultraviolet radiation. Progress in Organic Coatings, 127, pp. 348-358.

Matthew, A., Kyriaki, K., Shreyes, M., 2009. An investigation of graphite nanoplatelets as lubricant in grinding, International Journal of Machine Tools & Manufacture, 49, pp. 966-970.

McDonald, M. and Hamilton, J., 2009. Recent developments in soluble silicate-based binders. Powder and Bulk Engineering, pp. 30-35.

Meng, R., Deng, J., Duan, R., Liu, Y. and Zhang, G., 2019. Modifying tribological performances of AISI 316 stainless steel surfaces by laser surface texturing and various solid lubricants. Optics & Laser Technology, 109, pp. 401-411.

Minitab User Manual Release, 2016. 17.3.0, MINITAB Inc.

Miyoshi, K. ed., 2019. Solid lubrication fundamentals and applications. CRC Press.

Montgomery, DC., 2017. Design and analysis of experiments. John Wiley and sons.

Mróz, K.P., Kucharski, S., Doliński, K., Bigos, A., Mikułowski, G., Beltowska-Lehman, E. and Nolbrzak, P., 2016. Failure modes of coatings on steel substrate. Bulletin of the Polish Academy of Sciences. Technical Sciences, 64(1), pp. 249-256.

Mukhopadhyay, D., Banerjee, S. and Reddy, N.S.K., 2007. Investigation to study the applicability of solid lubricant in turning AISI 1040 steel. ASME. J. Manuf. Sci. Eng., 129(3), pp. 520-526.

Muratore, C. and Voevodin, A.A., 2006. Molybdenum disulfide as a lubricant and catalyst in adaptive nanocomposite coatings. Surface and coatings technology, 201(7), pp. 4125-4130.

Muratore, C., Voevodin, A.A., 2009. Chameleon Coatings: Adaptive Surfaces to Reduce Friction and Wear in Extreme Environments. Annu. Rev. Mater. Res., 39, pp. 297–324.

Orendorz, A., Brodyanski, A., Losch, J., Bai, L.H., Chen, Z.H., Le, Y.K., Ziegler, C. and Gnaser, H., 2007. Phase transformation and particle growth in nanocrystalline anatase TiO_2 films analyzed by X-ray diffraction and Raman spectroscopy. Surface Science, 601(18), pp. 4390-4394.

Pathanatecha, W. (2019). A Study of Various Parameters Affecting Adhesion of Coatings to Metal Substrates.

Paturi, U.M.R. and Narala, S.K.R., 2015. On a novel solid lubricant technique: A study on the tribological characteristics under dry slide condition. Proceedings of the Institution of Mechanical Engineers, Part J: Journal of Engineering Tribology, 229(12), pp. 1503-1512.

Pokorny, P., Tej, P. and Szelag, P., 2016. Discussion about magnesium phosphating. Metalurgija, 55(3), pp. 507-510.

Quitmeyer, J., 2006. Grasping the phosphate coating process: A properly maintained solution is key to achieving adhesion, corrosion protection, and lubrication. Metal finishing, 104(9), pp. 47-50.

Rajagopal, C., Vasu, K.I., 2000. Properties of Phosphate Coatings and Influencing Factors. In: Conversion Coatings: A Reference for Phosphating, Chromating, and Anodizing Processes. Tata McGraw-Hill, pp. 62-70.

Rao, D.N. and Krishna, P.V., 2008. The influence of solid lubricant particle size on machining parameters in turning. International Journal of Machine Tools and Manufacture, 48(1), pp. 107-111.

Rao, K.P. and Xie, C.L., 2006. A comparative study on the performance of boric acid with several conventional lubricants in metal forming processes. Tribology international, 39(7), pp. 663-668.

Rao, K.P., Prasad, Y.V.R.K., Xie, C.L., 2011. Further evaluation of boric acid vis-a-vis other lubricants for cold forming applications, Tribology International, 44, pp. 1118-1126.

Ravindran, P., Manisekar, K., Narayanasamy, R., & Narayanasamy, P. (2013). Tribological behaviour of powder metallurgy-processed aluminium hybrid composites with the addition of graphite solid lubricant. Ceramics International, 39(2), 1169-1182.

Reddy, N.S.K. and Rao, P.V., 2006. Experimental investigation to study the effect of solid lubricants on cutting forces and surface quality in end milling. International Journal of Machine Tools and Manufacture, 46(2), pp. 189-198.

Reddy, N.S.K., Nouari, M. and Yang, M., 2010. Development of electrostatic solid lubrication system for improvement in machining process performance. International Journal of Machine Tools and Manufacture, 50(9), pp. 789-797.

Reeves, C.J., Menezes, P.L., Lovell, M.R. and Jen, T.C., 2013. Tribology of solid lubricants. In Tribology for scientists and engineers, Springer, New York. pp. 447-494.

Renevier, N.M., Hamphire, J., Fox, V.C., Witts, J., Allen, T. and Teer, D.G., 2001. Advantages of using self-lubricating, hard, wear-resistant MoS2-based coatings. Surface and Coatings Technology, 142, pp. 67-77.

Renevier, N.M., Lobiondo, N., Fox, V.C., Teer, D.G. and Hampshire, J., 2000. Performance of MoS_2/metal composite coatings used for dry machining and other industrial applications. Surface and coatings technology, 123(1), pp. 84-91.

Renevier, N.M., Oosterling, H., Konig, U., Dautzenberg, H., Kim, B.J., Geppert, L., Koopmans, F.G.M. and Leopold, J., 2003. Performance and limitations of MoS_2/Ti composite coated inserts. Surface and Coatings Technology, 172(1), pp. 13-23.

Ripa, M., Frangu, L., 2004. A survey of artificial neural networks applications in wear and manufacturing processes. Journal of Tribology. 1, pp. 35-42.

Rossi, S., Chini, F., Straffelini, G., Bonora, P.L., Moschini, R. and Stampali, A., 2003. Corrosion protection properties of electroless Nickel/PTFE, Phosphate/MoS_2 and Bronze/PTFE coatings applied to improve the wear resistance of carbon steel. Surface and Coatings Technology, 173(2-3), pp. 235-242.

Rovani, A.C., Kouketsu, F., da Silva, C.H. and Pintaude, G. 2018. Surface Characterization of Three-Layer Organic Coating Applied on AISI 4130 Steel, Advances in Materials Science and Engineering 1, pp. 1-8.

Rudnicki, Z., Figiel, W., 2002. Neural nets applications in tribology research. Machine Operation Issues. 37, pp. 97-110.

Sahoo, P., Pal, S.K., 2007. Tribological performance optimization of electroless Ni–P coatings using the Taguchi method and grey relational analysis. Tribology letters. 28, pp. 191-201,

Sankara Narayanan, T.S.N., 2005. Surface pretretament by phosphate conversion coatings-A review. Reviews in Advanced Materials Science, 9, pp. 130-177.

Saravanakumar, A., Ravikanth, D., Rajeshkumar, L., Balaji, D., & Ramesh, M. (2021). Tribological Behaviour of MoS_2 and Graphite Reinforced Aluminium Matrix Composites. In IOP Conference Series: Materials Science and Engineering (Vol. 1059, No. 1, p. 012021). IOP Publishing.

Savan, A., Pfluger, E., Voumard, P., Schroer, A. and Simmonds, M., 2000. Modern solid lubrication: recent developments and applications of MoS_2. Lubrication Science, 12(2), pp. 185-203.

Shaji, S. and Radhakrishnan, V., 2002. Investigations on the application of solid lubricants in grinding. Proceedings of the Institution of Mechanical Engineers, Part B: Journal of Engineering Manufacture, 216(10), pp. 1325-1343.

Shaji, S. and Radhakrishnan, V., 2003. Analysis of process parameters in surface grinding with graphite as lubricant based on the Taguchi method. Journal of Materials Processing Technology, 141(1), pp. 51-59.

Shaji, S. and Radhakrishnan, V., 2003. Application of solid lubricants in grinding: investigations on graphite sandwiched grinding wheels. Machining science and technology, 7(1), pp. 137-155.

Shang, K., Zheng, S., Ren, S., Pu, J., He, D. and Liu, S., 2018. Improving the tribological and corrosive properties of MoS_2-based coatings by dual-doping and multilayer construction. Applied Surface Science, 437, pp. 233-244.

Shankara, A., Menezes, P.L., Simha, K.R. and Kailas, S.V., 2008. Study of solid lubrication with MoS_2 coating in the presence of additives using reciprocating ball-on-flat scratch tester, Sadhana 33, pp. 207-220.

Shen, M.X., Cai, Z.B., Peng, J.F., Peng, X.D. and Zhu, M.H., 2017. Antiwear properties of bonded MoS_2 solid lubricant coating under dual-rotary fretting conditions. Tribology Transactions, 60(2), pp. 217-225.

Singh, H., Mutyala, K.C., Mohseni, H., Scharf, T.W., Evans, R.D. and Doll, G.L., 2015. Tribological performance and coating characteristics of sputter-deposited Ti-doped MoS_2 in rolling and sliding contact. Tribology Transactions, 58(5), pp. 767-777.

Stojanović, B., Vencl, A., Bobić, I., Miladinović, S., & Skerlić, J. (2018). Experimental optimisation of the tribological behaviour of Al/SiC/Gr hybrid composites based on Taguchi's method and artificial neural network. Journal of the Brazilian Society of Mechanical Sciences and Engineering, 40(6), 1-14.

Sunil, T., Sandeep, M., Kumaraswami, R. and Shravan, A., 2016. A critical review on solid lubricants. Int. J. Mech. Eng. Technol, 7, pp. 193-199.

Suresh Kumar Reddy, N. and Venkateswara Rao, P., 2005. Performance improvement of end milling using graphite as a solid lubricant. Materials and manufacturing processes, 20(4), pp. 673-686.

Tamilselvi, M., Kamaraj, M.A., Devikala, S. and Selvi, J.A., 2015. Progress in zinc phosphate conversion coatings: a review, International Journal of Advanced Chemical Science and Applications 3, pp. 25-41.

Tedstone, A.A., Lewis, D.J., Hao, R., Mao, S.M., Bellon, P., Averback, R.S., Warrens, C.P., West, K.R., Howard, P., Gaemers, S. and Dillon, S.J., 2015. Mechanical properties of molybdenum disulfide and the effect of doping: an in situ TEM study. ACS applied materials and interfaces, 7(37), pp. 20829-20834.

Teer D.G., New solid lubricant coatings. Wear. 2001. 251(1-12), pp. 1068-1074.

Tran Khac, B.C., DelRio, F.W. and Chung, K.H., 2018. Interfacial strength and surface damage characteristics of atomically thin h-BN, MoS_2, and graphene. ACS applied materials and interfaces, 10(10), pp. 9164-9177.

Tyagi, R., Kumar, S., Kumar, V., Mohanty, S., Das, A. K., & Mandal, A. (2020). Analysis and Prediction of Electrical Discharge Coating Using Artificial Neural Network (ANN). In Advances in Simulation, Product Design and Development (pp. 177-189). Springer, Singapore.

Vadiraj, A., Kamaraj, M. and Sreenivasan, V.S., 2012. Effect of solid lubricants on friction and wear behaviour of alloyed gray cast iron. Sadhana, 37(5), pp. 569-577.

Vamsi Krishna, P., Srikant, R.R. and Nageswara Rao, D., 2011. Solid lubricants in machining. Proceedings of the Institution of Mechanical Engineers, Part J: Journal of Engineering Tribology, 225(4), pp. 213-227.

Vamsi Krishna, P., Srikant, R.R. and Rao, D.N., 2010. Experimental investigation to study the performance of solid lubricants in turning of AISI1040 steel. Proceedings of the Institution of Mechanical Engineers, Part J: Journal of Engineering Tribology, 224(12), pp. 1273-1281.

Vazirisereshk, M.R., Martini, A., Strubbe, D.A. and Baykara, M.Z., 2019. Solid lubrication with MoS2: a review. Lubricants, 7(7), pp. 1-35.

Velten, K., Reinicke, R., Friedrich, K., 2000. Wear volume prediction with artificial neural networks. Tribology International. 33, pp. 731-736.

Venu Gopal, A. and Venkateswara Rao, P., 2004. Performance improvement of grinding of SiC using graphite as a solid lubricant. Materials and manufacturing processes, 19(2), pp. 177-186.

Voevodin, A.A., Fitz, T.A., Hu, J.J. and Zabinski, J.S., 2002. Nanocomposite tribological coatings with “chameleon” surface adaptation. Journal of Vacuum Science & Technology A: Vacuum, Surfaces, and Films, 20(4), pp. 1434-1444.

Voevodin, A.A., Muratore, C. and Aouadi, S.M., 2014. Hard coatings with high temperature adaptive lubrication and contact thermal management. Surface and Coatings Technology, 257, pp. 247-265.

Voumard, P., Savan, A. and Pfluger, E., 2001. Advances in solid lubrication with MoS_2 multilayered coatings. Lubrication Science, 13(2), pp. 135-145.

Wan, H., Ye, Y., Chen, L., Chen, J. and Zhou, H., 2016. Influence of polyfluo-wax on the friction and wear behavior of polyimide/epoxy resin–molybdenum disulfide bonded solid lubricant coating. Tribology Transactions, 59(5), pp. 889-895.

Wenlong, S., Jianxin, D., Hui, Z. and Pei, Y., 2010. Study on cutting forces and experiment of MoS_2/Zr-coated cemented carbide tool. The International Journal of Advanced Manufacturing Technology, 49(9-12), pp. 903-909.

Wenlong, S., Jianxin, D., Hui, Z., Pei, Y., Jun, Z. and Xing, A., (a) 2011. Performance of a cemented carbide self-lubricating tool embedded with MoS_2 solid lubricants in dry machining. Journal of Manufacturing processes, 13(1), pp. 8-15.

Wenlong, S., Jianxin, D., Ze, W., Hui, Z., Pei, Y., Jun, Z. and Xing, A., (b) 2011. Cutting performance of cemented-carbides-based self-lubricated tool embedded with different solid lubricants. The International Journal of Advanced Manufacturing Technology, 52(5-8), pp. 477-485.

Xu, G. H., Zhu, M., Liu, J., Zhou, Z., & Liang, H. (2003). The effect of pre-treatment of substrate on fretting tribological behavior of MoS2 coatings. Wear, 255(1-6), 246-252.

Xu, J., Zhou, Z.R., Zhang, C.H., Zhu, M.H. and Luo, J.B., 2007. An investigation of fretting wear behaviors of bonded solid lubricant coatings. Journal of Materials Processing Technology, 182(1-3), pp. 146-151.

Xu, J., Zhu, M. H., Zhou, Z. R., Kapsa, P., & Vincent, L. (2003). An investigation on fretting wear life of bonded MoS2 solid lubricant coatings in complex conditions. Wear, 255(1-6), 253-258.

Xu, J., Zhu, M.H., Zhou, Z.R., Kapsa, P. and Vincent, L., 2003. An investigation on fretting wear life of bonded MoS2 solid lubricant coatings in complex conditions. Wear, 255(1-6), pp. 253-258.

Xu, Y., Xie, M., Li, Y., Zhang, G., Xu, X., Fan, X., Sun, Q., Li, H. and Zhu, M., 2020. The effect of Si content on the structure and tribological performance of MoS_2/Si coatings. Surface and Coatings Technology, 403, pp. 1-10.

Ye, Y., Chen, J. and Zhou, H., (a) 2009. An investigation of friction and wear performances of bonded molybdenum disulfide solid film lubricants in fretting conditions. Wear, 266(7-8), pp. 859-864.

Ye, Y., Chen, J. and Zhou, H., (b) 2009. Microstructure, tribological behavior, and corrosion-resistant performance of bonded MoS_2 solid lubricating film filled with nano-LaF_3. Journal of dispersion science and technology, 30(4), pp. 488-494.

Yin, Y.G., Lin, F.D., Yao, W., Xie, T. and Yu, J.W., 2011. Tribological properties of the surface bonded self-lubricating coating. In Advanced Materials Research 154, pp. 583-587.

Zhang, X., Luster, B., Church, A., Muratore, C., Voevodin, A.A., Kohli, P., Aouadi, S. and Talapatra, S., 2009. Carbon nanotube-MoS_2 composites as solid lubricants. ACS applied materials and interfaces, 1(3), pp.735-739.

Zhao, Z., Xin, H., Ren, Y., Guo, X., 2010. Application and comparison of BP neural network algorithm in MATLAB. International Conference on Measuring Technology and Mechatronics Automation. 1, pp. 590-593.

Zhu, M. H., & Zhou, Z. R. (2001). An investigation of molybdenum disulfide bonded solid lubricant coatings in fretting conditions. Surface and Coatings Technology, 141(2-3), 240-245.

Zhu, X., Lauwerens, W., Cosemans, P., Van Stappen, M., Celis, J.P., Stals, L.M. and He, J., 2003. Different tribological behavior of MoS2 coatings under fretting and pin-on-disk conditions. Surface and Coatings Technology, 163, pp. 422-428.

Outcome of the research

Publications in Reputed Journals:

1. Borgaonkar A., Syed I. and Sonawane, S.H. Fabrication and Characterization of Composite MoS_2-TiO_2 Coating Material. **IMechE, Part C: Journal of Mechanical Engineering Science**, Accepted on 15th April 2021 **Sage, (SCI)**

2. Borgaonkar A. and Syed I. Friction and wear behavior of composite MoS_2-TiO_2 coating material in dry sliding contact. **Journal of the Brazilian Society of Mechanical Sciences and Engineering.** 2021; 43: 1-13. **Springer, (SCI)**

3. Borgaonkar, A. V., and I. Syed. Effect of coatings on rolling contact fatigue and tribological parameters of rolling/sliding contacts under dry/lubricated conditions: a review. **Sādhanā.** 2020; 45(30): 1-16. **Springer, (SCI)**

4. Borgaonkar A., Syed I. Prediction of Tribological Behavior of Composite MoS_2-TiO_2 Coating Using Taguchi and Artificial Neural Network Approach, **Engineering Science and Technology, an International Journal**, **Elsevier, (SCI)**, Communicated on 10th April 2021, Status- Under review

Book chapters:

1. Borgaonkar A.V.**,** Syed I. Effect of temperature on the tribological performance of MoS_2-TiO_2 coating material. In: Voruganti H., Kumar K., Krishna P., Jin X. (eds) **Advances in Applied Mechanical Engineering. Lecture Notes in Mechanical Engineering, Springer** Singapore, 2020. pp. 611-618.

2. Borgaonkar, A.V., Syed, I. and Sonawane, S.H. Effects of Lubrication on Tribological Properties Coating Material of Composite MoS_2-TiO_2. In: M. T. Hameed Sultan et al. (eds) **Tribological Applications of Composite Materials, Springer** Singapore, 2020. pp. 267-281.